CHAPTER 5:

GENETIC CHARACTERISATION OF THE GMR>*RAD21*^{NC} MODIFIER LOCI

5.1 INTRODUCTION

The size and organisation of the *Drosophila* eye, like all organs and organisms, is determined by cell number, cell size and the structure and patterning of these cells. Cell number is a function of both cell division and cell death, while cell size is determined by cell growth and division. All of these processes are driven and regulated by a combination of intracellular and extracellular cues (Johnston and Gallant, 2002; Conlon and Raff, 1999). A class of genes exists to link environmental cues, such as nutrient availability, with metabolic processes such as protein synthesis that are essential in cell and organ growth. Other genes are responsible for directing the identity, structure and patterning of an organ, which are also crucial in determining the final size and appearance of the organ (Johnston and Gallant, 2002).

The genetic screen conducted to identify dominant modifiers of the GMR>*Rad21*^{NC} eye phenotype successfully identified 133 candidate genes as putative regulators of chromosome cohesion and segregation. However it is unlikely that all of these are directly affecting the cellular processes of cohesin and chromosome cohesion, or closely associated processes such as DNA replication, cell cycle regulation or chromosome segregation. A number of the genes observed to modify the GMR>*Rad21*^{NC} phenotype may be interacting through modulation of cell survival, cell differentiation and eye morphogenesis. One example is *klumpfuss,* (*klu*) the protein product of which drives cell proliferation and also has a role in apoptosis. In order to assess the function of the GMR>*Rad21*^{NC} modifiers identified in the primary screen, a range of secondary genetic assays were performed. These assays were designed to identify eye-specific modifiers, direct modifiers of apoptosis, modifiers of chromosome segregation and cell cycle progression, and modifiers acting through the tissue-specific Gal4driver.

Ectopic expression of RAD21^{NC} in the developing wing imaginal disc results in a reduced and disorganised wing phenotype (Keall, 2005; S. Page, unpublished). A moderately reduced-wing phenotype produced by ectopically expressing RAD21^{NC} under the control of the wing driver vgMQ-Gal4 was selected as an assay tool to assist in further analysing modifier loci of the GMR>*Rad21*^{NC} rough-eye phenotype.

The vgMQ>*Rad21*^{NC} reduced-wing assay was intended to identify modifier loci that are eye-specific in their effect as well as modifier loci that interact specifically with the original RAD21^{NC} transgenic line used for the rough-eye screen. RAD21 and cohesin are known to function in all somatic tissues (Warren *et al*., 2000) and so, based on this and the vgMQ-*Rad21*^{NC} reduced-wing phenotype, it was reasoned that the similar chromosomal abnormalities would be produced when RAD21^{NC} is ectopically expressed in any mitotically active tissue or organ. As control of cohesin and chromosome cohesion is anticipated to be highly conserved between somatic tissues, wing-specific *Rad21*^{NC} expression, which causes a reduced wing, was employed in an attempt to identify modifier loci that were eye-specific in their effects. Although many proteins are likely to be common to the developmental pathways of the eye and the wing, intrinsic differences between these tissues that make them unique provides an opportunity to assess the conservation of action for a given modifier allele. Equivalent modification by an allele of both the eye and wing phenotypes would be consistent with having a direct effect on chromosome cohesion and segregation. Heterozygosity for genes encoding cohesin subunits and known cohesin regulators were predicted to modify the *Rad21*^{NC} wing phenotype in the same or similar manner as the *Rad21*^{NC} eye phenotype.

A significant factor underlying the GMR>*Rad21*^{NC} phenotype is apoptosis. Inhibition of chromosome segregation results in cellular catastrophe with aneuploidy and broken DNA that can induce a cell to undergo apoptosis (Roos and Kaina, 2006). Although modification of the strength of the chromosome cohesion in the GMR>*Rad21*^{NC} model is predicted to reduce the frequency or severity of chromosome missegregation and thereby lessen apoptosis following cellular disaster, modifiers that act by directly influencing apoptosis were considered of secondary interest to this study. The GMR*hid* small eye phenotype assay and the GMR>*Rad21*^{NC}*, p35* eye phenotype assay were employed to identify modifier loci that directly influence apoptosis rates in the developing eye. As expression of the baculovirus p35 protein blocks all apoptosis, co-expression of *Rad21*^{NC} and *p35* under GMR in the eye was predicted to allow identification of modifier loci that influence the rate of apoptosis as these should not modify the GMR>*Rad21*^{NC} eye in the presence of *p35*. Whereas genes that are influencing the GMR>*Rad21*^{NC} eye phenotype through modification of chromosome segregation, cell cycle progression

and proliferation in the presence of aneuploidy should modify the GMR>*Rad21*^{NC}, *p35* eye phenotype. Modifiers of the GMR>*Rad21*^{NC}, *p35* eye phenotype are predicted to be of most interest to this study.

Finally, the GMR-Gal4 driver can yield a mild rough eye-phenotype on its own under certain circumstances or conditions. This phenotype was exploited to identify of modifier loci acting through modulation of the expression and/or cellular influences of the GAL4 transcription factor. This chapter describes these secondary assays and the analysis of the modifiers. The results of those four secondary assays were used in combination to ascertain which of the original list of GMR>*Rad21*^{NC} modifier loci act primarily via regulation of chromosome cohesion and segregation, and therefore worthy of further exploration as potential chromosome missegregation risk factors in human disease.

5.2 RESULTS

5.2.1 Rad21^{NC} *wing assay*

The wing assay was conducted by comparing variation in the size of the wing in individuals expressing RAD21^{NC} in a heterozygous mutant modifier background. Wing size variation was the primary consideration as this parameter could be relatively simply and objectively assessed. The wing assay was performed by crossing alleles of each modifier locusi alleles to the vgMQ-Gal4, UAS-*Rad21*^{NC}-*2HA* strain (referred to from here as vgMQ>*Rad21*^{NC}) followed by measurement of wing blade area for genotype quantitation (Figures 5.1 and 2.1). The mean sizes of the wing blades for test and control groups were compared using a Students' Unpaired T-test with a power ≥80% (for details see Materials and Methods section 2.7.3). A total of 109 alleles were tested using the vgMQ>*Rad21*^{NC} wing assay. Eighty-four of these were found to significantly modify the wing size via suppression (increased) or enhancement (decreased) of the wing blade area compared to controls. These data are presented in graphical form below in Figures 5.2 to 5.21, while the detailed statistical outcomes for each allele tested can be found in Appendix 5. The box and whisker plots used in this study were constructed using the smallest and largest wing measurement values (that are not outliers) as the

whiskers, and the 25th percentile, median (50th percentile) and the 75th percentile as the top, midline and bottom of the box, respectively.

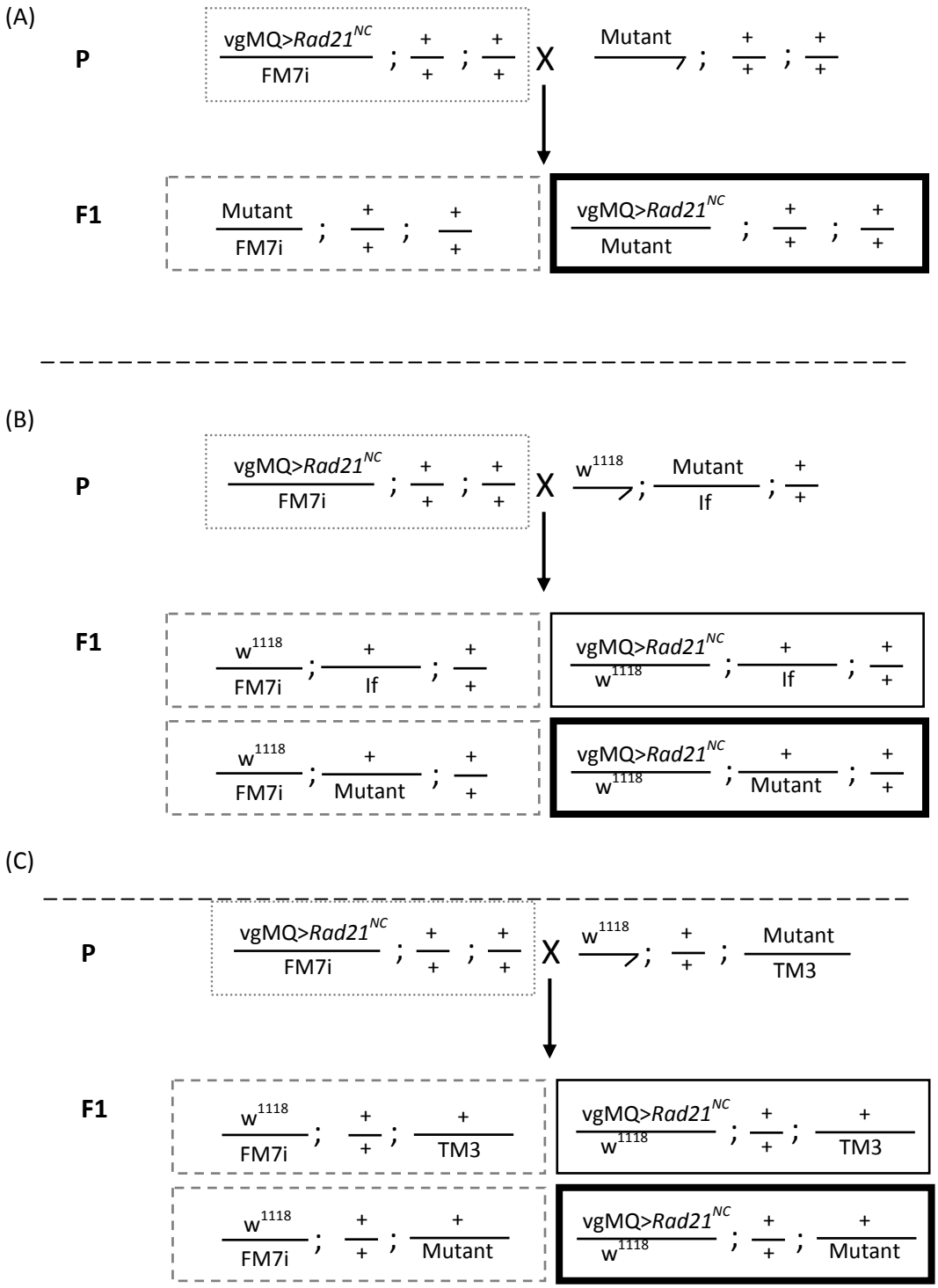

(D)

(i)

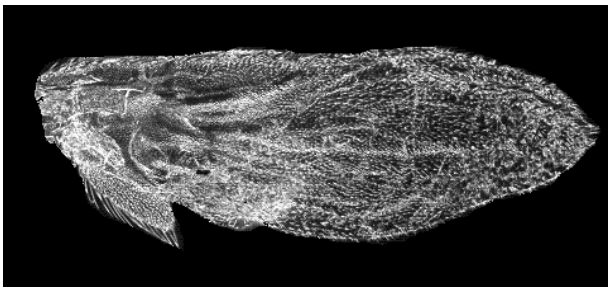

(ii)

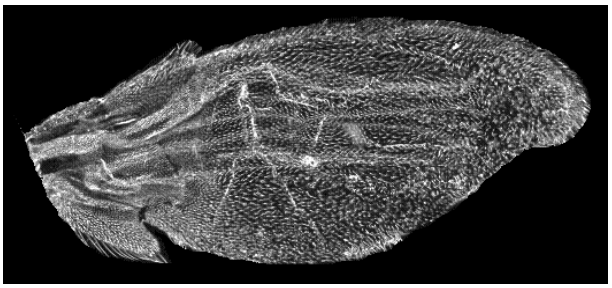

Figure 5.1: Crossing scheme and wing blade area analysis for the vgMQ>*Rad21*^{NC} assay. (A-C) Female flies from the vgMQ>*Rad21*^{NC}/FM7i; +/+; +/+ stock were crossed to males with mutant alleles carried on the 1st (A), 2nd (B) or 3rd (C) chromosome and balanced over the Y chromosome or appropriate marked balancer chromosomes. From the F1 progeny the test class (bold black box) and control class (black box) siblings were selected for comparison to identify changes in the vgMQ>*Rad21*^{NC} wing size in a heterozygous mutant background. The wings were also compared to parental (P) controls (grey box). (D) The mean wing blade area of the (i) vgMQ>*Rad21*^{NC}/+ control progeny was compared to the wing blade area of test progeny (ii) vgMQ>*Rad21*^{NC}/+; +/+; *Sep2*^{C207}. A minimum of 12 wings were measured for both test and control groups and only collected from female progeny to control for sex-specific size variances. A full description of the methods used can be found in Chapter 2 section 2.7.

5.2.1.1 Chromosome I modifier alleles

A total of 8 of the 13 chromosome I modifier alleles were tested in the vgMQ>*Rad21*^{NC} wing assay. Of these alleles, three were found to significantly modify the wing size compared to controls (Figure 5.2, Table 5.2).

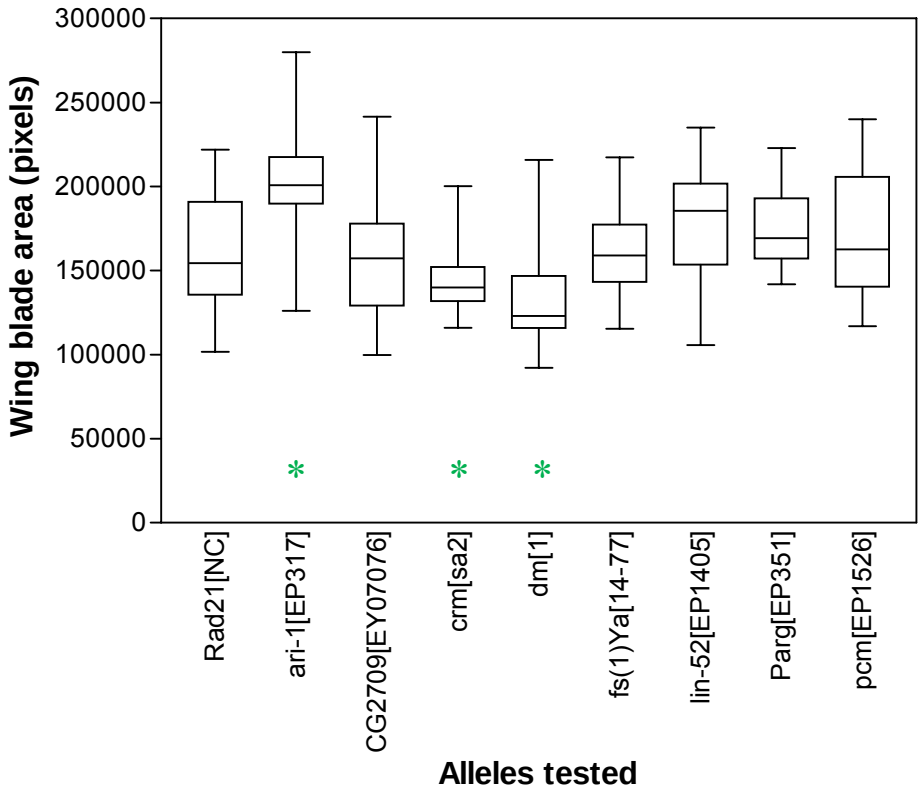

Figure 5.2: Wing analysis for chromosome I alleles. Modifier alleles of the vgMQ-*Rad21*^{NC} wing phenotype: *ari-1*^{EP317}/vgMQ>*Rad21*^{NC} (p=0.000) wings were significantly larger, while the *crm*^{sa2}/vgMQ>*Rad21*^{NC} (p=0.003) and *dm*^{1}/vgMQ>*Rad21*^{NC} (p=0.012) wings were signficantly smaller compared to the *vgMQ>Rad21*^{NC} stock control (Rad21[NC]) wings (*). The *fs(1)Ya*$^{14-77}$/ vgMQ>*Rad21*^{NC} and *Parg*^{EP351}/vgMQ>*Rad21*^{NC} wings were not significantly different from controls.

5.2.1.2 Chromosome II modifier alleles

A total of 29 of the 48 chromosome II modifier alleles were tested in the vgMQ>*Rad21*^{NC} wing assay. Of these alleles, 23 were found to significantly modify the wing size compared to either sibling controls or stock controls or both (Figures 5.3-5.8, Tables 5.3-5.4).

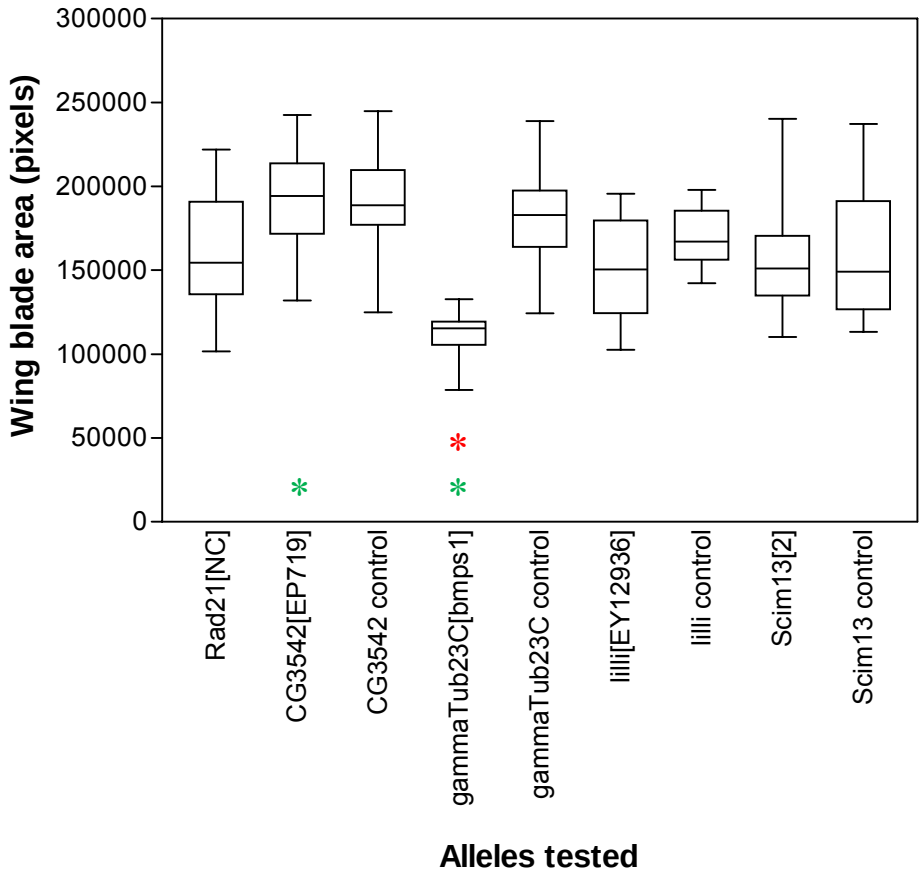

Figure 5.3: Wing analysis for chromosome II alleles, cytological regions 20-25. Modifier alleles of the vgMQ>*Rad21*^{NC} wing phenotype: vgMQ>*Rad21*^{NC}/+; *γ-Tub23C*^{bmps1}/+ (p=0.000) wings were significantly smaller than vgMQ>*Rad21*^{NC}/+ sibling control wings (*). The vgMQ>*Rad21*^{NC}/+; *CG3542*^{EP719}/+ (p=0.007) wings were significantly larger and vgMQ>*Rad21*^{NC}/+; *γ-Tub23C*^{bmps1}/+ (p=0.000) wings were significantly smaller than vgMQ>*Rad21*^{NC}/+ stock control (Rad21[NC]) wings (*). The vgMQ>*Rad21*^{NC}/+; *lilli*^{EY12936}/+ and vgMQ>*Rad21*^{NC}/+; *Scim13*^{2}/+ wings were not significantly different from either control.

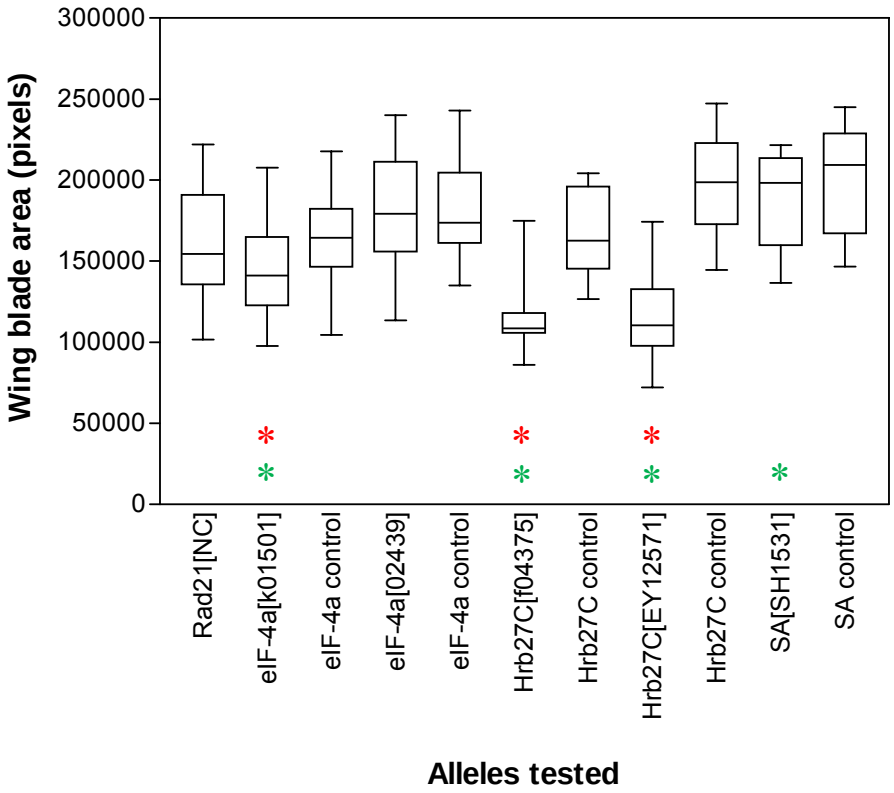

Figure 5.4: Wing analysis for chromosome II alleles, cytological regions 26-27. Modifier alleles of the vgMQ>*Rad21*^{NC} wing phenotype: vgMQ>*Rad21*^{NC}/+; *eIF-4a*^{k01501}/+ (p=0.020), vgMQ>*Rad21*^{NC}/+; *Hrb27C*^{f04375}/+ (p=0.000) and vgMQ>Rad21^{NC}/+; *Hrb27C*^{EY12571}/+ (p=0.000) wings were significantly smaller than vgMQ>Rad21^{NC}/+ sibling control wings (*). The vgMQ>*Rad21*^{NC}/+; *eIF-4a*^{k01501}/+ (p=0.020), vgMQ>Rad21^{NC}/+; *Hrb27C*^{f04375}/+ (p=0.000) and vgMQ>*Rad21*^{NC}/+; *Hrb27C*^{EY12571}/+ (p=0.000) wings were significantly smaller and the vgMQ>*Rad21*^{NC}/+; *SA*^{SH1531}/+ wings significantly larger than vgMQ>Rad21^{NC}/+ stock control (Rad21[NC]) wings (*). The vgMQ>*Rad21*^{NC}/+; *eIF-4a*^{02439}/+ wings were not significantly different from either control.

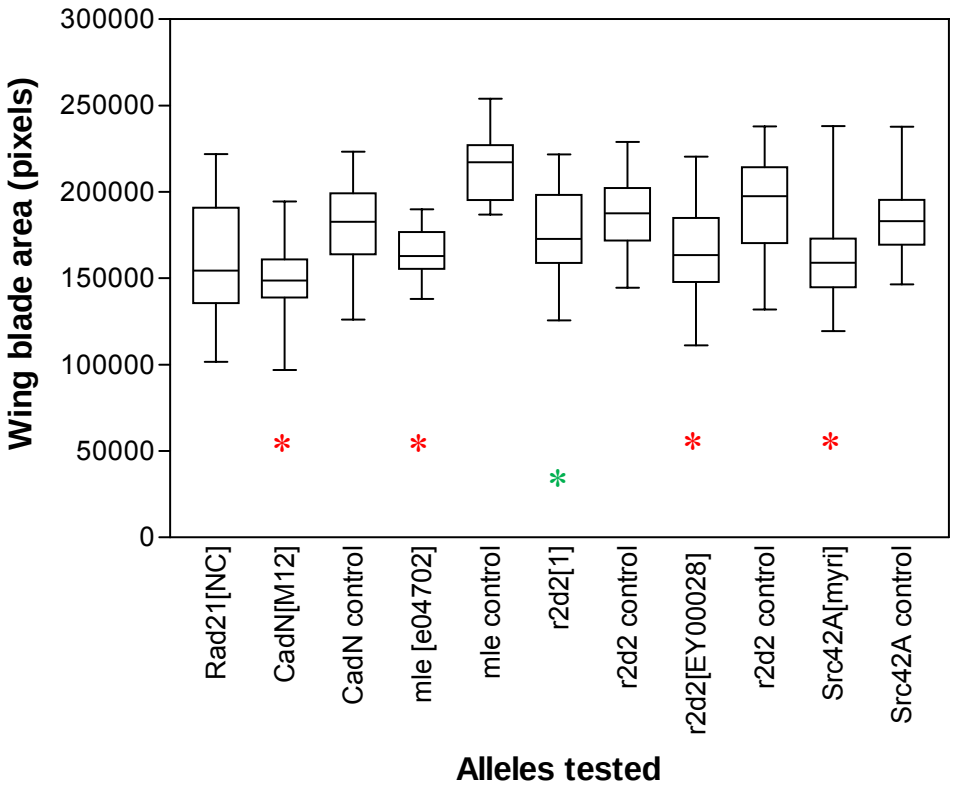

Figure 5.5: Wing analysis for chromosome II alleles, cytological regions 28-44. Modifier alleles of the vgMQ>*Rad21*^{NC} wing phenotype: vgMQ>*Rad21*^{NC}/+; *CadN*^{M12}/+ (p=0.000), vgMQ>*Rad21*^{NC}/+; *mle*^{e304702}/+ (p=0.000), vgMQ>*Rad21*^{NC}/+; *r2d2*^{EY00028}/+ (p=0.002) and vgMQ>*Rad21*^{NC}/+; *Src42A*^{myri}/+ (p=0.000) wings were significantly smaller than vgMQ>*Rad21*^{NC}/+ sibling control wings (*). The vgMQ>*Rad21*^{NC}/+; *r2d2*^{1}/+ (p=0.043) wings were significantly larger than vgMQ>*Rad21*^{NC}/+ stock control (Rad21[NC]) wings (*).

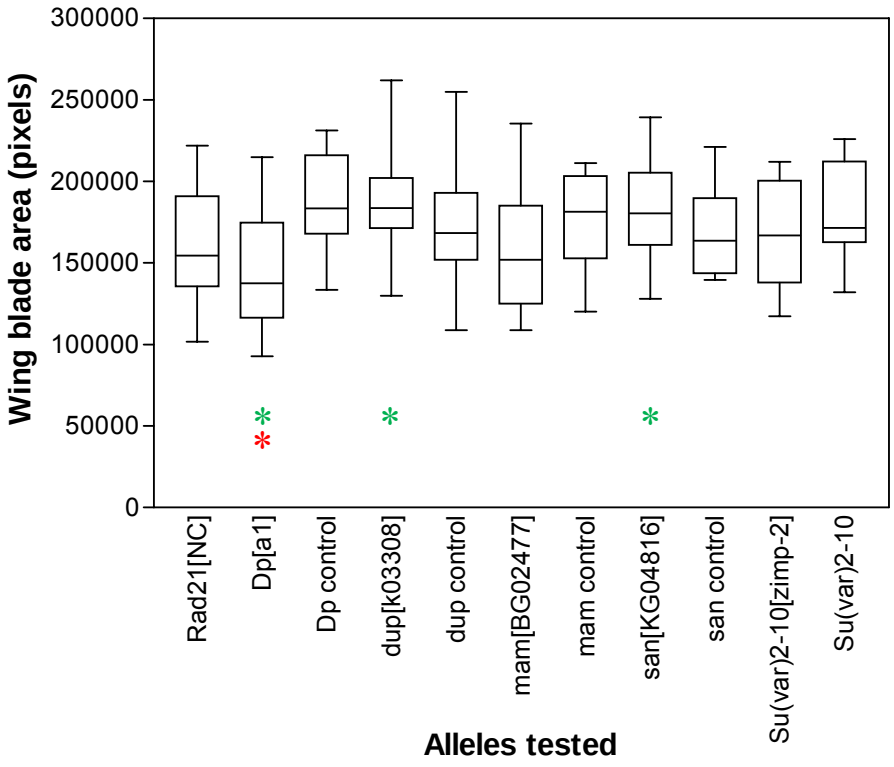

Figure 5.6: Wing analysis for chromosome II alleles, cytological regions 45-51. Modifier allele of the vgMQ>*Rad21*^{NC} wing phenotype: vgMQ>*Rad21*^{NC}/+; *Dp*^{a1}/+ (p=0.000) wings were significantly smaller than vgMQ>*Rad21*^{NC}/+ sibling control wings (*). The vgMQ>*Rad21*^{NC}/+; *Dp*^{a1}/+ (p=0.034) wings were significantly smaller and the vgMQ>*Rad21*^{NC}/+; *dup*^{k03308}/+ (p=0.005) and vgMQ>*Rad21*^{NC}/+; *san*^{KG04816}/+ (p=0.002) wings significantly larger than vgMQ>*Rad21*^{NC}/+ stock control (Rad21[NC]) wings (*). The vgMQ>*Rad21*^{NC}/+; *mam*^{BG02477}/+ and vgMQ>*Rad21*^{NC}/+; *Su(var)2-10*$^{zimp-2}$/+ wings were not significantly different from either control.

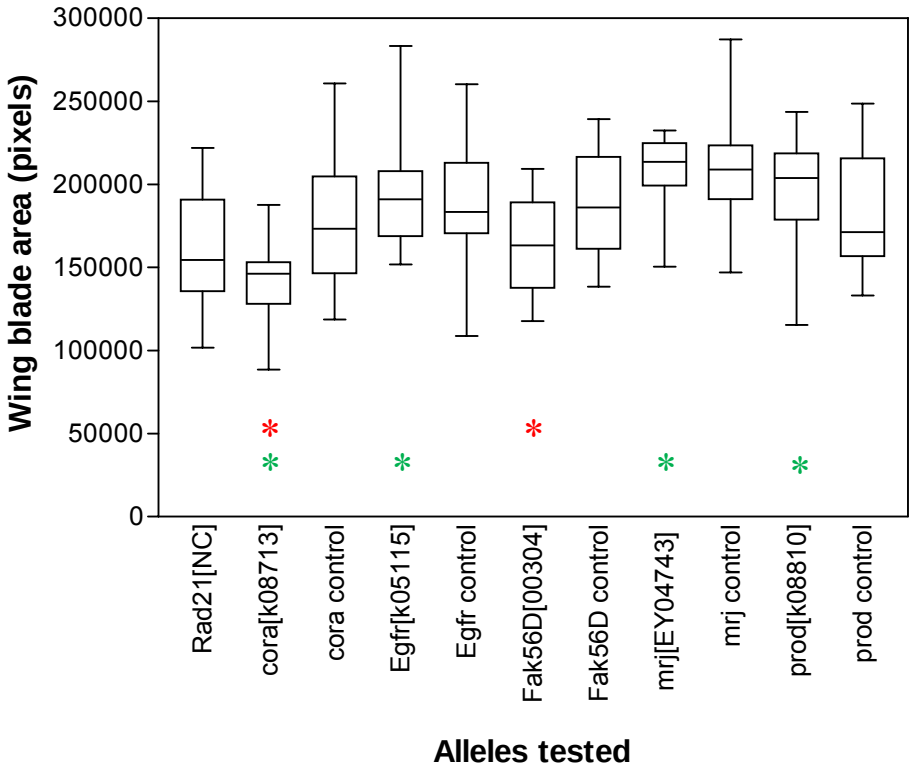

Figure 5.7: Wing analysis for chromosome II alleles, cytological regions 52-60. Modifier alleles of the vgMQ>*Rad21*^{NC} wing phenotype: vgMQ>*Rad21*^{NC}/+; *cora*^{k08713}/+ (p=0.000) and vgMQ>*Rad21*^{NC}/+; *Fak56D*^{00304}/+ (p=0.013) wings were significantly smaller than vgMQ>*Rad21*^{NC}/+ sibling control wings (*). The vgMQ>*Rad21*^{NC}/+; *cora*^{k08713}/+ (p=0.001) wings were significantly smaller and the vgMQ>*Rad21*^{NC}/+; *Egfr*^{k05115}/+ (p=0.001), vgMQ>*Rad21*^{NC}/+; *mrj*^{EY04743}/+ (p=0.000) and vgMQ>*Rad21*^{NC}/+; *prod*^{k08810}/+ (p=0.000) wings significantly larger than vgMQ>*Rad21*^{NC}/+ stock control (Rad21[NC]) wings (*).

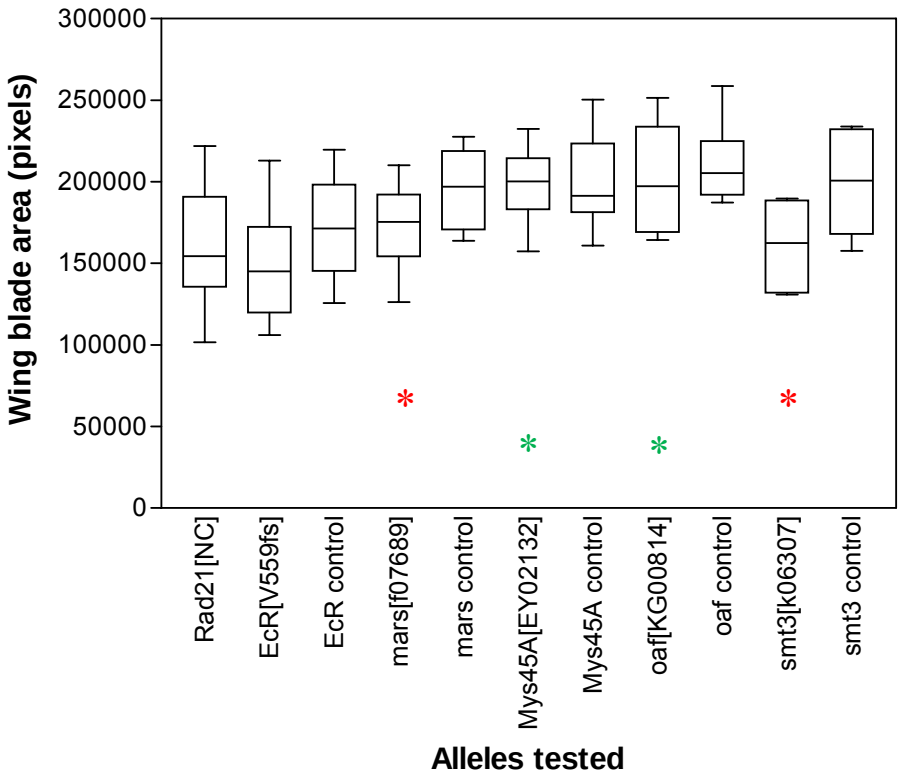

Figure 5.8: Wing analysis for alleles with power less than 80%. Modifier alleles of the vgMQ>*Rad21*^{NC} wing phenotype: vgMQ>*Rad21*^{NC}/+; *mars*^{f07689}/+ (p=0.019) and vgMQ>*Rad21*^{NC}/+; *smt3*^{k06307}/+ (p=0.033) wings were significantly smaller than vgMQ>*Rad21*^{NC}/+ sibling control wings (*). The vgMQ>*Rad21*^{NC}/+; *Mys45A*^{EY02132}/+ (p=0.000) and vgMQ>*Rad21*^{NC}/+; *oaf*^{KG00814}/+ (p=0.001) wings significantly larger than vgMQ>*Rad21*^{NC}/+ stock control (Rad21[NC]) wings (*). The vgMQ>*Rad21*^{NC}/+; *EcR*^{V559fs}/+ wings were not significantly different from either control. Assay power ranged from 50-70% power due to low test group and/or sibling control numbers.

5.2.1.3 Chromosome III modifier alleles

A total of 72 of the 86 chromosome III modifier alleles were tested in the vgMQ>*Rad21*^{NC} wing assay. Of these alleles, 58 were found to significantly modify the wing size compared to vgMQ>*Rad21*^{NC} sibling or stock controls or both (Figures 5.9-5.21, Tables 5.5.-5.9).

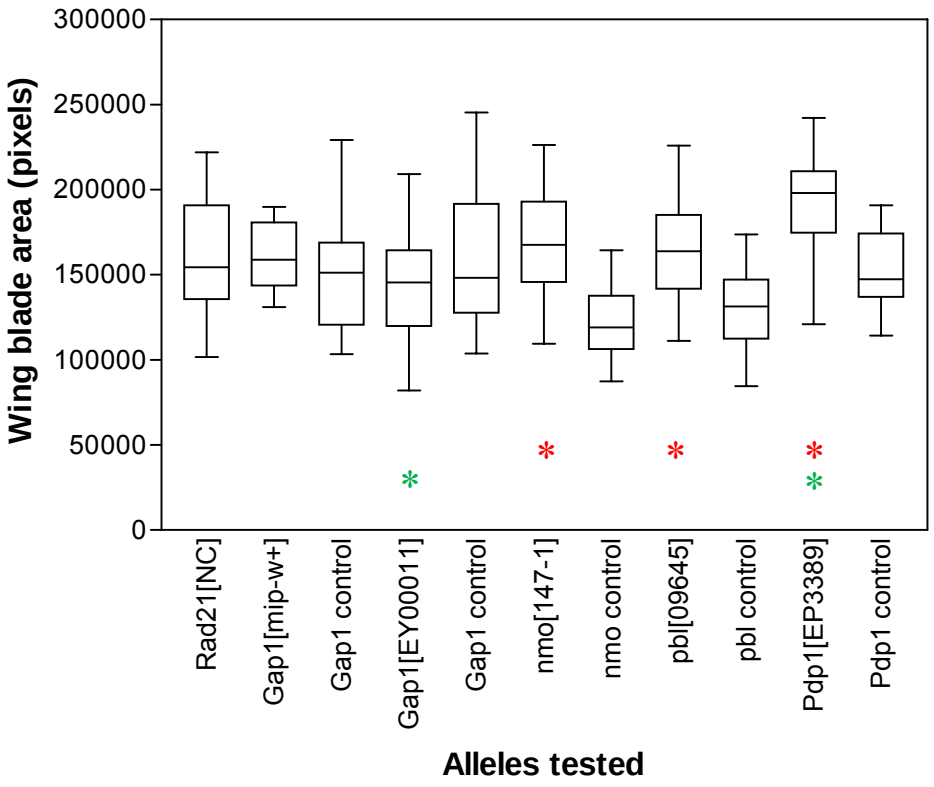

Figure 5.9: Wing analysis for chromosome III alleles, cytological regions 61-67C. Modifier alleles of the vgMQ>*Rad21*^{NC} wing phenotype: vgMQ>*Rad21*^{NC}/+; +/+; *nmo*$^{147-1}$/+ (p= 0.000), vgMQ>*Rad21*^{NC}/+; +/+; *pbl*^{09645}/+ (p= 0.000) and vgMQ>*Rad21*^{NC}/+; +/+; *Pdp1*^{EP3389}/+ (p=0.000) wings were significantly larger than vgMQ>*Rad21*^{NC}/+; +/+ sibling control wings (*). The vgMQ>*Rad21*^{NC}/+; +/+; *Gap1*^{EY00011}/+ (p=0.017) wings were significantly smaller and the vgMQ>*Rad21*^{NC}/+; +/+; *Pdp1*^{EP3389}/+ (p=0.000) wings significantly larger than vgMQ>*Rad21*^{NC}/FM7i stock control (Rad21[NC]) wings (*). The vgMQ>*Rad21*^{NC}/+; +/+; *Gap1*$^{mip\text{-}w+}$/+ wings were not significantly different from either control.

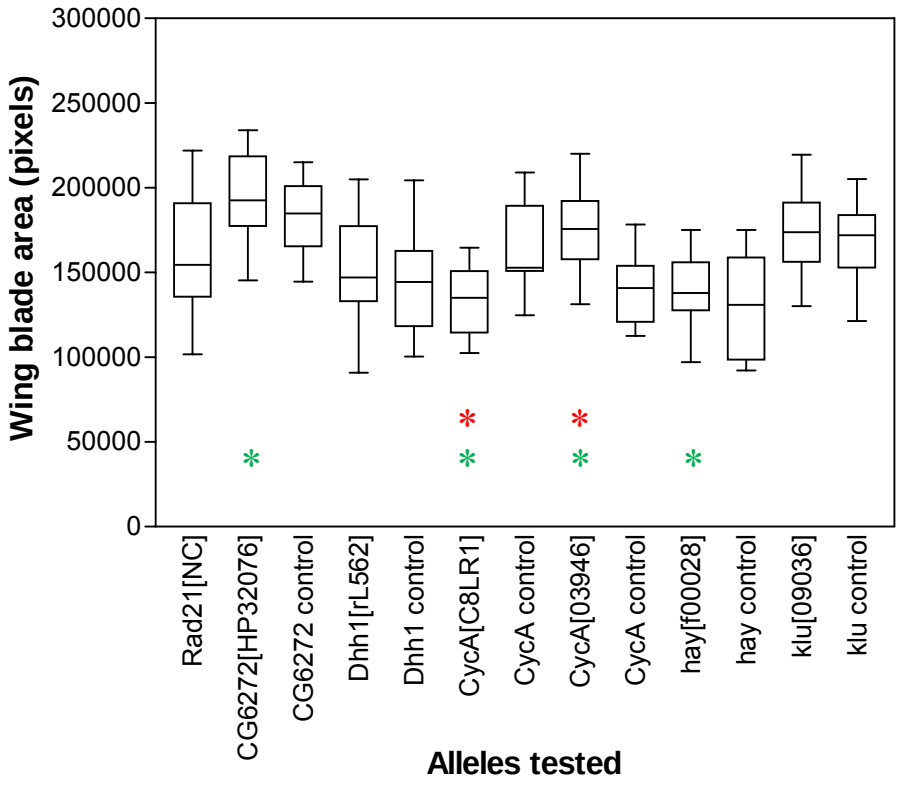

Figure 5.10: Wing analysis for chromosome III alleles, cytological regions 67D-68. Modifier alleles of the vgMQ>*Rad21*^{NC} wing phenotype: vgMQ>*Rad21*^{NC}/+; +/+; *CycA*^{C8LR1}/+ (p=0.000) wings were significantly smaller and vgMQ>*Rad21*^{NC}/+; *CycA*^{03946}/+ (p=0.000) were significantly larger than vgMQ>*Rad21*^{NC}/+ sibling control wings (*). The vgMQ>*Rad21*^{NC}/+; +/+; *CycA*^{C8LR1}/+ (p=0.000) and vgMQ>*Rad21*^{NC}/+; +/+; *hay*^{f00028}/+ (p=0.001) wings were significantly smaller and the vgMQ>*Rad21*^{NC}/+; +/+; *CG6272*^{HP32076}/+ (p=0.000) and vgMQ>*Rad21*^{NC}/+; +/+; *CycA*^{03946}/+ (p=0.042) wings significantly larger than vgMQ>*Rad21*^{NC}/FM7i stock control (Rad21[NC]) wings (*). The vgMQ>*Rad21*^{NC}/+; +/+; *Dhh1*^{rL562}/+ and vgMQ>*Rad21*^{NC}/+; +/+; *klu*^{09036}/+wings were not significantly different from either control.

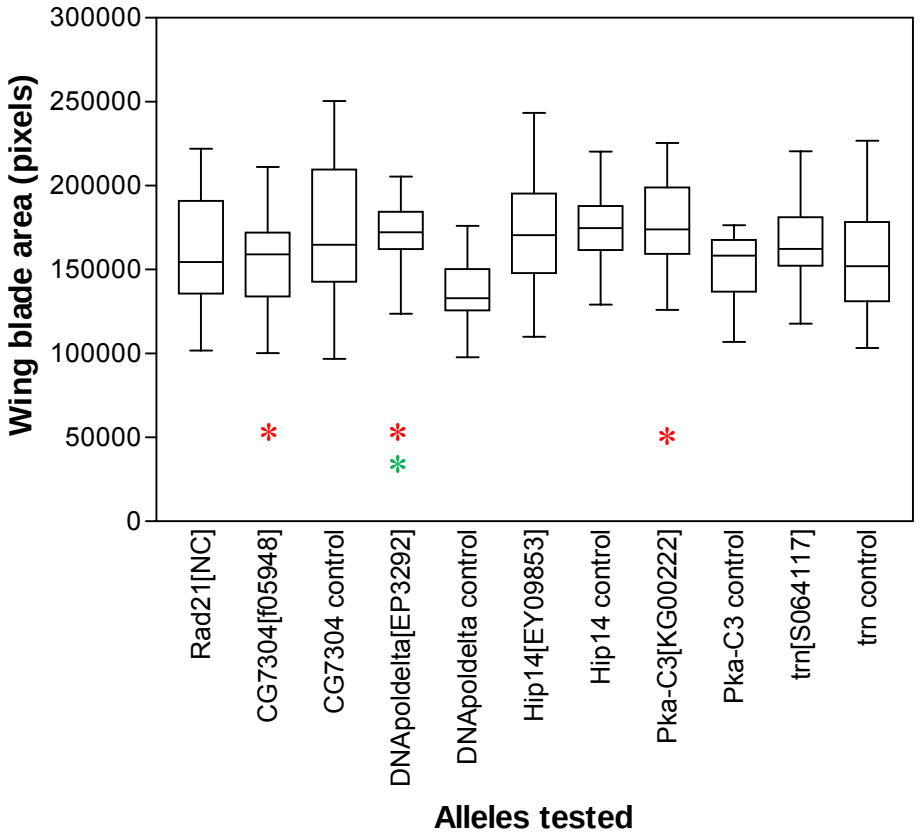

Figure 5.11: Wing analysis for chromosome III alleles, cytological regions 69-72C. Modifier alleles of the vgMQ>*Rad21*^{NC} wing phenotype: vgMQ>*Rad21*^{NC}/+; +/+; *CG7304*^{f05948}/+ (p=0.029) wings were significantly smaller and vgMQ>*Rad21*^{NC}/+; +/+; *DNApol-Δ*^{EP3292}/+ (p=0.000), vgMQ>*Rad21*^{NC}/+; +/+; *Pka-C3*^{KG00222}/+ (p=0.004) wings were significantly larger than vgMQ>*Rad21*^{NC}/+ sibling control wings (*). The vgMQ>*Rad21*^{NC}/+; +/+; *DNApol-Δ*^{EP3292}/+ (p=0.048) wings were significantly larger than vgMQ>*Rad21*^{NC}/FM7i stock control (Rad21[NC]) wings (*). The vgMQ>*Rad21*^{NC}/+; +/+; *Hip14*^{EY09853}/+ and vgMQ>*Rad21*^{NC}/+; +/+; *trn*^{S064117}/+ wings were not significantly different from either control.

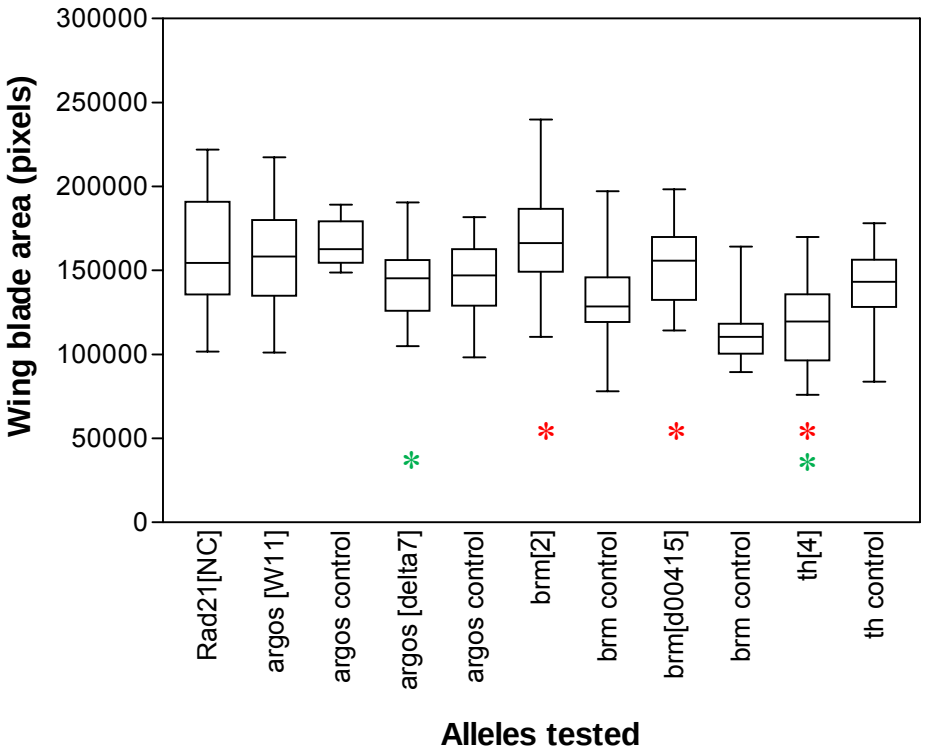

Figure 5.12: Wing analysis for chromosome III alleles, cytological regions 72C-73. Modifier alleles of the vgMQ>*Rad21*^{NC} wing phenotype: vgMQ>*Rad21*^{NC}/+; +/+; *brm*^{d00415}/+ (p=0.000) and vgMQ>*Rad21*^{NC}/+; +/+; *brm*^{2}/+ (p=0.000) and wings were significantly larger and vgMQ>*Rad21*^{NC}/+; +/+; *th*^{4}/+ (p=0.000) wings were significantly smaller than vgMQ>*Rad21*^{NC}/+ sibling control wings (*). The vgMQ>*Rad21*^{NC}/+; +/+; *argos*^{delta7}/+ (p=0.014) and vgMQ>*Rad21*^{NC}/+; +/+; *th*^{4}/+ (p=0.000) wings were significantly smaller than vgMQ>*Rad21*^{NC}/FM7i stock control (Rad21[NC]) wings (*). The vgMQ>*Rad21*^{NC}/+; +/+; *argo*^{W11}/+ wings were not significantly different from either control.

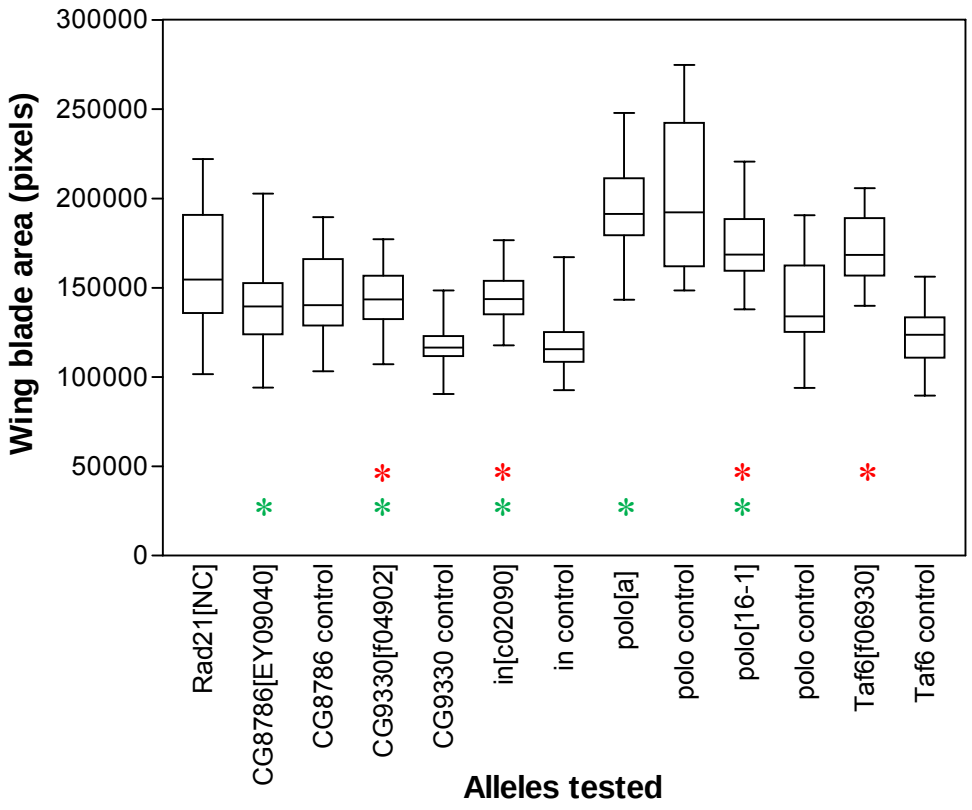

Figure 5.13: Wing analysis for chromosome III alleles, cytological regions 76-77B. Modifier alleles of the vgMQ>*Rad21*^{NC} wing phenotype: vgMQ>*Rad21*^{NC}/+; +/+; *CG9330*^{f04902}/+, vgMQ>*Rad21*^{NC}/+; +/+; *in*^{c02090}/+, vgMQ>*Rad21*^{NC}/+; +/+; *polo*$^{16\text{-}1}$/+ and vgMQ>*Rad21*^{NC}/+; +/+; *Taf6*^{f06930}/+ (p=0.000) wings were significantly larger than vgMQ>*Rad21*^{NC}/+ sibling control wings (*). The vgMQ>*Rad21*^{NC}/+; +/+; *CG8786*^{EY09040}/+ (p=0.002) wings were significantly smaller and the vgMQ>*Rad21*^{NC}/+; +/+; *CG9330*^{f04902}/+ (p=0.004), vgMQ>*Rad21*^{NC}/+; +/+; *in*^{c02090}/+ (p=0.005), vgMQ>*Rad21*^{NC}/+; +/+; *polo*^{a}/+ (p=0.000) and vgMQ>*Rad21*^{NC}/+; +/+; *polo*$^{16\text{-}1}$/+ (p=0.035) wings were significantly larger than vgMQ>*Rad21*^{NC} stock control (Rad21[NC]) wings (*).

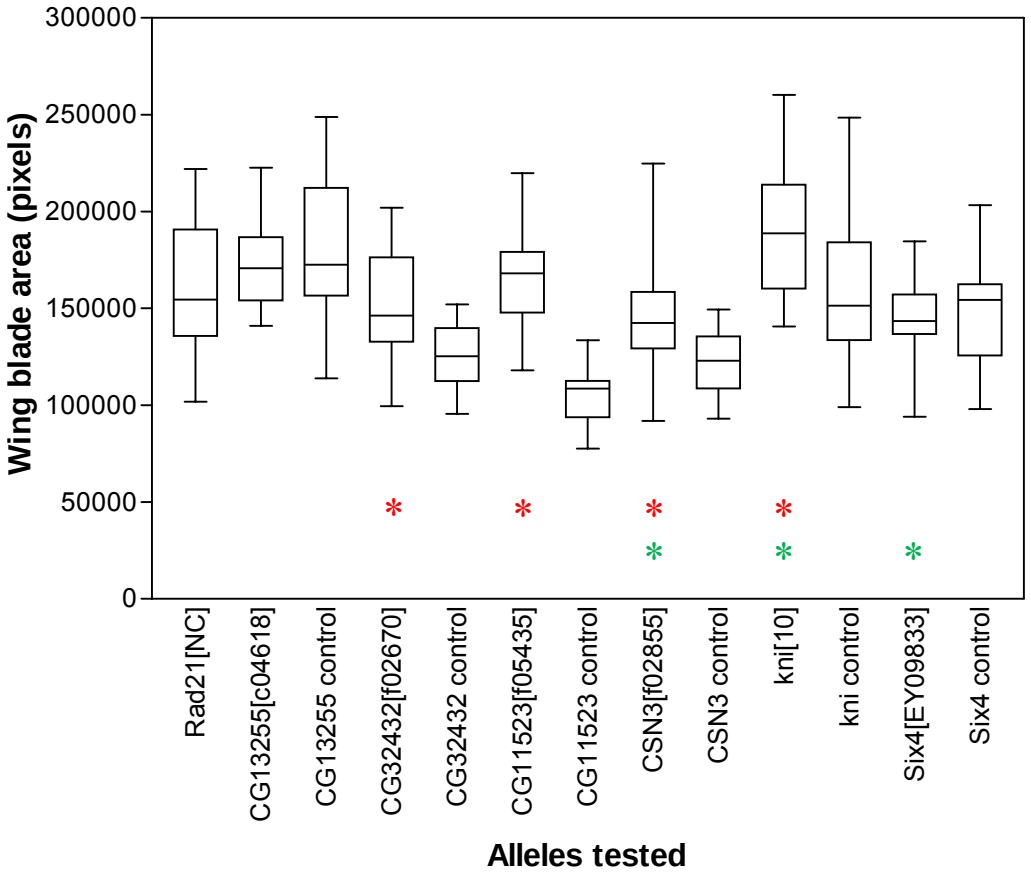

Figure 5.14: Wing analysis for chromosome III alleles, cytological regions 77E-78. Modifier alleles of the vgMQ>*Rad21*^{NC} wing phenotype: vgMQ>*Rad21*^{NC}/+; +/+; *CG32432*^{f02670}/+ (p=0.001), vgMQ>*Rad21*^{NC}/+; +/+; *CG11523*^{f05435}/+ (p=0.000), vgMQ>*Rad21*^{NC}/+; +/+; *CSN3*^{f02855}/+ (p=0.000) and vgMQ>*Rad21*^{NC}/+; +/+; *kni*^{10}/+ (p=0.008) wings were significantly larger than vgMQ>*Rad21*^{NC}/+ sibling control wings (*). The vgMQ>*Rad21*^{NC}/+; +/+; *CSN3*^{f02855}/+ (p=0.013) and vgMQ>*Rad21*^{NC}/+; +/+; *Six4*^{EY09833}/+ (p=0.020) wings were significantly smaller and the vgMQ>*Rad21*^{NC}/+; +/+; *kni*^{10}/+ (p=0.004) wings were significantly larger than vgMQ>*Rad21*^{NC}/FM7i stock control (Rad21[NC]) wings (*). The vgMQ>*Rad21*^{NC}/+; +/+; *CG13255*^{c04618}/+ wings were not significantly different from either control.

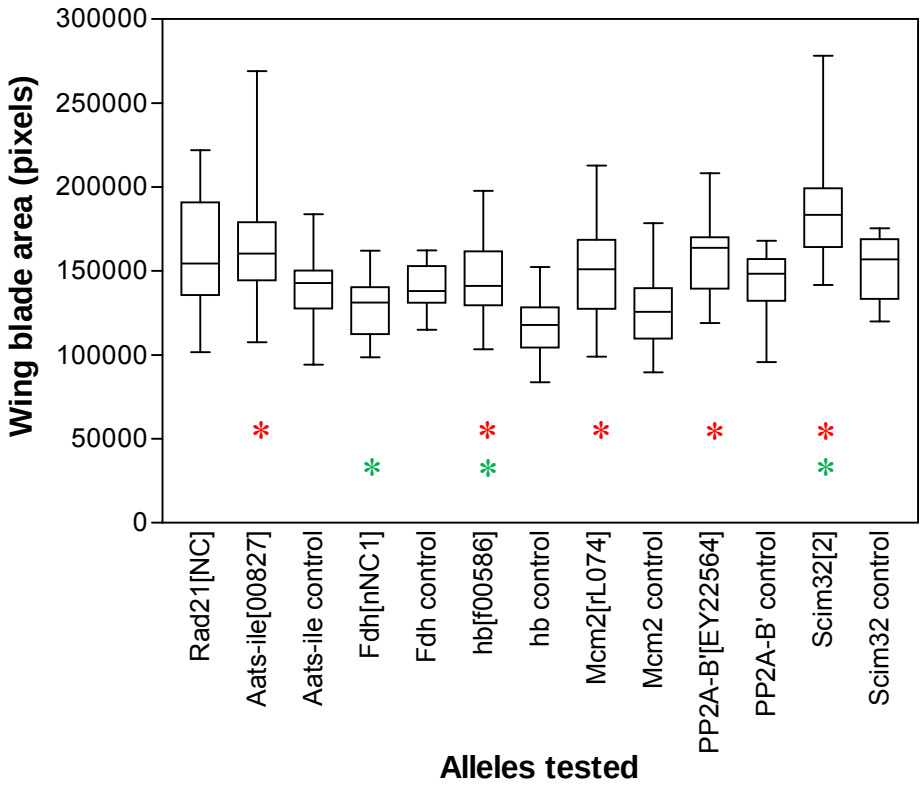

Figure 5.15: Wing analysis for chromosome III alleles, cytological regions 79-90F6. Modifier alleles of the vgMQ>*Rad21*^{NC} wing phenotype: vgMQ>*Rad21*^{NC}/+; +/+; *Aats-ile*^{00827}/+ (p=0.001), vgMQ>*Rad21*^{NC}/+; +/+; *hb*^{f00586}/+ (p=0.000), vgMQ>*Rad21*^{NC}/+; +/+; *Mcm2*^{rL074}/+ (p=0.001), vgMQ>*Rad21*^{NC}/+; +/+; *PP2A-B'*^{EY22564}/+ (p=0.019) and vgMQ>*Rad21*^{NC}/+; +/+; *Scim32*^{2}/+ (p=0.001) wings were significantly larger than vgMQ>*Rad21*^{NC}/+ sibling control wings (*). The vgMQ>*Rad21*^{NC}/+; +/+; *Fdh*^{nNC1}/+ (p=0.000) and vgMQ>*Rad21*^{NC}/+; +/+; *hb*^{f00586}/+ (p=0.010) wings were significantly smaller and the vgMQ>*Rad21*^{NC}/+; +/+; *Scim32*^{2}/+ (p=0.001) wings were significantly larger than vgMQ>*Rad21*^{NC}/FM7i stock control (Rad21[NC]) wings (*).

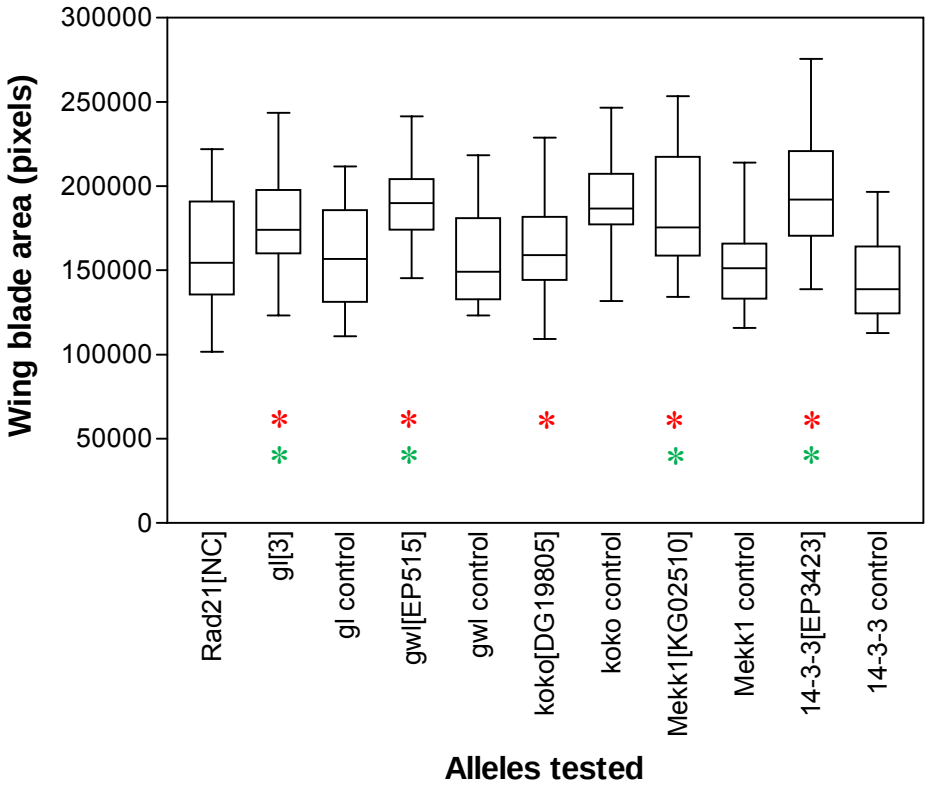

Figure 5.16: Wing analysis for chromosome III alleles, cytological regions 90F7-91. Modifier alleles of the vgMQ>*Rad21*^{NC} wing phenotype: vgMQ>*Rad21*^{NC}/+; +/+; *gl*^{3}/+ (p=0.001), vgMQ>*Rad21*^{NC}/+; +/+; *gwl*^{EP515}/+ (p=0.000), vgMQ>*Rad21*^{NC}/+; +/+; *Mekk1*^{KG02510}/+ (p=0.001) and vgMQ>*Rad21*^{NC}/+; +/+; *14-3-3ε*^{EP3423}/+ (p=0.000) wings were significantly larger and vgMQ>*Rad21*^{NC}/+; +/+; *koko*^{DG19805}/+ (p=0.000) wings were significantly smaller than vgMQ>*Rad21*^{NC}/+ sibling control wings (*). The vgMQ>*Rad21*^{NC}/+; +/+; *gl*^{3}/+ (p=0.045), vgMQ>*Rad21*^{NC}/+; +/+; *gwl*^{EP515}/+ (p=0.000), vgMQ>*Rad21*^{NC}/+; +/+; *Mekk1*^{KG02510}/+ (p=0.001) and vgMQ>*Rad21*^{NC}/+; +/+; *14-3-3ε*^{EP3423}/+ (p=0.000) wings were significantly larger than vgMQ>*Rad21*^{NC} stock control (Rad21[NC]) wings (*).

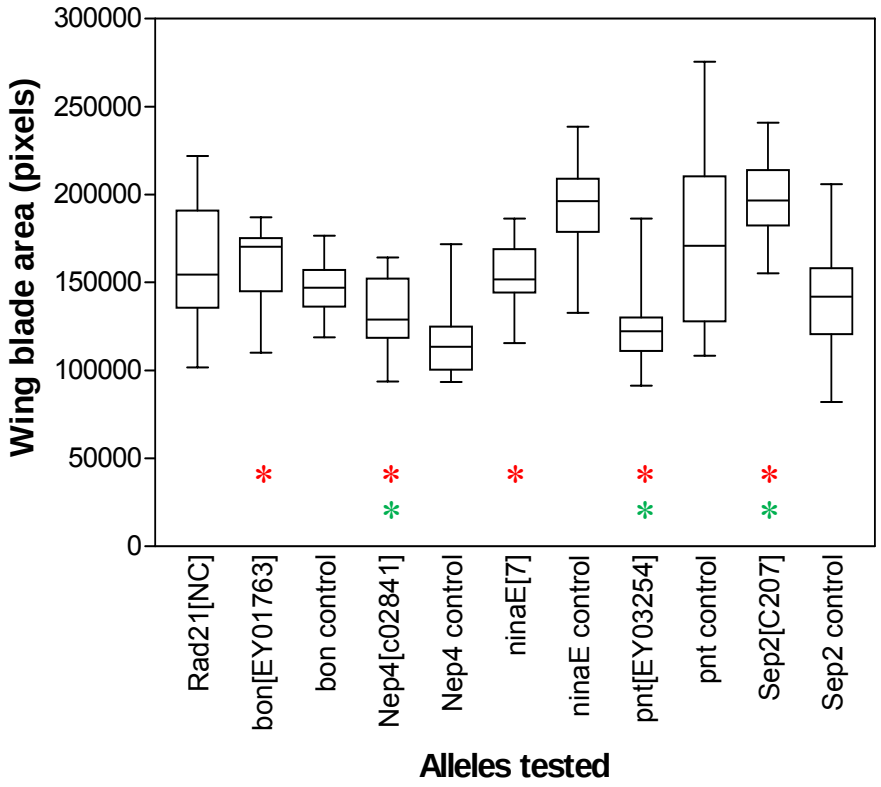

Figure 5.17: Wing analysis for chromosome III alleles, cytological region 92-94. Modifier alleles of the vgMQ>*Rad21*^{NC} wing phenotype: the vgMQ>*Rad21*^{NC}/+; +/+; *bon*^{EY01763}/+ (p=0.037), vgMQ>*Rad21*^{NC}/+; +/+; *Nep4*^{c02841}/+ (p=0.032) and vgMQ>*Rad21*^{NC}/+; +/+; *Sep2*^{C207}/+ (p=0.000) wings were significantly larger, while the vgMQ>*Rad21*^{NC}/+; +/+; *ninaE*^{7}/+ (p=0.000) and vgMQ>*Rad21*^{NC}/+; +/+; *pnt*^{EY03254}/+ (p=0.000) wings were significantly smaller than vgMQ>*Rad21*^{NC}/+ sibling control wings (*). The vgMQ>*Rad21*^{NC}/+; +/+; *Nep4*^{c02841}/+ (p=0.000) and vgMQ>*Rad21*^{NC}/+; +/+; *pnt*^{EY03254}/+ (p=0.000) wings were significantly smaller and the vgMQ>*Rad21*^{NC}/+; +/+; *Sep2*^{C207}/+ (p=0.000) wings were significantly larger than vgMQ>*Rad21*^{NC}/FM7i stock control (Rad21[NC]) wings (*).

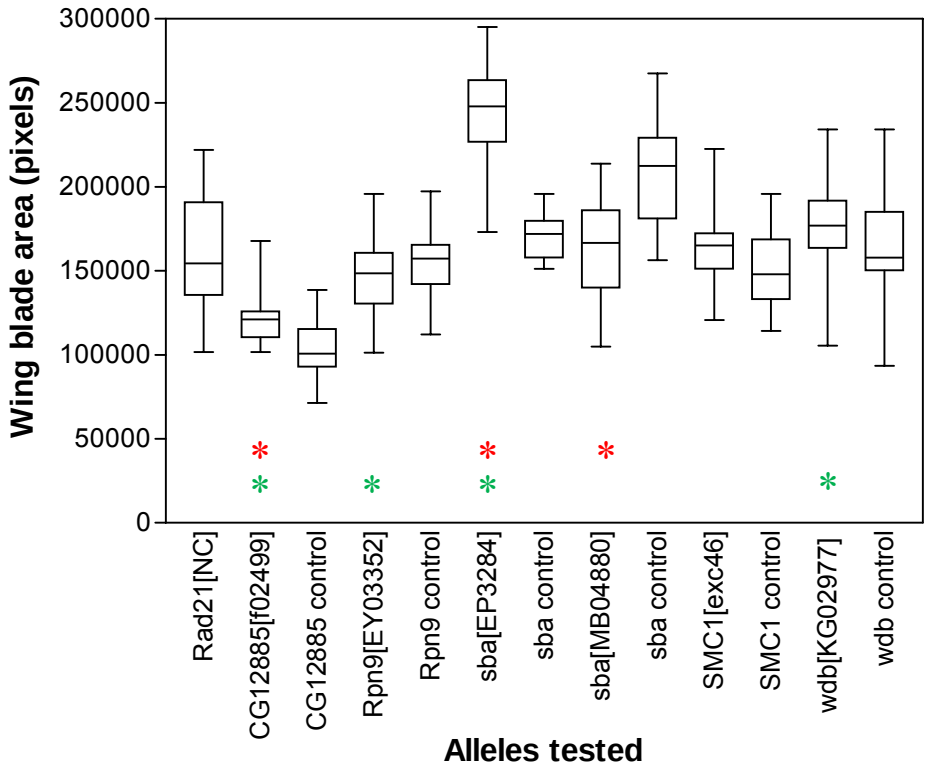

Figure 5.18: Wing analysis for chromosome III alleles, cytological regions 95-100. Modifier alleles of the vgMQ>*Rad21*^{NC} wing phenotype: vgMQ>*Rad21*^{NC}/+; +/+; *CG12885*^{f02499}/+ (p=0.003), vgMQ>*Rad21*^{NC}/+; +/+; *sba*^{EP3284}/+ (p=0.000) and vgMQ>*Rad21*^{NC}/+; +/+; *sba*^{MB04880}/+ (p=0.000) wings were significantly larger than vgMQ>*Rad21*^{NC}/+ sibling control wings (*). The vgMQ>*Rad21*^{NC}/+; +/+; *CG12885*^{f02499}/+ (p=0.000) and vgMQ>*Rad21*^{NC}/+; +/+; *Rpn9*^{EY03352}/+ (p=0.017) wings were significantly smaller and the vgMQ>*Rad21*^{NC}/+; +/+; *sba*^{EP3284}/+ (p=0.000) and vgMQ>*Rad21*^{NC}/+; +/+; *wdb*^{KG02977}/+ (p=0.025) wings were significantly larger than vgMQ>*Rad21*^{NC}/FM7i stock control (Rad21[NC]) wings (*). The vgMQ>*Rad21*^{NC}/+; +/+; *SMC1*^{exc46}/+ wings were not significantly different from either control.

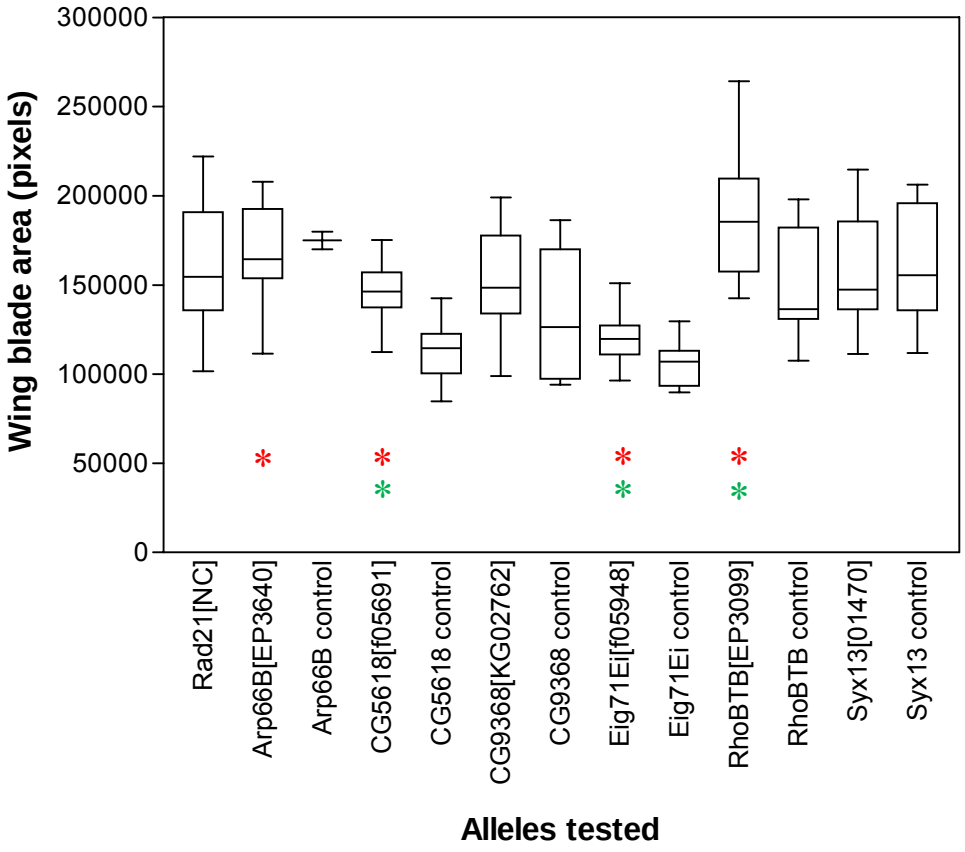

Figure 5.19: Wing analysis for chromosome III alleles, cytological regions 60-77B, with power less than 80%. Modifier alleles of the vgMQ>*Rad21*^{NC} wing phenotype: the vgMQ>*Rad21*^{NC}/+; +/+; *Arp66B*^{EP3640}/+ (p=0.001), vgMQ>*Rad21*^{NC}/+; +/+; *CG5618*^{f05961}/+ (p=0.000), vgMQ>*Rad21*^{NC}/+; +/+; *Eig71Ei*^{f04943}/+ (p=0.012) and vgMQ>*Rad21*^{NC}/+; +/+; *RhoBTB*^{EP3099}/+ (p=0.001) wings were significantly larger than vgMQ>*Rad21*^{NC}/+ sibling control wings (*). The vgMQ>*Rad21*^{NC}/+; +/+; *CG5618*^{f05961}/+ (p=0.012) and vgMQ>*Rad21*^{NC}/+; +/+; *Eig71Ei*^{f04943}/+ (p=0.000) wings were significantly smaller and the vgMQ>*Rad21*^{NC}/+; +/+; *RhoBTB*^{EP3099}/+ (p=0.003) wings were significantly larger than vgMQ>*Rad21*^{NC}/FM7i stock control (Rad21[NC]) wings (*). The vgMQ>*Rad21*^{NC}/+; +/+; *Syx13*^{01470}/+ wings were not significantly different from either control. Assay power ranged from 60-79% power due to low test group and/or sibling control numbers.

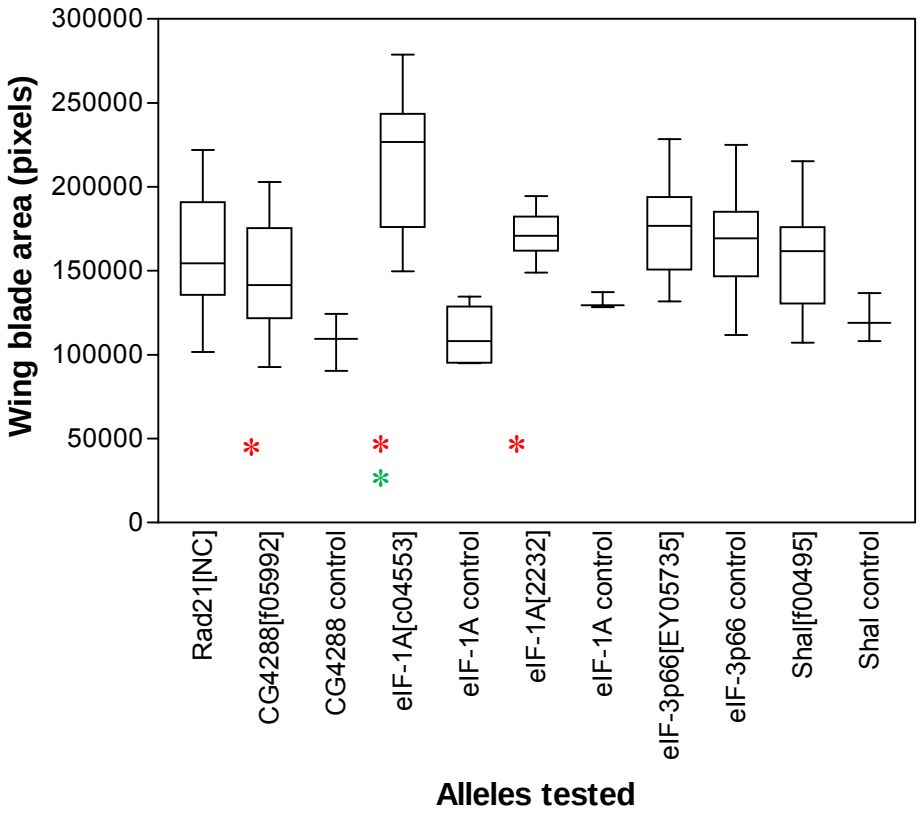

Figure 5.20: Wing analysis for chromosome III alleles, cytological regions 77E-100, with power less than 80%. Modifier alleles of the vgMQ>*Rad21*^{NC} wing phenotype: the vgMQ>*Rad21*^{NC}/+; +/+; *CG4288*^{f05992}/+ (p=0.032), vgMQ>*Rad21*^{NC}/+; +/+; *eIF-1A*^{c04533}/+ (p=0.000) and vgMQ>*Rad21*^{NC}/+; +/+; *eIF-1A*^{2232}/+ (p=0.000) wings were significantly larger than vgMQ>*Rad21*^{NC}/+ sibling control wings (*). The vgMQ>*Rad21*^{NC}/+; +/+; *eIF-1A*^{c04533}/+ (p=0.000) wings were significantly larger than vgMQ>*Rad21*^{NC}/FM7i stock control (Rad21[NC]) wings (*). The vgMQ>*Rad21*^{NC}/+; +/+; *eIF-3p66*^{EY05735}/+ and vgMQ>*Rad21*^{NC}/+; +/+; *Shal*^{f00495}/+ wings were not significantly different from either control. Assay power ranged from 40-79% power due to low test group and/or sibling control numbers.

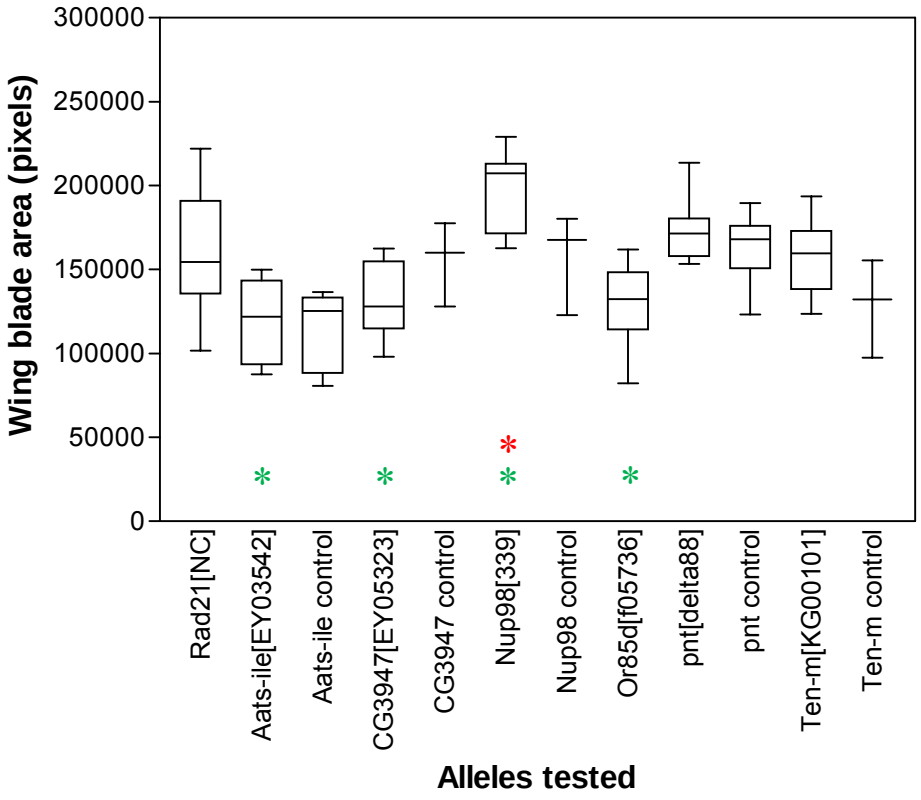

Figure 5.21: Wing analysis for chromosome III genes with insufficient numbers for strong analysis. Modifier alleles of the vgMQ>*Rad21*^{NC} wing phenotype: the vgMQ>*Rad21*^{NC}/+; +/+; *Nup98*^{339}/+ (p=0.008) wings were significantly larger than vgMQ>*Rad21*^{NC}/+ sibling control wings (*). The vgMQ>*Rad21*^{NC}/+; +/+; *Aats-ile*^{EY03542}/+ (p=0.001), vgMQ>*Rad21*^{NC}/+; +/+; *G3947*^{EY05323}/+ (p=0.002) and vgMQ>*Rad21*^{NC}/+; +/+; *Or85d*^{f05736}/+ (p=0.000) wings were significantly smaller and the vgMQ>*Rad21*^{NC}/+; +/+; *Nup98*^{339}/+ (p=0.002) wings were significantly larger than vgMQ>*Rad21*^{NC}/FM7i stock control (Rad21[NC]) wings (*). The vgMQ>*Rad21*^{NC}/+; +/+; *pnt*^{delta88}/+ wings were not significantly different from either control. Assay power ranged from 55-65% power due to low test group and/or sibling control numbers.

*5.2.2 The GMR*hid *apoptosis assay*

In the sensitised cellular climate of a proliferating, RAD21^{NC}-expressing cell, slight changes in regulators of apoptosis are likely to significantly modify rates of cell death. Genes that are able to promote cell survival in the presence of aneuploidy are very interesting candidates for this study; however, general regulators of apoptosis are of secondary interest as these are unlikely to be influencing chromosome segregation. In order to identify general regulators of apoptosis that are also able to modify an apoptosis-based phenotype in the absence of aneuploidy, the GMR*hid* small-eye phenotype was employed as an assay tool.

The GMR*hid* small-eye phenotype is produced through promotion of apoptosis, by induction of HID expression via the eye-specific GMR promoter. The product of the *hid* gene, head involution defective (HID) promotes apoptosis by inhibiting the anti-apoptotic activities of DIAP1 (Goyal *et al.*, 2000; Wang *et al.*, 1999), leading to activation of caspases and the apoptosis cascade. *Hid*, under the control of GMR, results in the apoptotic death of all photoreceptor cells in the ommatidia, thus producing a very small eye consisting of undifferentiated cuticle and a dense band of bristles (Grether *et al*., 1995).

The apoptotic activity of HID is directly regulated by the EGFR/Ras/MAPK pathway and therefore GMR*hid* has also been utilised by many researchers as a readout for regulators for the EGFR/Ras/MAPK pathway (Bergmann *et al*., 1998; Kurada and White, 1998). The EGFR/Ras/MAPK pathway is required for cell proliferation, cell growth, cell differentiation and cell death in a variety of tissues and species (Johnson and Vaillancourt, 1994; Bergmann *et al*., 1998; Freeman, 1998). Regulators of EGFR/Ras/MAPK signalling can influence multiple cellular functions depending on the cellular context. The initial GMR>*Rad21*^{NC} modifier screen indentified a significant number of EGFR/Ras/MAPK regulators and effectors, therefore the GMR*hid* phenotype was used as an assay tool to identify modifier loci that may be influencing the GMR>*Rad21*^{NC} rough-eye phenotype through modulation of the EGFR/Ras/MAPK pathway and HID-induced apoptosis.

Mutant alleles of individual modifier loci were crossed to the GMR*hid*, SM1/+ stock (Figure 5.22) and the eye phenotypes of test and control progeny visualised and compared via microscopic examination. Images of modified GMR*hid* small-eyes in various mutant backgrounds have been compiled according to the location of the loci by chromosome, chromosome arm and cytological region in Appendix 6. In total 112 alleles were tested for modification of the GMR*hid* small-eye phenotype, and of these 45 were found to significantly modify the size and/or organisation of the eye compared to sibling controls. Sixty-seven alleles were found not to modify the GMR*hid* phenotype when compared to sibling controls. These data allowed loci that modify the GMR>*Rad21*^{NC} eye phenotype independently of a direct effect on apoptosis to be identified.

*5.2.2.1 GMR*hid *modifier alleles*

A total of 2 of the 13 chromosome I modifier alleles were tested in the GMR*hid* assay and both of these alleles were found to suppress the size of the GMR*hid* eye (Table 5.2, Appendix 6). A total of 35 of the 48 chromosome II modifier alleles were tested in the GMR*hid* assay. Thirteen of these alleles were found to modify the eye phenotype: 11 alleles were found to suppress and 2 alleles enhance the GMR*hid* eye phenotype (Tables 5.3, 5.4 and 5.9, Appendix 6). A total of 68 of the 86 chromosome III modifier alleles were tested in the GMR*hid* assay. Of these alleles, 30 were found to modify the eye phenotype and all were found to suppress the GMR*hid* eye phenotype (Tables 5.5-5.9; Appendix 6).

In support of the GMR*hid* phenotype being a readout for the activity of the EGFR/Ras/MAPK pathway, alleles of *Fak56D, Gap1, klu* and *Mekk1*, which are known EGFR/Ras/MAPK pathway components and regulators, all suppressed the GMR*hid* eye phenotype (Figure 5.23). Alleles of other EGFR/Ras/MAPK genes, including *Egfr, trn, pnt* and *14-3-3-ε*, did not modify the GMR*hid* phenotype; however, this may be due to the nature of the protein or the specific alleles tested. None of the cohesin subunits (*SA, SMC1* and *SMC3*) or cohesin regulators (*san, PP2A-B', polo, gwl* and *Nup98*) modified the GMRhid phenotype (Tables 5.3-5.9).

(A)

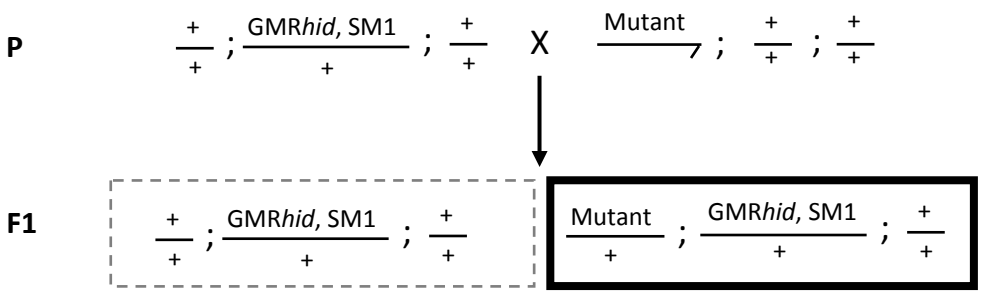
P
+/+ ; GMRhid, SM1/+ ; +/+
X
Mutant/+ ; +/+ ; +/+
F1
+/+ ; GMRhid, SM1/+ ; +/+
Mutant/+ ; GMRhid, SM1/+ ; +/+

(B)

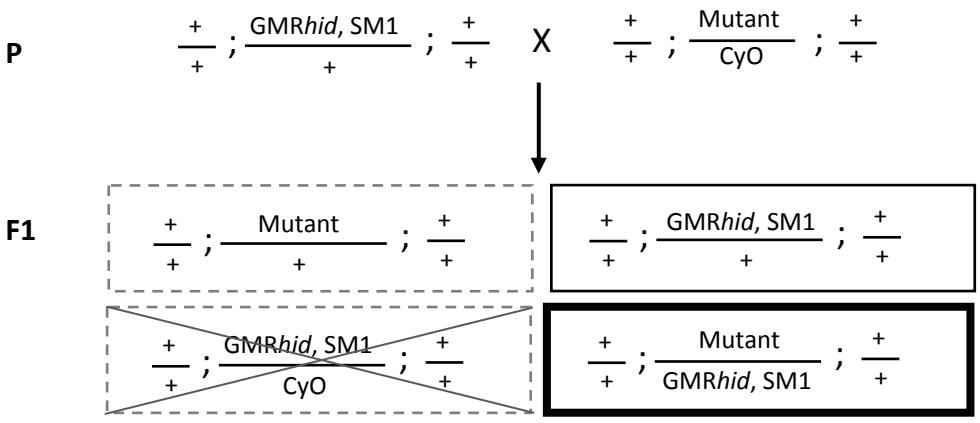
P
+/+ ; GMRhid, SM1/+ ; +/+
X
+/+ ; Mutant/CyO ; +/+
F1
+/+ ; Mutant/+ ; +/+
+/+ ; GMRhid, SM1/+ ; +/+
+/+ ; GMRhid, SM1/CyO ; +/+
+/+ ; Mutant/GMRhid, SM1 ; +/+

(C)

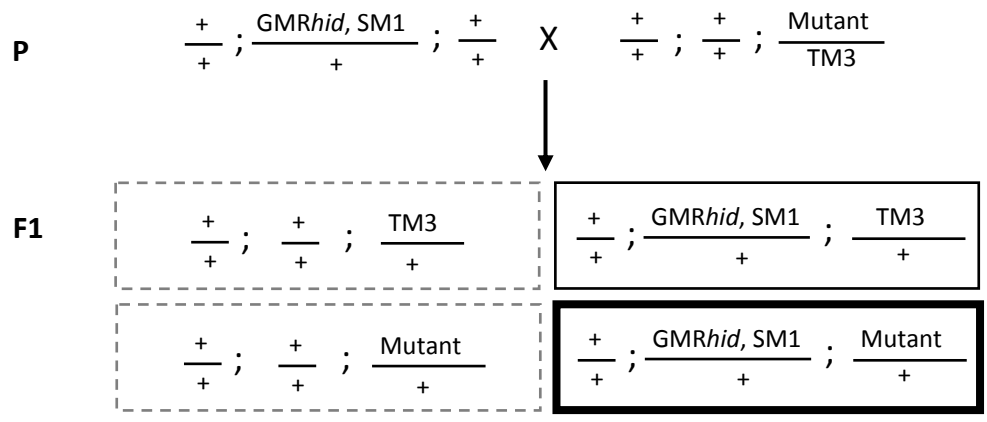
P
+/+ ; GMRhid, SM1/+ ; +/+
X
+/+ ; +/+ ; Mutant/TM3
F1
+/+ ; +/+ ; TM3/+
+/+ ; GMRhid, SM1/+ ; TM3/+
+/+ ; +/+ ; Mutant/+
+/+ ; GMRhid, SM1/+ ; Mutant/+

Figure 5.22: GMR*hid* assay crossing scheme. (A-C) Female flies from the +/+; GMR*hid*, SM1/+; +/+ stock were crossed to males with mutant alleles carried on the 1st (A), 2nd (B) or 3rd (C) chromosome and balanced over the Y chromosome or appropriate marked balancer chromosomes. From the F1 progeny the test class (bold black box) and control class (black box) siblings were selected for comparison to identify changes in the GMR*hid* eye phenotype in a heterozygous mutant background. Other sibling classes were discarded or were had non-viable genotypes.

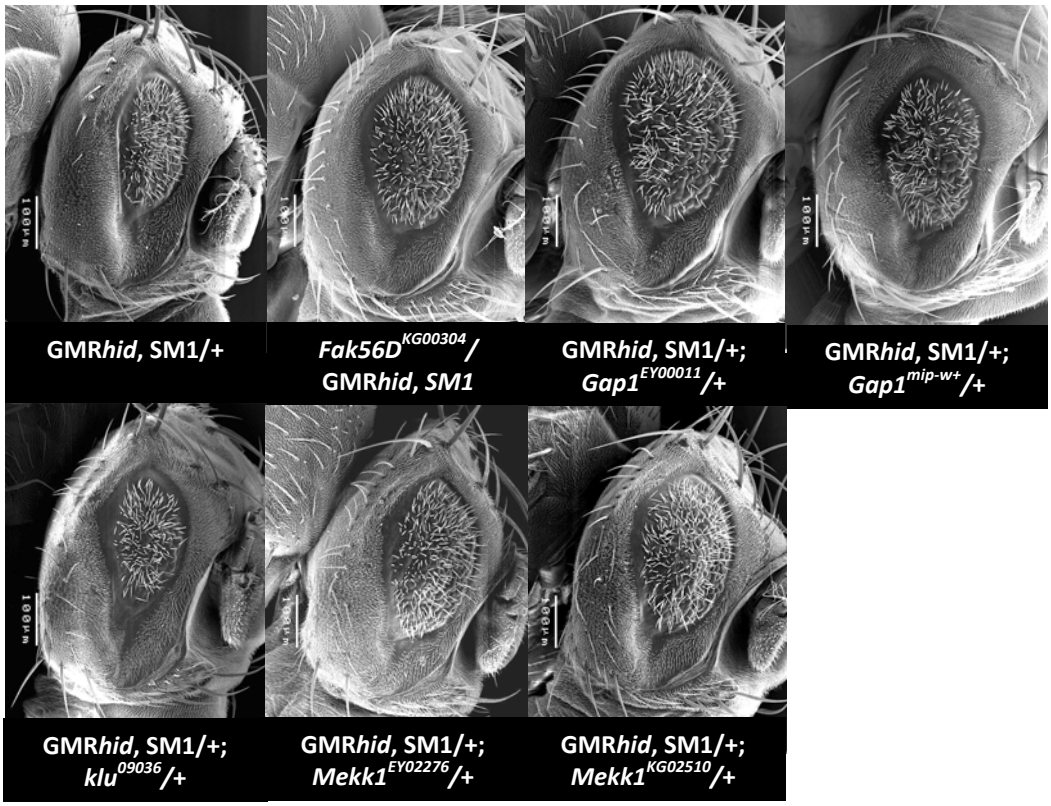

Figure 5.23: Modifier alleles of the GMR*hid* phenotype. Modifier alleles of the GMR*hid*/+ phenotype: *Fak56D*^{KG00304}/GMR*hid*, SM1, GMR*hid*, SM1/+; *Gap1*^{EY00011}/+, GMR*hid*, SM1/+; *Gap1*$^{mip\text{-}w+}$/+, GMR*hid*, SM1/+; *klu*^{09036}/+, GMR*hid*, SM1/+; *Mekk1*^{EY02276}/+ and GMR*hid*, SM1/+; *Mekk1*^{KG02510}/+ were observed to suppress the phenotype compared to GMR*hid,* SM1/+ controls.

5.2.3 GMR>Rad21^{NC}, p35 *assay*

When expressed in the *Drosophila* eye imaginal disc, the baculovirus p35 protein has been shown to inhibit all apoptosis that occurs either as a normal part of eye development or as a result of DNA damage following irradiation (Hay *et al.*, 1994). It was previously shown that introducing UAS-*p35* along with UAS-*Rad21^{NC}* resulted in inhibition of apoptosis induced by *Rad21^{NC}* expression as revealed by acridine orange staining (see Figure 3.9). Adult flies carrying GMR-Gal4, UAS-*p35* and UAS-*Rad21^{NC}* transgenes display only partial suppression of the GMR>*Rad21^{NC}* rough-eye phenotype, with introduction of a second copy of the UAS-*p35* transgene having very little additional effect (Figure 5.24). Thus, the introduction of p35 does not completely suppress the GMR>RAD21^{NC} eye phenotype, indicating that factors other than cell death contribute significantly to the GMR>RAD21^{NC} eye phenotype.

Two factors that are highly likely to be influencing the GMR>*Rad21^{NC}* eye phenotype are cell proliferation and cell differentiation. The fact that the anti-apoptotic protein p35 strongly suppresses the size defect of the GMR>*Rad21^{NC}* eye indicates that many cells expressing RAD21^{NC} die by apoptosis during eye development. However, the observation that p35 only partially inhibits the phenotype suggests that at least some of these cells are incapable of further cell division or growth, possibly due to mitotic catastrophe or because they have an unviable aneuploid karyotype. Additionally, cell and tissue differentiation are known to be influenced by the rate of cell cycle progression (Budirahardja and Gonczy, 2009). As this is altered in the GMR>*Rad21^{NC}* eye, via slowing of M-phase, suppression of apoptosis would be expected to have little effect on this aspect of the GMR>*Rad21^{NC}* eye phenotype.

As the cleavage-resistant RAD21 induces cell death as well as M phase delay (Section 3.2.6.3), it is hypothesised that genetic modifier loci that specifically counteract or antagonise these effects are more likely to directly influence chromosome segregation and are therefore of significant interest in this study. With p35 inhibiting all apoptosis in the eye-antennal imaginal disc it was therefore predicted that any interaction observed when GMR>UAST-*Rad21^{NC}*, UAS-*p35* was

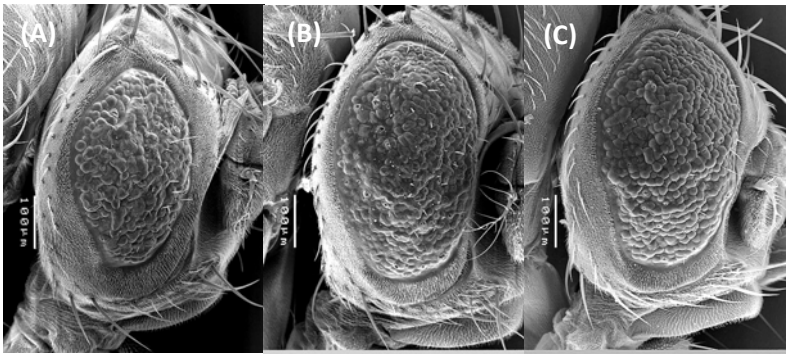

Figure 5.24: Suppression of apoptosis in the GMR>*Rad21^{NC}* eye. (A) The size defect of the GMR>UAST-*Rad21^{NC}*/+ rough-eye phenotype can be suppressed by (B) the co-expression of the anti-apoptotic protein p35 (GMR>UAST-*Rad21^{NC}*, UAS-*p35*/+). (C) The addition of a second copy of the *p35* transgene (GMR>UAST-*Rad21^{NC}*, UAS-*p35*/UAS-*p35*) has little further influence on size of the eye and only slightly suppresses the organisation defect.

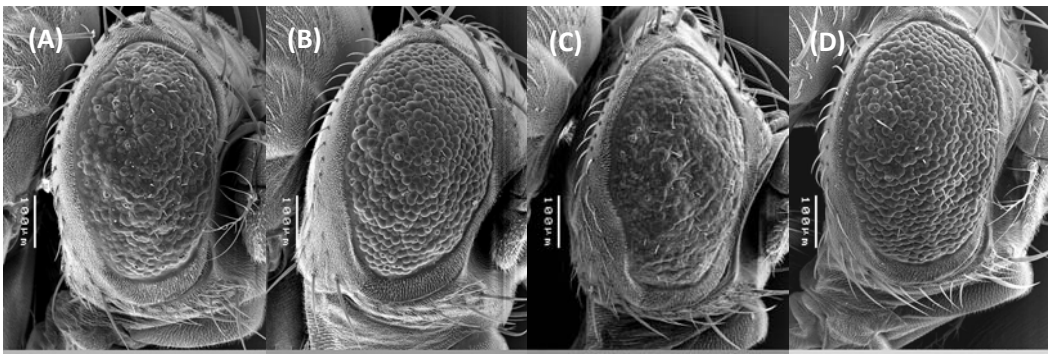

Figure 5.25: Modification of the GMR>*Rad21^{NC}*, *p35* eye phenotype by cell cycle and cell proliferation regulators. (A) The GMR>UAST-*Rad21^{NC}*, UAS-*p35* eye phenotype, showed suppression of organisation (B) when CDK1 was ectopically expressed (GMR>UAST-*Rad21^{NC}*, UAS-*p35*/UAS-*cdk1*) and enhancement of organisation (C) when CYCLIN B was ectopically expressed (GMR>UAST-*Rad21^{NC}*, UAS-*p35*/UAS-*cycB*). (D) When EGFR expression was reduced, suppression of both the size and organisation defects was observed (GMR>UAST-*Rad21^{NC}*, UAS-*p35*/*Egfr^{k05115}*).

crossed into a heterozygous mutant background would be a result of the mutant allele influencing factors other than apoptosis. Modifier alleles capable of altering this phenotype were predicted to be influencing factors such as cell cycle progression and cell proliferation based on the ability of known cell proliferation and cell cycle regulators like *Egfr, Cdk1* and *Cyclin B* to modify the GMR>*Rad21*^{NC}, *p35* eye phenotype (Figure 5.25).

Modifier alleles of the GMR>*Rad21*^{NC} and GMR>*Rad21*^{NC}, *p35* eye phenotypes were hypothesised to meet one of more of the following capabilities:

1) Allow cell proliferation in the presence of mitotic catastrophe
2) Modify the cell cycle resulting in:
    a) modification of chromosome segregation efficacy
    b) modification of cell differentiation and/or recruitment of cells to ommatidia
3) Modify chromosome segregation resulting in:
    a) modification of cell cycle progression and cell differentiation/recruitment of cells to ommatidia
    b) modification of cell proliferation

Mutant alleles of individual modifier loci were crossed to the GMR>*Rad21*^{NC}, *p35*/CyO stock (Figure 5.26) and the eye phenotypes of test and control progeny visualised and compared via microscopic examination. Images of modified GMR>*Rad21*^{NC}, *p35* rough-eyes in specific heterozygous mutant backgrounds have been compiled below according to the location of the genes by chromosome, chromosome arm and cytological region as shown in Appendix 6. A total of 105 alleles were tested against the GMR>*Rad21*^{NC}, *p35* small eye phenotype. Of these alleles 67 were found to significantly modify the size and/or organisation of the eye compared to sibling controls (Appendix 6), while 38 alleles were found not to modify the GMR>*Rad21*^{NC}, *p35* phenotype compared to sibling controls. Of the 67 modifying alleles, 61 alleles suppressed and 6 alleles enhanced the GMR>*Rad21*^{NC}, *p35* phenotype (Tables 5.2 to 5.9).

(A)

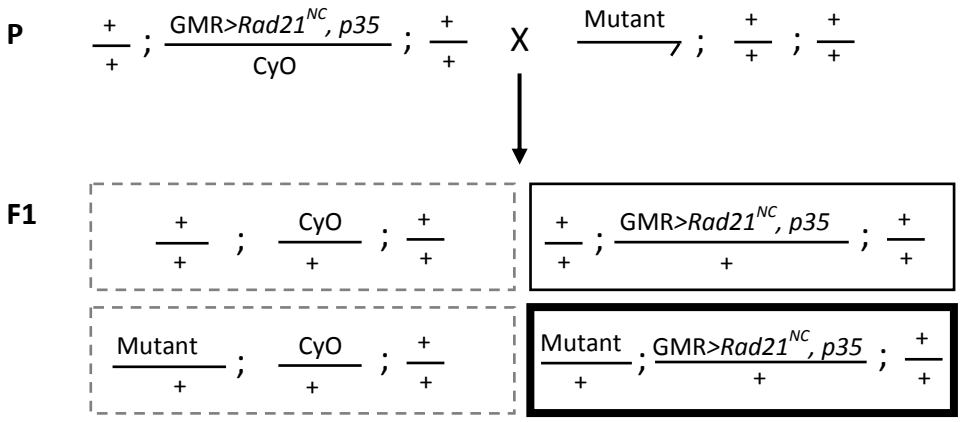
P
+/+ ; GMR>Rad21^NC, p35 / CyO ; +/+
X
Mutant / + ; +/+ ; +/+
F1
+/+ ; CyO/+ ; +/+
+/+ ; GMR>Rad21^NC, p35 / + ; +/+
Mutant/+ ; CyO/+ ; +/+
Mutant/+ ; GMR>Rad21^NC, p35 / + ; +/+

(B)

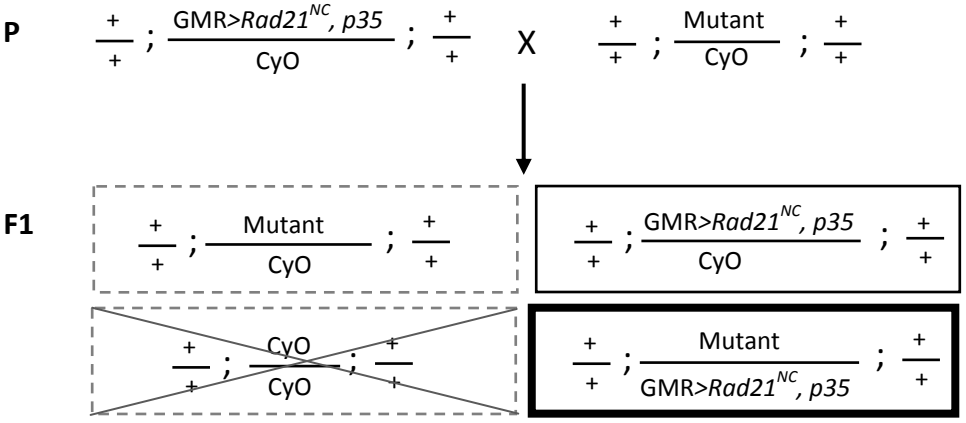
P
+/+ ; GMR>Rad21^NC, p35 / CyO ; +/+
X
+/+ ; Mutant / CyO ; +/+
F1
+/+ ; Mutant/CyO ; +/+
+/+ ; GMR>Rad21^NC, p35 / CyO ; +/+
+/+ ; CyO/CyO ; +/+
+/+ ; Mutant / GMR>Rad21^NC, p35 ; +/+

(C)

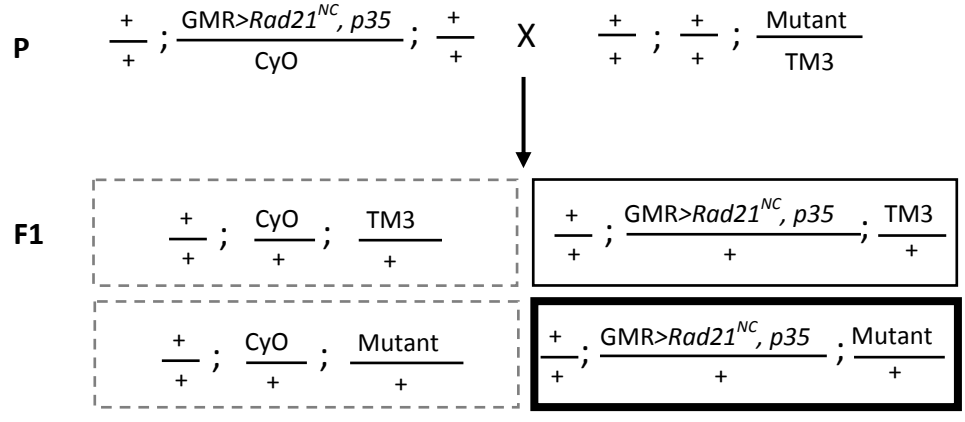
P
+/+ ; GMR>Rad21^NC, p35 / CyO ; +/+
X
+/+ ; +/+ ; Mutant / TM3
F1
+/+ ; CyO/+ ; TM3/+
+/+ ; GMR>Rad21^NC, p35 / + ; TM3/+
+/+ ; CyO/+ ; Mutant/+
+/+ ; GMR>Rad21^NC, p35 / + ; Mutant/+

Figure 5.26: GMR>*Rad21^{NC}, p35* assay crossing scheme. (A-C) Female flies from the +/+; GMR>*Rad21^{NC}, p35*/CyO; +/+ stock were crossed to males with mutant alleles carried on the 1st (A), 2nd (B) or 3rd (C) chromosome and balanced over the Y chromosome or appropriate marked balancer chromosomes. From the F1 progeny the test class (bold black box) and control class (black box) siblings were selected for comparison to identify changes in the GMR>*Rad21^{NC}, p35* phenotype in a heterozygous mutant background. Other sibling classes were discarded or were had non-viable genotypes.

5.2.3.1 GMR>*Rad21^{NC}, p35 modifier alleles*

A total of 3 of the 13 chromosome I modifier alleles were tested in the GMR>*Rad21^{NC}, p35* assay and all were found to be able to modify the eye phenotype modify (Table 5.2, Appendix 6). A total of 34 of the 48 chromosome II modifier alleles were tested in the GMR>*Rad21^{NC}, p35* assay. Thirteen of these alleles were found to modify the eye phenotype, 10 alleles suppress the eye phenotype, while 3 alleles enhance the GMR>*Rad21^{NC}, p35* eye phenotype (Tables 5.3, 5.4 and 5.9, Appendix 6). A total of 68 of the 86 chromosome III modifier alleles were tested in the GMR>*Rad21^{NC}, p35* assay. Fifty-one of these alleles were found to modify the eye phenotype: 48 alleles suppressed the phenotype, while 3 alleles enhanced the GMR>*Rad21^{NC}*, *p35* eye phenotype (Tables 5.5 to 5.9, Appendix 6).

In support of the GMR>*Rad21^{NC}, p35* phenotype being suitable to identify regulators of chromosome cohesion and cell cycle progression, alleles of *SA, Scim13, oaf, CycA, JIL-1, polo, Mcm2, PP2A-B', Nup98* and *SMC1*were all found to be able to suppress the GMR>*Rad21^{NC}, p35* phenotype (Figure 5.27). All of these genes have previously been shown to regulate aspects of DNA replication, chromosome segregation and cell division. Alleles of *san, gwl, dup* and *Dp*, also regulators of cohesin and cell division, did not modify the GMR>*Rad21^{NC}, p35* phenotype. Many of the modifier loci associated with the EGFR/Ras/MAPK signalling pathway (*Egfr, klu, trn, pnt, Mekk1, Fak56D* and *Gap1*) also modified the GMR>*Rad21^{NC}, p35* phenotype (Tables 5.3-5.9).

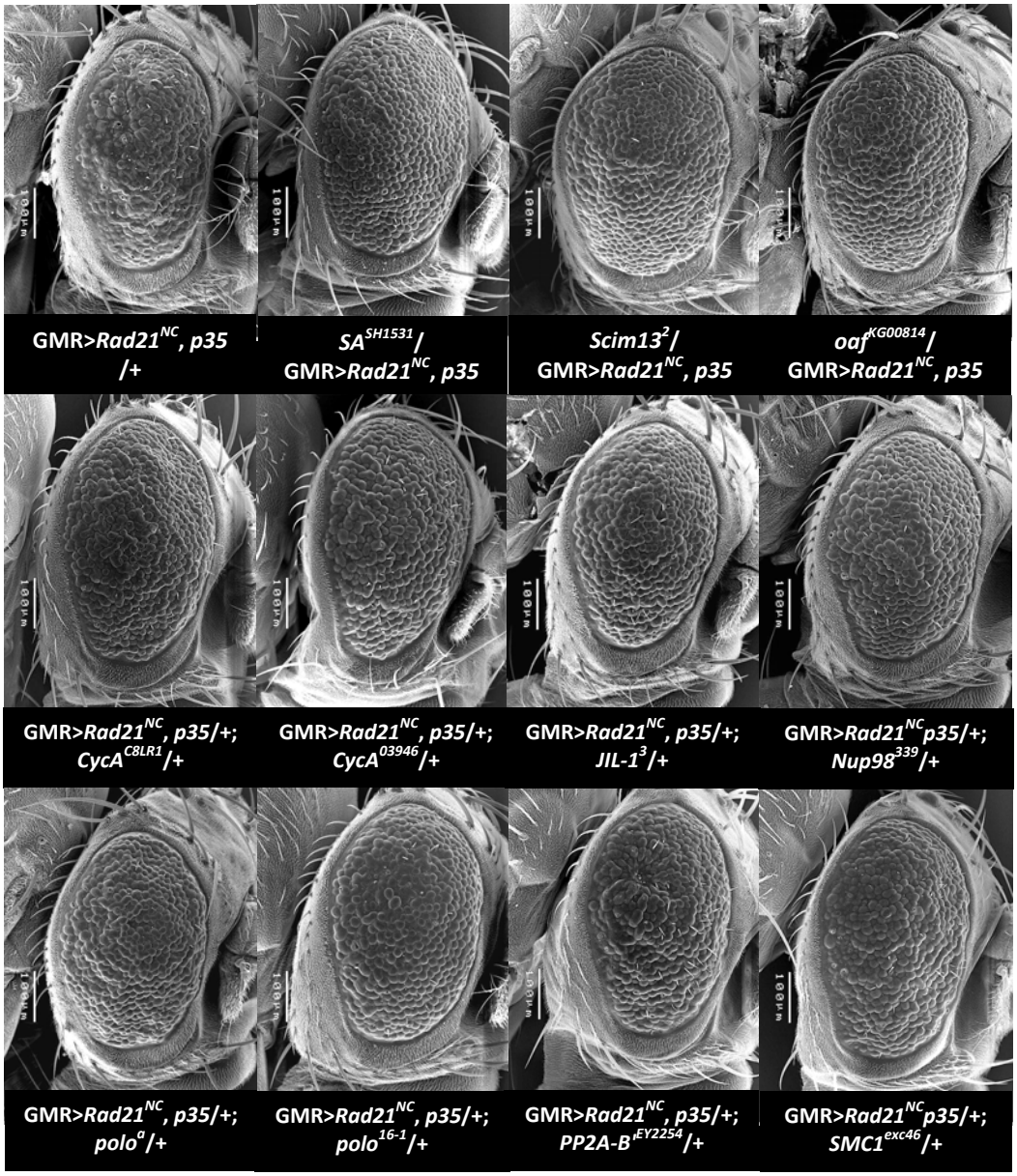

Figure 5.27: Modifier alleles of the GMR>*Rad21^{NC}*, *p35* eye phenotype. Modifier alleles of the GMR>*Rad21^{NC}*, *p35*/+ phenotype: *SA^{SH1531}*/GMR>*Rad21^{NC}*, *p35*, *Scim13^{2}*/GMR>*Rad21^{NC}*, *p35*, *oaf^{KG00814}*/GMR>*Rad21^{NC}*, *p35*, GMR>*Rad21^{NC}*, *p35*/+; *CycA^{C8LR1}*/+, GMR>*Rad21^{NC}*, *p35*/+; *CycA^{03946}*/+, GMR>*Rad21^{NC}*, *p35*/+; *JIL-1^{3}*/+, GMR>*Rad21^{NC}*, *p35*/+; *Nup98^{339}*/+, GMR>*Rad21^{NC}*, *p35*/+; *polo^{a}*/+. GMR>*Rad21^{NC}*, *p35*/+; *polo$^{16-1}$*/+, GMR>*Rad21^{NC}*, *p35*/+; *PP2A-B$^{'EY2254}$*/+ and GMR>*Rad21^{NC}*, *p35*/+; *SMC1^{exc46}*/+ were observed to suppress the phenotype compared to GMR>*Rad21^{NC}*, *p35*/+ controls.

5.2.4 GMR-Gal4 assay

As mentioned previously, a phenotype of disorganised ommatidia can be produced in GMR-Gal4 homozygotes at 25˚C and in GMR-Gal4 heterozygotes raised at 29˚C in the absence of a UAS-transgene. This phenotype appears to be largely due to increased apoptosis in the developing eye imaginal disc (Kramer and Staveley, 2003). This increase in apoptosis has been hypothesised to be due to GAL4 swamping the nuclear import channels or by alteration of the expression of genes whose identities are unknown (Kramer and Staveley, 2003). Whatever the mechanism, the increase in apoptosis that Kramer and Staveley observed in the developing 3rd instar eye imaginal discs of GMR-Gal4 heterozygotes raised at 25˚C introduces another variable to the GMR>*Rad21*^{NC} eye phenotype that needs to be taken into consideration when analysing the outcome of the genetic screen. Mutant alleles that are able to influence GAL4 expression levels could subsequently alter transgene expression levels directly or the level of apoptosis occurring in the eye indirectly. To further characterise the effect of the GMR-Gal4 driver on the GMR>*Rad21*^{NC} modifier loci identified, the mild ommatidial disorganisation phenotype produced in GMR-Gal4 heterozygotes at 29˚C (Figure 5.28) was used as a tool to determine the effects of modifier loci on GAL4 expression and eye development. Ectopic expression of Cyclin B (and other transgenes) suppressed the GMR>*Rad21*^{NC} heterozygote (29˚C) eye phenotype as did reduced expression of ARGOS (Figure 5.29). ARGOS is involved in ommatidial rotation and also regulates apoptosis within the developing eye (Sawamoto *et al.*, 1998). These observations suggest that protein production, eye structure development and apoptosis are all capable of influencing the GMR-Gal4 eye phenotype and potentially influence the GMR>*Rad21*^{NC} phenotype through the GMR-Gal4 driver.

Mutant alleles of individual modifier loci were crossed to the GMR-Gal4/CyO stock (Figure 5.30) and the eye phenotypes of test and control progeny visualised and compared via microscopic examination. Images of modified GMR-Gal4 disorganised-eyes in specific mutant backgrounds have been compiled according to the location of the genes by chromosome, chromosome arm and cytological region in Appendix 6. A total of 103 alleles were tested against the GMR-Gal4 eye phenotype. Of these alleles 51 were found to significantly modify the organisation and/or size of the eye compared to sibling controls, while 52 alleles were found not

to modify the GMR-Gal4 phenotype compared to sibling controls. Of the 51 modifying alleles, 44 alleles suppressed and 7 alleles enhanced the GMR-Gal4 phenotype.

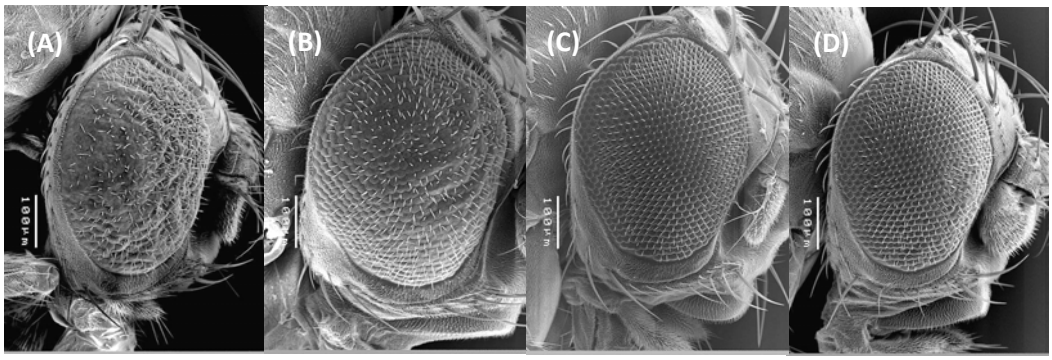

Figure 5.28: The effects of the GMR-Gal4 driver. (A) Homozygous GMR-Gal4/GMR-Gal4 25˚C, (B) Heterozygous GMR-Gal4/+ 29˚C, (C) Heterozygous GMR-Gal4/+ 25˚C, (D) Homozygous GMR-Gal4, UAST-*Rad21*^{WT}-2HA 25˚C.

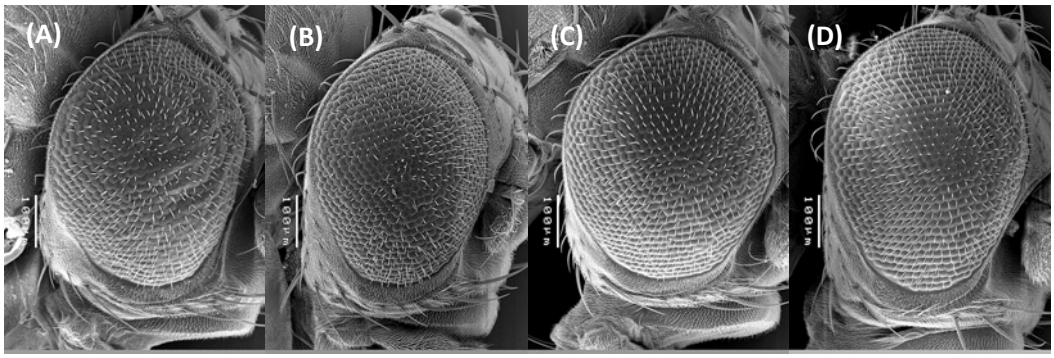

Figure 5.29: Regulators of the cell cycle and ommatidial development influence the GMR-Gal4 phenotype. (A) The mild disorganisation phenotype of the heterozygous GMR-Gal4/+ eye at 29˚C, is suppressed (B) by misexpression of CYCLIN B (GMR-Gal4/UAS-CycB, and by reduction (C and D) of ARGOS expression (argos$^{\Delta 7}$ and argos^{W11}, respectively).

(A)

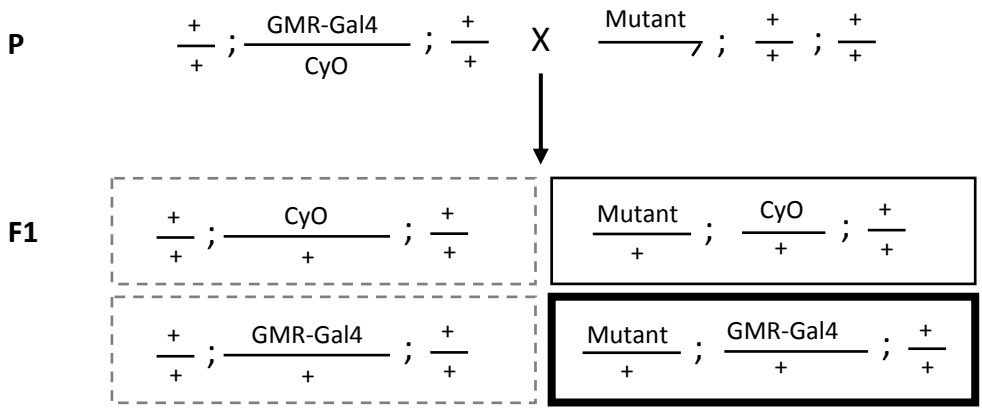
P
+/+ ; GMR-Gal4/CyO ; +/+
X
Mutant ; +/+ ; +/+
F1
+/+ ; CyO/+ ; +/+
Mutant/+ ; CyO/+ ; +/+
+/+ ; GMR-Gal4/+ ; +/+
Mutant/+ ; GMR-Gal4/+ ; +/+

(B)

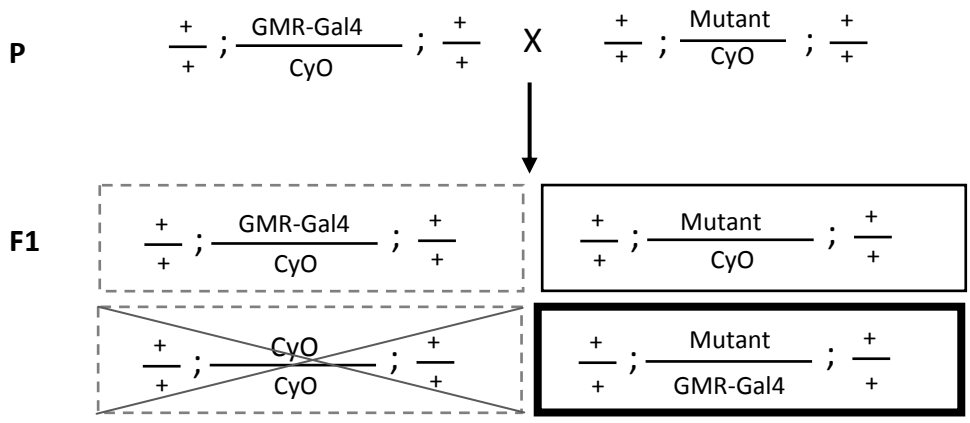
P
+/+ ; GMR-Gal4/CyO ; +/+
X
+/+ ; Mutant/CyO ; +/+
F1
+/+ ; GMR-Gal4/CyO ; +/+
+/+ ; Mutant/CyO ; +/+
+/+ ; CyO/CyO ; +/+
+/+ ; Mutant/GMR-Gal4 ; +/+

(C)

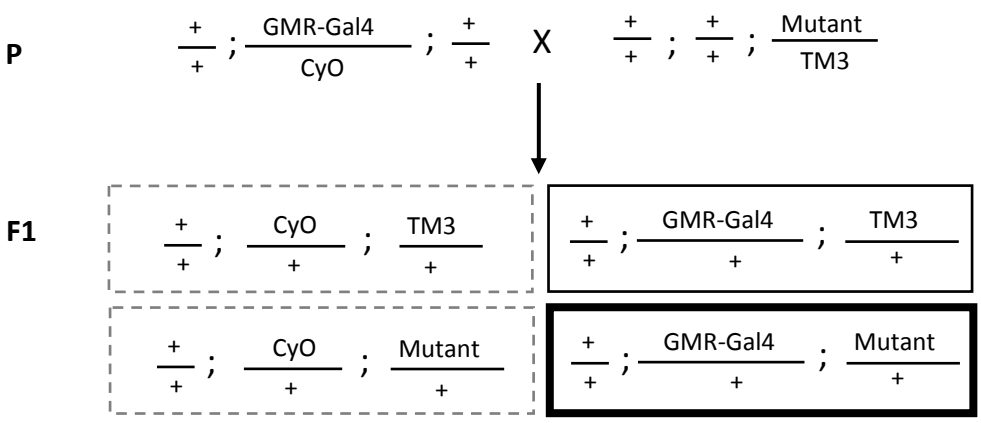
P
+/+ ; GMR-Gal4/CyO ; +/+
X
+/+ ; +/+ ; Mutant/TM3
F1
+/+ ; CyO/+ ; TM3/+
+/+ ; GMR-Gal4/+ ; TM3/+
+/+ ; CyO/+ ; Mutant/+
+/+ ; GMR-Gal4/+ ; Mutant/+

Figure 5.30: GMR-Gal4 assay crossing scheme. (A-C) Female flies from the +/+; GMR-Gal4/CyO; +/+ stock were crossed to males with mutant alleles carried on the 1st (A), 2nd (B) or 3rd (C) chromosome and balanced over the Y chromosome or appropriate marked balancer chromosomes. From the F1 progeny the test class (bold black box) and control class (black box) siblings were selected for comparison to identify changes in the GMR-Gal4/+ phenotype in a heterozygous mutant background. Other sibling classes were discarded or were had non-viable genotypes.

5.2.4.1 GMR-Gal4 modifier loci

A total of 3 of the 13 chromosome I modifier alleles were tested in the GMR-Gal4 assay with only 1 found to be a GMR-Gal4 modifier locus (Table 5.2, Appendix 6). A total of 31 of the 48 chromosome II modifier alleles were tested in the GMR-Gal4 assay. Nine of these alleles were found to modify the eye phenotype, five of the alleles suppressed the GMR-Gal4 eye phenotype, while four alleles enhanced the GMR-Gal4 eye phenotype (Tables 5.3, 5.4 and 5.9, Appendix 6). A total of 69 of the 86 chromosome III modifier alleles were tested in the GMR-Gal4 assay. Forty-one of these alleles were found to modify the eye phenotype, 38 alleles suppressed the GMR-Gal4 eye phenotype, while 3 alleles enhanced the GMR-Gal4 eye phenotype (Tables 5.5-5.9, Appendix 6).

The GMR-Gal4 eye phenotype was both suppressed and enhanced by the modifier alleles tested (Figures 5.31 and 5.32). As anticipated, eye-specific loci *gl* and *ninaE* modified the GMR-Gal4 eye phenotype (Figure 5.30). Unexpectedly, alleles of the cohesin subunit *SA* and the cohesin regulators *gwl, Nup98, polo* and *san* also modified the GMR-Gal4 eye phenotype (Figure 5.32). Overall a wide variety of loci were able to influence the GMR-Gal4 phenotype, with functions including gene expression, EGFR signalling pathway, cell division, chromosome segregation, protein expression regulation, and metabolism.

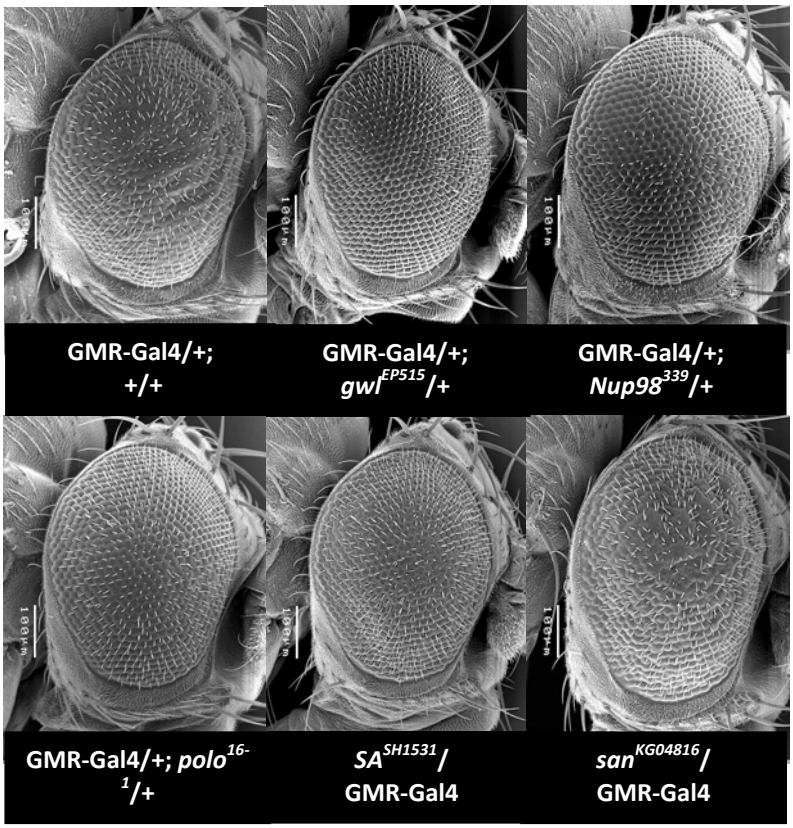

Figure 5.31: Modification of the GMR-Gal4 phenotype by eye development regulators. Modifier alleles of the GMR-Gal4/+ phenotype at 29˚C: GMR-Gal4/+; gl^{3}/+ suppressed and GMR-Gal4/+; $ninaE^{7}$/+ enhanced the GMR-Gal4/+ eye phenotype compared to controls.

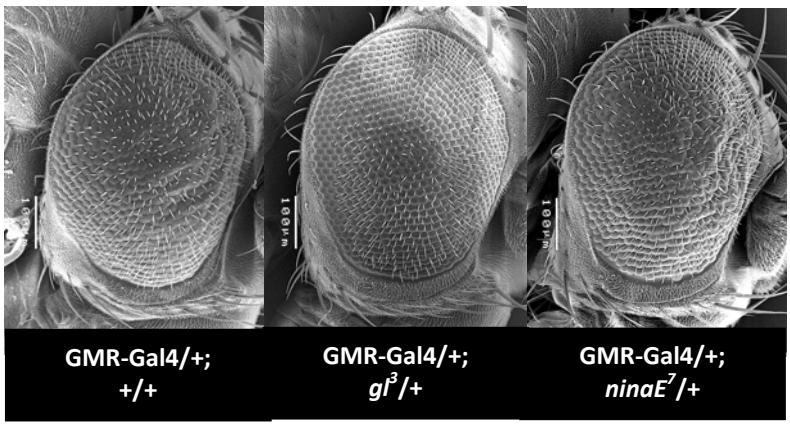

Figure 5.32: Modification of the GMR-Gal4 eye phenotype by cohesin components and cohesin regulators. Modifier loci of the GMR-Gal4/+ phenotype at 29˚C: GMR-Gal4/+; gwl^{EP515}/+, GMR-Gal4/+; $Nup98^{339}$/+, GMR-Gal4/+; $polo^{16\text{-}1}$/+, and SA^{SH1531}/GMR-Gal4 suppressed the GMR-Gal4 eye phenotype, while and $san^{KG04816}$/GMR-Gal4 enhanced the GMR-Gal4 eye phenotype compared to controls.

5.2.5 Summary of the genetic screen and secondary assays

The modifier loci identified in the primary GMR>*Rad21*^{NC} genetic screen and the outcomes of all the secondary screen assays performed are summarised in Tables 5.2-5.9 below. For the 133 identified modifier loci 97 of these had a 2nd allele tested and 61 of these also modified the GMR>*Rad21*^{NC} eye phenotype. Due to time and fly stock constraints only fifteen 2nd modifying alleles were included in further assays and analyses. Of the 125 alleles included in the secondary assays, 84 were identified as modifier alleles of the vgMQ>*Rad21*^{NC} wing phenotype (77% of alleles tested), 45 were identified as modifier alleles of the GMR*hid* phenotype (40% of alleles tested), 67 were identified as modifier alleles of the GMR>*Rad21*^{NC}*, p35* phenotype (64% of alleles tested) and 51 were identified as modifier alleles of the GMR-Gal4 phenotype (50% of alleles tested). The breakdown of secondary assay suppressors and enhancers is presented in Table 5.1 below; of note the vast majority of eye phenotype modifier alleles were suppressors while the wing modifier alleles displayed a much more equally balanced distribution between suppressors and enhancers.

The strong skew towards suppression was maintained with the other eye phenotypes used, but was less obvious with the wing phenotype (Table 5.10, purple shaded square) with a significant number of GMR>*Rad21*^{NC} suppressor alleles being vgMQ>*Rad21*^{NC} enhancer alleles. There were no extremely obvious correlations between the outcomes of the secondary assays for individual alleles, although there did appear to be significantly fewer GMR*hid* modifiers that were also vgMQ>*Rad21*^{NC} and GMR-Gal4 modifiers (Table 5.10, blue shaded squares), and significantly more GMR>*Rad21*^{NC}, *p35* modifiers that were also GMR-Gal4 modifiers relative to comparisons between other secondary assays (Table 5.10, yellow shaded square).

Table 5.1: Comparison of allele distribution within the secondary assays

ASSAY	*Rad21*^{NC} eye	Wing assay	GMR*hid* assay	p35 assay	GMR-Gal4 assay
N°. modifying alleles	*133 alleles*	*84 alleles (77% tested)*	*45 alleles (40% tested)*	*67 alleles (64% tested)*	*51 alleles (50% tested)*
Rad21^{NC} **eye**		67% 33%	96% 4%	95% 5%	88% 12%
Wing assay			28% 11% 61%	40% 16% 44%	38% 11% 51%
GMR*hid* assay				42% - 58%	28% 4% 68%
p35 assay					51% 2% 47%
GMR-Gal4 assay					

Table Key

Alleles that modified phenotypes in the same direction (i.e. suppressed both, enhanced both or modified neither) are shown in red.

Alleles that modified the phenotypes in the opposite direction (i.e. suppressed one and enhanced the other) are shown in black

Alleles that modified one phenotype and not the other are shown in green.

N.B. Percentages are based on the modifier allele information in Tables 5.2-5.9.

Table 5.2: Summary of chromosome I modifier alleles and genetic assays

Allele	Rad21^{NC} eye modification	2nd Interacting allele	Rad21^{NC} wing modification	GMRhid eye modification	GMR>Rad21^{NC}, p35 eye modification	GMR-Gal4 eye modification
ari-1^{EP317}	Suppression	No	Suppression*	NT	NT	NT
CG2709^{EY07076}	Suppression	Yes	None	Suppression	NT	Suppression
crm^{sa2}	Suppression	No	Enhancement*	NT	Suppression	None
dm^{1}	Enhancement	Yes	Enhancement*	NT	NT	NT
fs(1)Ya$^{14-77}$	Suppression	No	None	NT	NT	NT
Klp3A$^{mei-352}$	Suppression	No	NT	NT	NT	NT
lin-52^{EP1405}	Suppression	NT	None	NT	Suppression	NT
Mcm3^{4249}	Suppression	NT	NT	NT	NT	NT
mit(1)15^{13807}	Suppression	No	NT	NT	NT	NT
nej^{EP950}	Suppression	NT	NT	NT	NT	NT
Parg^{EP351}	Suppression	NT	None	NT	NT	NT
pcm^{EP1526}	Suppression	NT	None	NT	Suppression	None
snf^{1}	Suppression	No	NT	Suppression	NT	NT

* Alleles that demonstrated significant difference in mean compared to vgMQ>*Rad21*^{NC} sibling controls and * alleles that demonstrated significant difference in mean compared to vgMQ>*Rad21*^{NC} stock controls. NT = Not Tested.

Table 5.3: Summary of chromosome II (regions 21-34) modifier alleles and genetic assays.

Allele	Rad21^{NC} eye modification	2nd Interacting allele	Rad21^{NC} wing modification	GMRhid eye modification	GMR>Rad21$^{N}_{C}$, p35 eye modification	GMR-Gal4 eye modification
bowl^{2}	Suppression	No	NT	NT	NT	NT
cdc2^{10728}	Suppression	NT	NT	NT	NT	NT
cdc14^{EY10303}	Suppression	NT	NT	NT	NT	NT
CG3542^{EP719}	Suppression	NT	Suppression*	Suppression	None	None
CG9643^{EY07345}	Suppression	NT	NT	NT	NT	NT
CG11070^{EP2597}	Suppression	NT	NT	None	Suppression	None
CG17221^{c00569}	Suppression	NT	NT	NT	NT	NT
cup^{KG01851}	Enhancement	No	NT	NT	NT	NT
cort^{QW55}	Suppression	Yes	NT	None	None	Suppression
esc^{1240}	Suppression	No	NT	NT	NT	NT
γTub23C^{bmps1}	Enhancement	NT	Enhancement**	Enhancement	Enhancement	Enhancement
Hrb27C^{EY12571}	Enhancement	Yes	Enhancement**	None	Enhancement	Enhancement
Hrb27C^{f04375}	Suppression	Yes	Enhancement**	None	None	None
lilli^{EY12936}	Enhancement	NA	None	None	Enhancement	Enhancement
oaf^{KG00814}	Suppression	No	Suppression*	Suppression	Suppression	None
Rca1^{03300}	Suppression	No	NT	NT	NT	NT
r2d2^{1}	Enhancement	Yes	Suppression*	None	None	None
r2d2^{EY00028}	Suppression	Yes	Enhancement*	None	None	None
SA^{SH1531}	Suppression	NA	Suppression*	None	Suppression	Suppression
Scim13^{2}	Suppression	NA	None	Suppression	Suppression	None
smt3^{k06307}	Suppression	Yes	Enhancement*	None	None	None
vir-1^{EY08717}	Suppression	NT	NT	NT	NT	NT

Table 5.4: Summary of chromosome II (regions 35-60) modifier alleles and genetic assays.

Allele	Rad21^{NC} eye modification	2nd Interacting allele	Rad21^{NC} wing modification	GMRhid eye modification	GMR>Rad21^{NC}, p35 eye modification	GMR-Gal4 eye modification
CadN^{MI2}	Suppression	NT	Enhancement*	Enhancement	None	Suppression
CadN2^{BG02611a}	Suppression	Yes	NT	None	Suppression	None
CG2264^{KG02847b}	Enhancement	No	NT	Suppression	None	NT
CG5559^{KG02182}	Suppression	Yes	NT	Suppression	NT	NT
CG30484^{10102}	Suppression	NT	NT	NT	NT	NT
cora^{k08713}	Suppression	Yes	Enhancement**	Suppression	None	None
cora^{EY07598}	Suppression	Yes	NT	Suppression	None	NT
dl^{UY2278}	Enhancement	No	NT	NT	NT	NT
Dp^{a1}	Suppression	Yes	Enhancement**	Suppression	None	None
lat^{EP1168}	Suppression	No	NT	NT	NT	NT
mam^{BG02407}	Enhancement	Yes	None	None	None	None
mars^{f07689}	Suppression	NT	Enhancement*	None	None	None
mrj^{EY04743}	Suppression	NT	Suppression*	Suppression	Suppression	NT
Mys45A^{EY02132}	Suppression	No	Suppression*	None	Suppression	Suppression
san^{KG04816}	Suppression	NA	Suppression*	None	None	Enhancement
shark^{1}	Suppression	No	NT	NT	NT	NT
Su(var)2-10^{zimp-2}	Suppression	Yes	None	None	None	None

Table 5.5: Summary of chromosome III (regions 61-72) modifier alleles and genetic assays.

Allele	Rad21^{NC} eye modification	2nd Interacting allele	Rad21^{NC} wing modification	GMRhid eye modification	GMR>Rad21^{NC}, p35 eye modification	GMR-Gal4 eye modification
Arp66B^{EP3640}	Suppression	NT	Enhancement*	Suppression	Suppression	None
brm^{d00415}	Suppression	Yes	Suppression*	None	Suppression	Suppression
brm^{2}	Suppression	Yes	Suppression*	None	Suppression	Suppression
CG6272^{HP32076}	Suppression	NT	Suppression*	Suppression	None	Suppression
CG7304^{f05948}	Suppression	Yes	Enhancement*	None	None	Suppression
Dhh1^{rL562}	Suppression	NT	None	Suppression	Suppression	Suppression
DNApol-Δ^{EP3292}	Suppression	NT	Suppression**	None	NT	Suppression
Ect4^{e03740}	Suppression	Yes	NT	None	Suppression	Suppression
Eig71Et^{f04943}	Suppression	NT	Suppression* Enhancement*	None	None	Suppression
hay^{f00028}	Enhancement	NT	Enhancement*	None	Suppression	Suppression
Hip14^{EY09853}	Suppression	No	None	Suppression	NT	NT
JIL-1^{3}	Suppression	Yes	NT	None	Suppression	Suppression
klu^{09036}	Suppression	No	None	Suppression	Suppression	Suppression
nmo^{j147-1}	Suppression	Yes	Suppression*	Suppression	Suppression	None
pbl^{09645}	Suppression	Yes	Suppression*	Suppression	Suppression	Suppression
Pdp1^{EP3389}	Suppression	Yes	Suppression**	None	Suppression	None
Pka-C3^{KG00222}	Suppression	No	Suppression*	None	Suppression	None
Syx13^{01470}	Suppression	Yes	None	Suppression	Suppression	None
th^{4}	Enhancement	Yes	Enhancement**	None	None	None
trn^{S064117}	Suppression	No	None	None	Suppression	None
vih^{7061}	Suppression	NT	NT	NT	NT	NT

Table 5.6: Summary of chromosome III (regions 73-78) modifier alleles and genetic assays.

Allele	Rad21^{NC} eye modification	2nd Interacting allele	Rad21^{NC} wing modification	GMRhid eye modification	GMR>Rad21^{NC}, p35 eye modification	GMR-Gal4 eye modification
asf1^{LA00872}	Suppression	NT	NT	Suppression	NT	NT
CG3947^{EY05323}	Suppression	Yes	Enhancement*	Suppression	None	NT
CG5618^{f05961}	Suppression	NT	Suppression* Enhancement*	Suppression	Suppression	Suppression
CG8786^{EY09040}	Suppression	NT	Enhancement*	Suppression	None	Suppression
CG9330^{f04902}	Suppression	Yes	Suppression* Enhancement*	None	None	Suppression
CG9368^{KG02762}	Suppression	NT	None	None	Suppression	Suppression
CG13255^{c04618}	Suppression	NT	None	None	Suppression	Suppression
CG32432^{f02670}	Suppression	No	Suppression*	None	Enhancement	None
CSN3^{f02855}	Suppression	No	Suppression* Enhancement*	None	Suppression	Suppression
Gyc76C^{EY02825}	Suppression	NT	NT	NT	NT	NT
in^{c02090}	Suppression	NT	Suppression* Enhancement*	Suppression	Suppression	NT
kni^{10}	Suppression	No	Suppression**	None	None	Suppression
polo^{a}	Suppression	Yes	Suppression*	None	Suppression	None
polo$^{16-1}$	Suppression	Yes	Suppression**	None	Suppression	Suppression
RhoBTB^{EP3099}	Suppression	NT	Suppression**	NT	Suppression	Suppression
Shal^{f00495}	Suppression	No	None	None	Suppression	Suppression
Six4^{EY09833}	Suppression	Yes	Enhancement*	None	NT	None
Taf6^{f06930}	Suppression	No	Suppression*	None	Suppression	Suppression
Toll-9^{c05666}	Suppression	NT	NT	NT	NT	NT

Table 5.7: Summary of chromosome III (regions 79-91) modifier alleles and genetic assays.

Allele	Rad21^{NC} eye modification	2nd Interacting allele	Rad21^{NC} wing modification	GMRhid eye modification	GMR>Rad21^{NC}, p35 eye modification	GMR-Gal4 eye modification
Aats-ile^{00827}	Suppression	Yes	Suppression*	None	Suppression	Suppression
Aats-ile^{EY03542}	Suppression	Yes	Enhancement*	None	None	None
CG4570^{EY02388}	Suppression	NT	NT	NT	NT	NT
CG11523^{f05435}	Suppression	No	Suppression*	None	Suppression	Suppression
eIF-1A^{2232}	Enhancement	Yes	Suppression*	Suppression	NT	NT
eIF-1A^{c04533}	Suppression	Yes	Suppression**	NT	NT	NT
Fdh^{nNC1}	Suppression	No	Enhancement*	None	Suppression	Suppression
gl^{1}	Suppression	Yes	NT	Suppression	NT	None
gl^{3}	Suppression	Yes	Suppression**	Suppression	Suppression	Suppression
gwl^{EP515}	Suppression	No	Suppression**	None	None	Suppression
hb^{f00586}	Enhancement	NT	Suppression* Enhancement*	None	NT	Suppression
koko^{DG19805}, *Vha100-2*^{DG19805}	Suppression	NT	Enhancement*	Suppression	None	NT
Mekk1^{KG02510}	Suppression	Yes	Suppression**	Suppression	None	Enhancement
Mekk1^{EY02276}	Suppression	Yes	NT	Suppression	Suppression	None
Or85d^{f05736}	Suppression	No	Enhancement*	None	Suppression	None
PP2A-B"^{EY22564}	Suppression	Yes	Suppression*	None	Suppression	None
Scim32^{2}	Suppression	NA	Suppression**	Suppression	None	None
Ten-m^{EY03921}	Suppression	Yes	NT	None	None	None
Ten-m^{KG00101}	Suppression	Yes	None	Suppression	Suppression	None
14-3-3ε^{EP3423}	Suppression	No	Suppression**	None	None	None

Table 5.8: Summary of chromosome III (regions 92-100) modifier alleles and genetic assays.

Allele	Rad21^{NC} eye modification	2nd Interacting allele	Rad21^{NC} wing modification	GMRhid eye modification	GMR>Rad21^{NC}, p35 eye modification	GMR-Gal4 eye modification
bon^{EY01763}	Suppression	Yes	Suppression*	None	Suppression	Suppression
cdc2c^{2}	Suppression	Yes	NT	NT	NT	NT
CG4288^{f05992}	Suppression	Yes	Suppression*	None	Suppression	Suppression
CG12885^{f02499}	Suppression	Yes	Suppression* Enhancement*	None	Suppression	Suppression
CG31163^{BG00076}	Suppression	NT	NT	NT	NT	NT
eIF-36p66^{EY05735}	Suppression	NT	None	Suppression	None	Suppression
Nep4^{c02841}	Suppression	NT	Suppression* Enhancement*	Suppression	Suppression	NT
ninaE^{7}	Suppression	NT	Enhancement*	Suppression	Suppression	Enhancement
Nup98^{339}	Suppression	Yes	Suppression**	None	Suppression	Suppression
Pli^{BG02732}	Suppression	No	NT	Suppression	NT	NT
pnt^{EY03254}	Enhancement	Yes	Enhancement**	None	Enhancement	Enhancement
pnt^{A88}	Suppression	Yes	None	NT	NT	NT
Rab1^{e01287}	Suppression	NT	NT	NT	NT	NT
Rpn9^{EY03352}	Suppression	Yes	Enhancement*	Suppression	None	Suppression
sba^{MB04880}	Suppression	Yes	Enhancement*	None	Suppression	None
sba^{EP3284}	Suppression	Yes	Suppression**	NT	NT	NT
Sep2^{C207}	Suppression	Yes	Suppression**	None	Enhancement	Suppression
Tbp-1^{04210b}	Suppression	NT	NT	Suppression	Suppression	None

Table 5.9: Summary of miscellaneous modifier alleles and genetic assays

Allele	$Rad21^{NC}$ eye modification	2^{nd} Interacting allele	$Rad21^{NC}$ wing modification	GMRhid eye modification	GMR>$Rad21^{NC}$, p35 eye modification	GMR-Gal4 eye modification
dup^{k03308}	Suppression	Yes	Suppression*	Suppression	None	None
EcR^{V559fs}	Enhancement	NT	None	None	None	None
Egfr^{k05115}	Suppression	No	Suppression*	None	Suppression	None
eIF-4A^{02439}	Suppression	Yes	None	None	None	None
eIF-4A^{k01501}	Suppression	Yes	Enhancement**	None	None	None
Fak56D^{KG00304}	Suppression	Yes	Enhancement*	Suppression	Suppression	None
mle^{e04702}	Suppression	No	Enhancement*	None	None	Suppression
myb^{4472}	Suppression	NT	NT	NT	NT	NT
prod^{k08810}	Suppression	NT	Suppression*	None	None	None
Src42A^{myri}	Suppression	No	Enhancement*	None	None	None
argos$^{\Delta 7}$	Suppression	Yes	Enhancement*	NT	NT	Suppression
argos^{W11}	Suppression	Yes	None	NT	NT	Suppression
CycA^{C8LR1}	Suppression	Yes	Enhancement**	None	Suppression	None
CycA^{03946}	Suppression	Yes	Suppression**	None	Suppression	None
Gap1^{B2}	Suppression	Yes	NT	None	Suppression	None
Gap1$^{mip\text{-}w+}$	Suppression	Yes	None	Suppression	Suppression	None
Gap1^{EY00011}	Suppression	Yes	Enhancement*	Suppression	Suppression	NT
Mcm2^{rL074}	Suppression	NT	Suppression*	Suppression	Suppression	None
SMC1^{exc46}	Suppression	Yes	None	None	Suppression	None
SMC3$^{exc11.5}$	Suppression	NT	NT	NT	NT	NT
wdb^{KG02977}	Suppression	NT	Suppression*	None	Suppression	None

5.3 DISCUSSION

5.3.1 Validity of the secondary assays

5.3.1.1 Rad21^{NC} *wing assay*

The vgMQ>*Rad21*^{NC} wing phenotype was developed to identify modifier loci that were not eye-specific in their function. Eye development loci such as *Six4, gl* and *ninaE* were anticipated to not be able to modify the vgMQ>*Rad21*^{NC} wing phenotype. Known cohesin subunits and cohesin regulators that were found to suppress the GMR>*Rad21*^{NC} eye phenotype were also predicted to suppress the wing phenotype due to the conservation of cohesin function between somatic tissues. Consistent with the prediction that cohesion-specific regulators would also modify the vgMQ>*Rad21*^{NC} phenotype, 80% of modifier loci that are directly linked to cohesin or closely linked to cellular processes that underlie cohesin regulation and function were found to modify the vgMQ>*Rad21*^{NC} phenotype relative to controls. In addition, the eye development gene *Six4* did not modify the vgMQ>*Rad21*^{NC} phenotype, while the eye-development gene *ninaE* only modified the wing phenotype compared to sibling controls and not vgMQ>*Rad21*^{NC} controls. Surprisingly, the *glass* allele tested displayed significant suppression of the vgMQ>*Rad21*^{NC} wing compared to both sibling and stock controls.

The tendency for some sibling control groups to differ significantly in wing size from the test group and the stock control is possibly due to genetic interactions with mutations carried on the balancer chromosomes. This would explain the failure of some alleles to modify the wing size significantly compared to sibling controls, while modifying the wing significantly compared to stock controls. The failure of the cohesin subunit SMC1 to significantly modify the wing size compared to controls may be due to a lack of sensitivity in the wing phenotype assay.

Questions remain as to which parameters are relevant in assessing genetic interaction with *Rad21*^{NC} in the wing; however, no obvious variations in wing structure, organisation or general appearance were noted while performing this assay. Intriguingly, inhibition of apoptosis through the introduction of the baculovirus p35 protein into the vgMQ>*Rad21*^{NC} background did not result in a significant change in

the size of the wing (S. Page, unpublished). From analysis of the GMR>*Rad21*^{NC}, *p35* eye, it was predicted that p35 is able to only rescue the replicating *Rad21*^{NC}-expressing cells and not the progeny of these cells, which suffer mitotic catastrophes and presumably fail to replicate again. Overall it would appear that this wing phenotype and the analysis used are not sufficiently sensitive to detect small differences in cell number that may be induced in some heterozygous mutant backgrounds that otherwise produced an observable change in the crystalline-like arrays of the adult eye ommatidia.

*5.3.1.2 GMR*hid *assay*

It was predicted that alleles of GMR>*Rad21*^{NC} modifier loci that also modulate the GMR*hid* phenotype (through modification of apoptosis) would not modify the GMR>*Rad21*^{NC}, *p35* eye where no apoptosis is occurring. For the most part modifier alleles that altered the GMR*hid* eye phenotype did not alter the GMR>*Rad21*^{NC}, *p35* eye phenotype (58% of tested alleles, Table 5.1), indicating that many modifier alleles of the GMR*hid* eye phenotype are likely to be directly influencing apoptosis. Alleles that are capable of modifying both the *hid* and *Rad21*^{NC} eye phenotypes are predicted to be influencing cellular pathways and events including those upstream of HID-induced apoptosis, such as the Ras/mitogen-acitivated protein kinase (MAPK) pathways and effectors.

The EGFR/Ras/MAPK pathway (discussed in detail in section 6.3.8) has many and varied roles during development, influencing cell proliferation, cell differentiation and programmed cell death. Besides a general role for this pathway in regulating rates of cell division, specific members of the EGFR/Ras/MAPK pathway have specialised roles in aspects of chromosome and cell division (discussed in detail in Chapter 6) that make modifiers of this pathway of particular interest to this study.

As sensitivity to EGFR/Ras/MAPK signalling activity is limited to the GMR>*hid* eye phenotype and not observed for the apoptosis inducers *reaper* (*rpr*) and *grim* (Bergmann *et al*., 1998), these genes could be considered for examining apoptosis *in vivo* that is independent of the effects of EGFR/Ras/MAPK signalling. While general regulators of apoptosis are not of direct interest in this study, regulators of

EGFR/Ras/MAPK signalling that are potentially influencing the cell cycle and chromosome segregation are most certainly worthy of further investigation.

5.3.1.3 GMR>Rad21^{NC}, p35 assay

Loci able to modify the GMR>*Rad21^{NC}, p35* eye phenotype were predicted to predominantly influence the phenotype through modulation of chromosome cohesion and/or cell cycle progression. In support of these hypothesised mechanisms, known regulators of chromosome segregation and cell cycle (*SA, Scim13, oaf, polo, PP2A-B', SMC1, wdb* and *Gap1*) were found to modify this phenotype. Loci associated with the spindle, cytokinesis, chromatin regulation and DNA replication modified both the GMR>*Rad21^{NC}* and GMR>*Rad21^{NC}, p35* eye phenotypes. Additionally, many of the EGFR/Ras/MAPK-associated genes were found to modify the GMR>*Rad21^{NC}, p35* phenotype, indicating that cell proliferation and differentiation are able to influence chromosome segregation in a GMR>*Rad21^{NC}, p35* mutant background.

Many of the identified loci that are associated with general gene expression modified the GMR>*Rad21^{NC}, p35* phenotype, which could support the idea that these loci are modulating chromosome cohesion through changes in the abundance of the ectopically expressed transgenes or other essential gene products. However, almost all the identified loci with fundamental roles in eye development were also able to modify the GMR>*Rad21^{NC}, p35* phenotype. This indicates that factors that directly regulate cell differentiation and proliferation may also influence the eye phenotype without influencing chromosome cohesion directly.

5.3.1.4 GMR-Gal4 assay

The GMR-Gal4 assay was anticipated to identify modifier alleles that were influencing the GMR>*Rad21^{NC}* phenotype by modulating the activity of the GMR promoter and Gal4 protein activity. Exactly 50% of the alleles tested using the GMR-Gal4 assay were found to be able to modify the eye phenotype (Table 5.1) and with no apparent directional pattern to the modification, based on loci function or the types of mutations employed, it may be a non-specific interaction with the GMR-Gal4 phenotype.

Unexpectedly, the cohesin component *SA* and the cohesin regulators *gwl, Nup98, polo* and *san* were able to modify the GMR-Gal4 phenotype. This may be indicative of cohesin being able to influence Gal4 expression or the expression of genes capable of influencing the GMR-Gal4 eye phenotype, such as those involved in protein production or apoptosis, . However, further characterisation of the GMR-Gal4 phenotype is required to fully understand these genetic interactions. Therefore, GMR> *Rad21*^{NC} modifier loci have not been discounted from further investigation based on modification of the GMR-Gal4 eye phenotype alone and all results have been considered in the context of all the assays performed and published data.

5.3.2 Refinement of the GMR>Rad21^{NC} *modifier list*

It was originally anticipated that a clear pattern would emerge from the secondary genetic assays described above, which would allow plausible novel chromosome cohesion regulator candidates to be identified on the basis of shared characteristics with known cohesion regulators. In support of this, the cohesin subunits and cohesin regulators tested were generally found to modify the vgMQ>*Rad21*^{NC} wing phenotype, not modify the GMR*hid* phenotype, to modify the GMR>*Rad21*^{NC}*, p35* phenotype and possibly modify the GMR-Gal4 phenotype. Loci involved in DNA replication, cell cycle regulation, cytokinesis and spindle regulation almost always modified the wing phenotype and mostly modified the GMR>*Rad21*^{NC}*, p35* phenotype, but were much less consistent in their modfication of the GMRhid eye and vgMQ>*Rad21*^{NC} wing phenotypes.

This provides a loose framework for identifying other modifier loci that directly influence the fidelity of chromosome cohesion. The lack of a strong and consistent set of characteristics, however, is most likely a reflection of the multifunctional nature of proteins and cellular pathways. Many of the identified loci have recognised roles in multiple cellular activities. Loci that were found to modify all the assay phenotypes (*γTub23C, pbl, CG5618, gl* and *ninaE*) were predicted to have a general influence on tissue development and therefore be poor candidates for regulators of chromosome cohesion. However, the known functions of *γTub23C* and *pbl* in cell division would suggest otherwise and it is therefore difficult to disregard these genes on the basis of the secondary assay results. Hypothesised modes of

genetic modulation of the GMR>*Rad21*^{NC} phenotype and chromosome cohesion and segregation are considered in-depth in the following chapter.

CHAPTER 6: FINAL DISCUSSION

6.1 INTRODUCTION

Loss of chromosome cohesion has been implicated as a significant contributor to chromosome missegregation and aneuploidy. The majority of cell cycle and chromosome cohesion studies have been performed in highly informative yeast systems, human cell cultures and *Xenopus* cell-free extracts. Use of multicellular models, like *Drosophila melanogaster*, offers an opportunity to better understand these complex genetic pathways in metazoans species. A relatively high level of conservation exists between the *Drosophila* and human genomes, with greater than 60% of known human disease gene having an identified *Drosophila* orthologue (Fortini *et al.*, 2000). *Drosophila* has proven a valuable tool for investigating the molecular basis of human diseases and therefore was chosen for this study to further our knowledge and understanding of potential genetic risk factors for human aneuploidy conditions.

Neverless, there are currently no recognised and testable genetic risk factors for meiotic aneuploidy and human aneuploidy syndromes, which may be due to the predominant focus on the maternal-age effect. We hypothesised that impaired function of genes that regulate chromosome cohesion and segregation will be an underlying aetiological factor in a subset of cases of human aneuploidy syndromes. Therefore this study aimed to identify regulators of chromosome cohesion and segregation that can influence chromosome segregation accuracy in a metazoan context.

6.2 THIS STUDY

At the commencement of this study it was clear that much of the molecular network underlying chromosome segregation remained to be determined and that metazoan species, such as *Drosophila*, could provide unique insights into these processes. The aim of this study was to identify novel regulators of chromosome cohesion and segregation. To achieve this, a chromosome missegregation model was used that employed a non-cleavable form of the cohesin component *Rad21* to impede chromosome segregation. When ectopically expressed in the replicating cells of the

developing *Drosophila* eye this cleavage-resistant variant produced a reduced and disorganised eye phenotype (Chapter 3). The underlying cellular phenotype demonstrated increased levels of tetraploidy, aneuploidy, lagging chromosomes and fragments of broken chromosomes. This eye phenotype proved modifiable by second site heterozygous mutations in genes encoding known regulators of cohesin and chromosome segregation, such as *NippedB*, *Separase* and *Cyclin B*. Following this characterisation the chromosome missegregation phenotype was utilised as a screening tool to identify regulators of chromosome segregation capable of modifying chromosome cohesion (Chapter 4). The genetic screen performed as part of this study identified 133 candidate loci that were able to modify the GMR>*Rad21*^{NC} chromosome missegregation model and thereby have been linked to chromosome segregation. The screen was carried out using mutant alleles of loci that fell within the breakpoints of deletions previously identified as GMR>*Rad21*^{NC} modifiers. The number of modifying loci is greater than originally anticipated, however, this may reflect the molecular complexity of chromosome segregation, the inter-connectedness of cellular pathways and the multi-functional nature of proteins.

A series of secondary assays were designed in the expectation that they would allow modifiers that influence the eye phenotype through specific mechanisms to be identified (Chapter 5). The lack of a single defining set of characteristics identified by the secondary assays reflects the diverse nature of the candidate loci identified and highlights the value of a tertiary aneuploidy assay. Detailed examination of the relevant literature revealed many direct and indirect links between the candidate loci and chromosome cohesion and segregation, as will be examined in the following section

6.3 EXPLORATION OF CANDIDATE GENE FUNCTIONS

6.3.1 Cohesin and cohesin regulators

This screen identified alleles of three of the four cohesin subunits (*SMC1, SMC3, SA*), cohesion establishment factor *san*, and known cohesin regulators *polo*, *PP2A-B'* (the protein phosphatase 2A regulatory subunit), *gwl* and *Nup98* as modifiers of the GMR>*Rad21*^{NC} chromosome missegregation model. Decreasing the cellular levels

of cohesin subunits or san, via heterozygosity, would be predicted to result in a reduction in chromosomally-bound cohesin, thereby allowing the chromosomes to separate more easily. Mutant alleles of *SA, SMC1, SMC3* and *san* all suppressed the GMR>*Rad21*^{NC} phenotype, consistent with the expectation that reducing the expression level of these proteins will reduce the number of both wildtype and cleavage-resistant cohesin molecules impeding chromosome segregation (Figure 6.1).

Reduction of the cellular levels of cohesin regulators polo kinase and PP2A via heterozygosity would be predicted to strengthen and weaken centromeric cohesin through decreased and increased activation of the prophase dissociation pathway, respectively (Sumara *et al.*, 2002; Riedel *et al*., 2006). Similar to heterozygous polo, increased expression of gwl kinase, which antagonises the activity of polo (Archambault *et al.*, 2007), should also result in more centromeric cohesin at anaphase (Figure 6.1). Although low levels of cohesin are known to remain on the chromosome arms until anaphase (Nakajima *et al.*, 2007), the most significant cohesin population after prophase is the centromeric cohesin; therefore, it was satisfying to observe that regulators of centromeric cohesin were identified as modifiers of the GMR>*Rad21*^{NC} phenotype. These mutants are predicted to decrease the level of centromeric cohesin and thereby decrease the strength of the impediment to chromosome segregation. With fewer cleavage-resistant cohesin molecules present at the centromere the probability of the chromosomes segregating correctly to form viable daughter cells. Consistent with these predictions, the mutant alleles of *PP2A-B'* examined suppressed of the GMR>*Rad21*^{NC} phenotype. Unexpectedly, the *polo* and *gwl* allele tested suppressed the GMR>*Rad21*^{NC} when increased centromeric cohesion would be expected to enhance the phenotype as this would result in increased strength of the impediment to chromosome segregation. However, the involvement of polo kinase in other mitotic events (Karaiskou *et al.*, 1999; Ayaydin *et al.*, 2000; Carmena *et al.,* 1998) would suggest that polo, and its regulator gwl kinase, are able to suppress the GMR>*Rad21*^{NC} phenotype through these other mechanisms. Polo also has a key role in regulating mitotic cyclin activation and this is discussed in section 6.3.2.

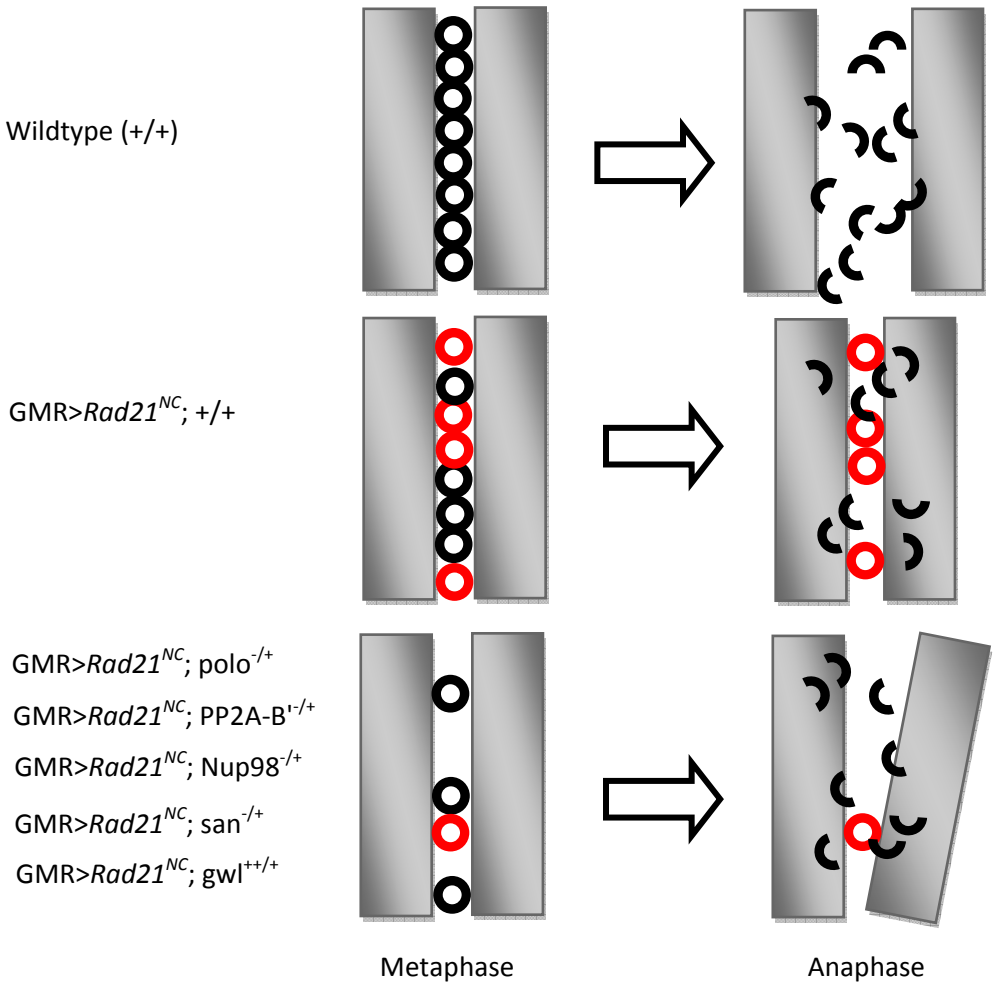

Figure 6.1: Cohesin subunits and cohesin regulators. Cohesin complexes (black circles) normally hold sister-chromatids together until the onset of anaphase, when an cohesin molecules remaining on the chromosomes are cleaved by Separase. Non-cleavable cohesin (red circles) are resistant to Separase activity and remain on the chromosomes after the onset of anaphase impeding chromosome segregation. Decreasing the levels of cohesin regulators *polo, PP2A*, *Nup98* and *san*, and increasing the levels of *gwl* all result in decreased cohesin molecules (cleavable and non-cleavable) at the onset of anaphase. Therefore fewer molecules are present to impede chromosome segregation and the GMR>*Rad21*^{NC} phenotype is suppressed.

Nup98 acts in unison with Rae1 to regulate nuclear mRNA export (Blevins *et al.*, 2003). At the onset of metaphase when the function of these proteins switches to regulation of the APC/C^{Cdh1} to prevent the premature degradation of securin, which functions to inhibit Separase (Jeganathan *et al.*, 2005; Baker *et al.*, 2007). Premature activation of Separase is predicted to significantly reduce the population of cleavable chromosome-bound cohesin prior to the onset of anaphase and therefore decrease the work required of the other cohesin-removal pathways. Consistent with these predictions, the Nup98 mutant allele was observed to suppress the GMR>*Rad21*^{NC} phenotype. Under normal conditions only a select subset of cohesin molecules are cleaved by Separase at the onset of anaphase, as most cohesin molecules are removed by other pathways prior to anaphase (Hauf *et al*., 2005; Sumara *et al.*, 2002). If Separase is active in the cell prior to anaphase, the cleavage-dependent and –independent pathways will indiscriminately remove cohesin molecules, thereby reducing the cleavage-resistant impediment to chromosome separation prior to the onset of anaphase.

Many other cellular processes can potentially influence the levels of chromosome-bound cohesin and the ability of chromosomes to segregate accurately, and these are discussed in the following sections. The normal functioning of a cell depends on a cellular network that is highly complex, being made up of numerous interlinked and inter-dependent pathways. How the broad groups of genes identified in this study interlink to influence chromosome cohesion and segregation is presented schematically below (Figure 6.2). Each of these processes is considered in turn in the sections below. Alternative mechanisms for how some genes identified in this study are influencing the GMR>*Rad21*^{NC} phenotype have also been postulated where direct modulation of chromosome segregation is considered less likely.

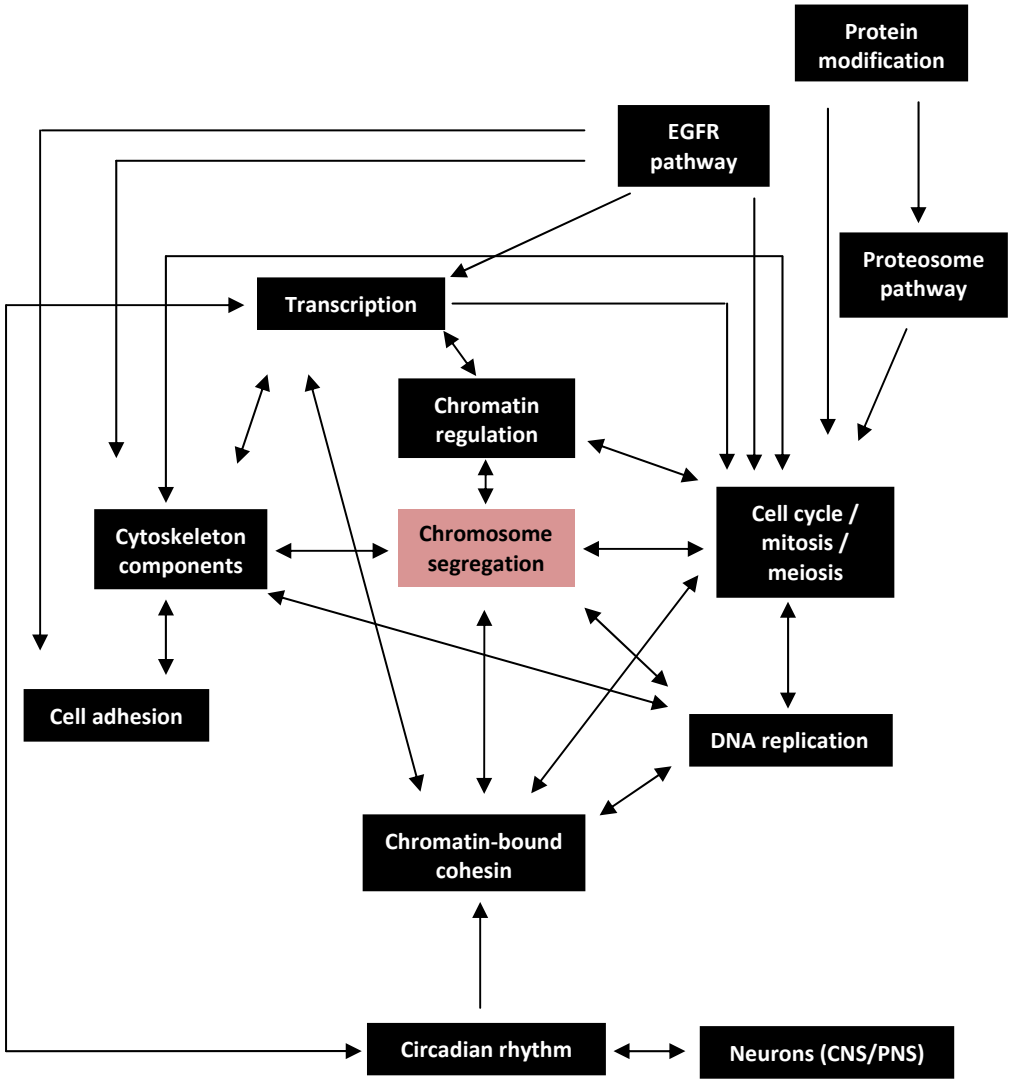

Figure 6.2: Inter-regulation of cellular processes.

6.3.2 DNA replication and the cell cycle

DNA replication is a discrete phase of the cell cycle that is regulated at a number of levels to ensure proper timing and accurate replication of the genome. DNA replication is closely linked with the loading of cohesin onto chromosomes and establishment of cohesion (Wang *et al*. 2000; Edwards *et al*. 2003; Skibbens *et al*. 1999). It is therefore explicable that several DNA replication genes have been

identified by the GMR>*Rad21*^{NC} modifier screen. Genes identified include those required for the initiation of DNA replication (*Mcm3, lat, dup*), formation of replication forks (*crm*) and polymerisation of nucleotides (*DNApolΔ*). As discussed in-depth in section 1.4.8, the replication fork facilitates establishment of cohesive cohesin onto chromosomes and cohesin loaded after S-phase is not able to establish cohesion (Moldovan *et al*., 2006; Mayer *et al*., 2001; Kenna and Skibbens, 2003; Edwards *et al*., 2003). Subtle perturbation in the action of these DNA replication genes is therefore likely to cause a reduction in the establishment of cohesion in S phase.

The delay in chromosome segregation and consequent delay of the exit from mitosis induced by non-cleavable cohesin is believed to have a significant influence on the final GMR>*Rad21*^{NC} phenotype (section 3.2.3.3). This cell cycle transition delay is likely to sensitise the cells to subtle changes in levels of key cell cycle regulators, such as those identified in this study (*Cyclin A, Cyclin B, cdc2, cdc2c, polo, myb, Dp,Rca1 vih* and *Rpn9*). Cdc2c is the binding partner of Cyclin E, and this complex regulates the entry into S phase (Sukhanova and Du, 2008; Sauer *et al*., 1995). CycA and CycB are binding partners for cdc2 and are integral in driving the cell into mitosis (Ohi and Gould, 1999) and the sequential destruction of Cyclins A and B is necessary for exit from mitotsis (Su *et al.*, 1998; Sigrist *et al.*, 1995). *Drosophila Myb, Dp and polo* are also involved in the regulation of the G2/M transition. Myb and Dp are responsible for regulating the transcription of the G2/M transition factors (Berckmans and De Vevlder, 2009). Polo regulates the G2/M transition by activating cdc25 (string kinase), which in turn activates the Cyclin B/cdc2 kinase (Lobjois *et al.*, 2009; Kumagai and Dunphy, 1996). Rca1, vih and Rpn9 modulate cell cycle progression through regulation of APC/C-mediated destruction of the mitotic cyclins (Mathe *et al.*, 2004; Zielke *et al.,* 2006; Grosskortenhaus and Sprenger, 2002; Wollenberg and Swaffield, 2001), which is discussed in greater detail in section 6.3.9. Further delaying the progression of the cell cycle would be predicted to allow cells more time to resolve chromosome non-disjunction and therefore would have been identified as GMR>*Rad21*^{NC} suppressors.

6.3.3 Chromatin structure and cohesin loading

A number of loci associated with the regulation of chromosome structure were identified in this study (*asf1, fs(1)Ya, JIL-1, Parg, prod* and *Su(var)2-10*), as well as a number of loci that regulate the expression of specific coding regions (*bon, brm, esc* and *Parg*). Accurate segregation of chromosomes is also contingent on the chromosomes being correctly packaged and condensed, most visibly during mitotic (and meiotic) prophase. Nuclear DNA is complexed with histones and other chromatin-associated proteins to form chromatin and is regulated at a number of organisational levels. Genes associated with various aspects and regulatory mechanisms of chromatin structure and regulation were identified in this study and are presented below in Figure 6.3.

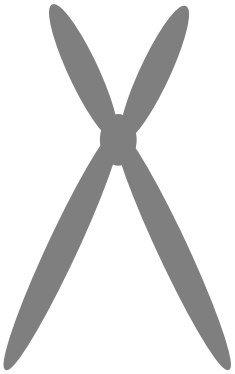

Figure 6.3: Chromatin structure effectors and regulators identified in the GMR>*Rad21*^{NC} screen. Overall chromosome structure is dependent on nucleosome assembly (*asf1*), higher orders of folding and specialised areas of heterochromatin and patterns of condensation (*JIL-1, fs(1)Ya, prod, Su(var)2-10*). Targeted regions of the chromatin can be modified to promote gene expression or effect gene silencing through ATP-driven remodelling (*brm*) or modification of histone tails (*esc*) or DNA methylation (*Parg*). (Deng *et al.*, 2008; Shrogen-Knaak *et al.*, 2006; Gurley *et al.*, 1978; Kingston *et al.,* 1996; Terriente-Felix and de Celis, 2009; Razin and Cedar, 1991; Rodriguez *et al.*, 2006; Erlich, 2006).

As discussed in section 1.4.6, a subset of cohesin loading has been associated with chromatin remodelling factors SNF2h (Hakimi *et al.,* 2002). Additionally, cohesin loading is specificially recruited to and concentrated at regions of heterochromatin (Nonaka *et al.*, 2002; Pidoux and Allshire, 2004; Bernard *et al.*, 2001). Therefore, it is predicted that regulators of chromatin structure have a direct effect on the amount of cohesin associated with cohesin or that chromosomal structural defects are influencing chromosome segregation.

6.3.4 Cytoskeleton components, spindle and cytokinesis

A significant number of loci associated with the cytoskeletal machinery and the mitotic spindle were identified as modifiers of the GMR>*Rad21*^{NC} phenotype. These included a centrosome structural protein (*γTub23C*) and centrosome regualtory proteins (*mars, polo, SMC1*), a kinetochore-associated microtubule protein (mit(1)15), a spindle pole protein (*vih*), mitotic spindle regulators (*cdc14* and eIF-1A) and microtubule movement regulators (*Klp3A, Gap1* and *polo*). The microtubules of the mitotic spindle are integral to accurate chromosome alignment and segregation (Figure 6.4) (Rao *et al*., 2009; King, 2008; Vogt *et al.*, 2008) . Not only the integrity of the structure of the spindle is key to accurate chromosome segregation, the spindle is also the target of the spindle checkpoint, The spindle checkpoint is the cell surveillance system that in normal cells prevents the segregation of unaligned and misaligned chromosomes by inhibiting the activities of the APC/C and the onset of anaphase (Kang and Yu, 2009; Lu et al., 2009; Qi and Yu, 2006). Subtle changes in the levels of kinetochore and spindle factors have been observed to result in severe chromosome segregation defects (Bakhoum *et al*., 2009) and therefore it would be predicted that heterozygosity or overexpression the mitotic spindle-associated factors identified as modifiers of the GMR>*Rad21*^{NC} phenotype are directly modifying the accuracy of chromosome segregation.

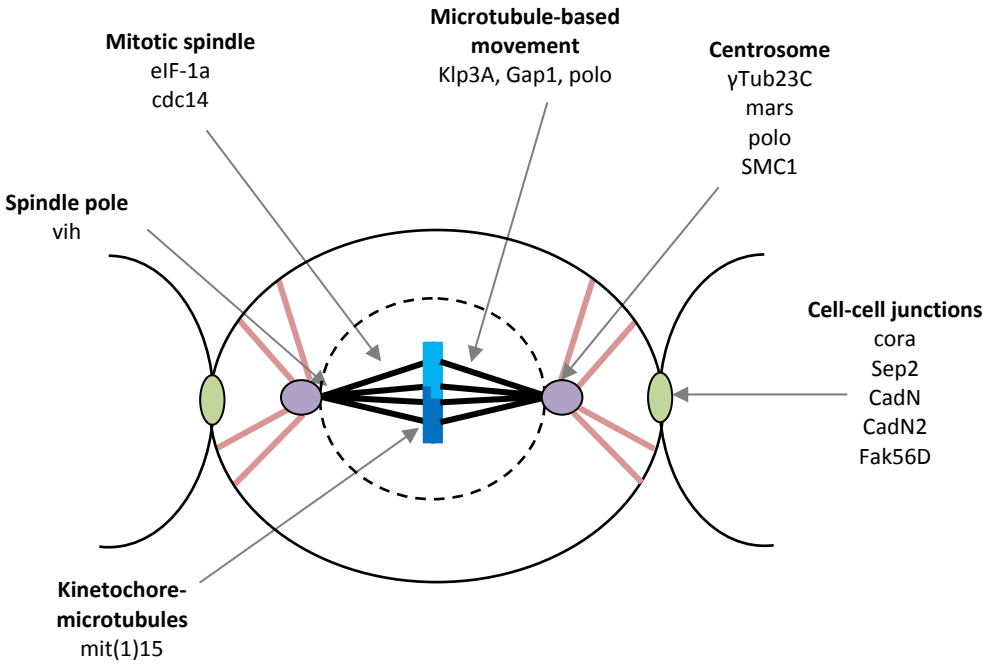

Figure 6.4: Mitotic spindle and M phase. The centrosome plays a central role in cell division as the point of nucleation of mitotic microtubules (de Sainte Phalle and Sullivan). Microtubules are responsible for the positioning of duplicated centrosomes and spindle poles, alignment of the chromosomes at the metaphase plate (Heald, 2000) and the poleward movement of chromosomes at anaphase (de Sainte Phalle and Sullivan, 1998; Matthies *et al*., 1996). The astral and spindle microtubules allow a dividing cell to generate the tension required to satisfy the spindle assembly checkpoint and provide the structures to facilitate accurate chromosome segregation (Zhou *et al.*, 2002; de Sainte Phalle and Sullivan, 1998).

Centrosomes have been linked to age-specific chromosome segregation abnormalities in human, murine, porcine and *Drosophila* oocytes (Schatten and Sun, 2009; Miao *et al*., 2009a; Miao *et al.*, 2009b; Schatten *et al*., 1999). Other key factors that have been associated with oocyte aging are MAPK and the maturation/mitosis promoting factor (MPF), with MAPK and MPF activity being demonstrated to gradually decreasing as oocytes age. MAPK associates with centrosome components and is thought to be necessary for centrosome and

microtubule stabilisation (Lee *et al.*, 2007; Sun *et al.*, 2002; Saavedra *et al.,* 1999). The Cyclin B subunit of the MPF is essential for the recruitment and stabilisation of the pericentriolar matrix protein NuMA (Sun and Schatten, 2007; Gehmlich *et al*., 2004). The centrosome-MAPK link is very intriguing as this provides a direct link between regulators of MAPK and the physical segregation of chromosomes.

Following the completion of mitosis, cells undergo cytokinesis to divide the cell mass and sequester the segregated chromosomes into the two daughter cells (Figure 6.5). The position of the spindle determines the site at which the cell membrane will furrow to initiate cytokinesis (Burgess and Chang, 2005; D'Avino *et al.,* 2005). There are a number of spindle-associated factors that influence the furrow positioning, including the spindle microtubules, the astral microtubules and chromosome passenger proteins (von Dassow, 2009; Vagnarelli and Earnshaw, 2004). The spindle microtubules appear to dictate the position of the cleavage plane midway between the spindle poles, while the astral microtubules appear to initiate furrow ingression by signalling to the cell cortex (Scholey *et al.*, 2003). The centrosomes are also integral in the completion of cytokinesis, although how they contribute is currently unclear (Khodjakov and Rieder, 2001; Piel *et al*., 2001).

Failure of cytokinesis results in tetraploidy and aneuploidy due to the replicated and segregated chromosomes not being sequestered into two daughter cells. Mutations that block the initiation of the cytokinetic furrow lead to failure of cytokinesis. For example, failure of the mitotic spindle to anchor at the anaphase cortex and altered expression of cytokinesis factors can result in failure of cytokinesis initiation and completion (Wilke*r et al*., 2007). Abnormalities in cytokinesis can also result in aneuploidy, for example mis-positioning of the contractile ring can result in chromosome missegregation and aneuploidy (Werner *et al.,* 2007). It is predicted that altered expression levels of cytokinetic factors will affect daughter cell chromosome inheritance through abnormal cytokinesis or complete failure of cytokinesis.

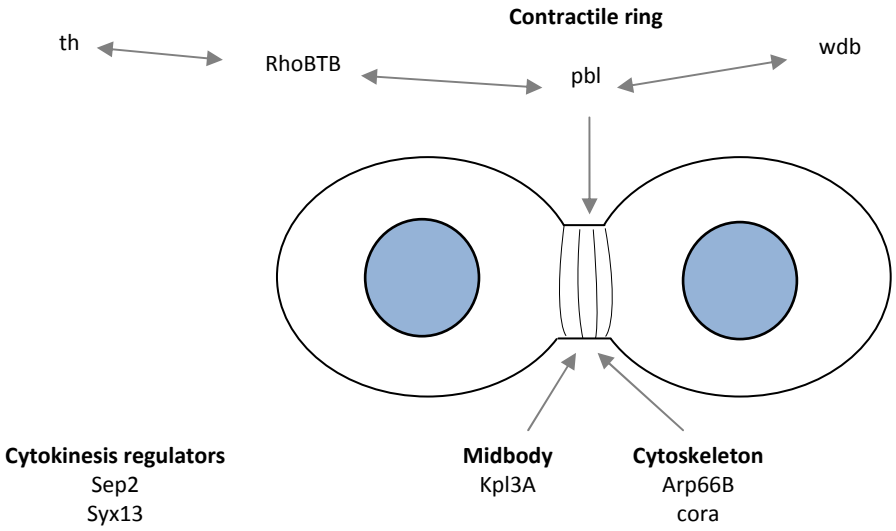

Figure 6.5: Cytokinesis. Once the chromosomes have been evenly divided between the spindle poles the cell mass must also be divided to distribute the organelles and other essential cellular contents equally between the two daughter cells in a process known as cytokinesis. At the site of furrow ingression a contractile ring forms, using actin and myosin II filaments to create a furrow that ingresses into the cell mass and finally undergoes abscission to completely separate the two daughter cells (Robinson *et al.,* 2002; Cao and Wang, 1990).

6.3.5 Cell junctions and cell division

Several genes involved in cell adhesion were identified as modifiers of the GMR>*Rad21*^{NC} phenotype, these include cadherins (*CadN, CadN2*), a focal adhesion kinase (*Fak56D*), a septin (*Sep2*) and a transmembrane protein (*Ten-m*). The main cell adhesion molecules with a recognised role in cell cycle signalling are integrins, cadherins, Merlin (neurofibromatosis 2), and their associated proteins (Figure 6.6). Integrins are associated with the ECM and frequently act in conjunction with growth factor receptors such as EGFR to promote cell proliferation by upregulating Cyclins D and E (Figure 6.6) (Streuli, 2009; Klein *et al*., 2007; Bjorge *et al.*, 2000; Erpel and Courtneidge, 1995). In contrast, cadherins and Merlin are located on the lateral walls of a cell and transmit contact inhibition signals that inhibit cell proliferation by down-regulating the G1-S cyclins (Klein *et al*., 2007; Pugacheva *et al.*, 2006). Consequently these loci may modify the GMR>*Rad21*^{NC} phenotype via modulation of the cell cycle. The signalling pathways activated by these adhesion molecules regulate not only the G1 cell cycle machinery to influence the entry in S-phase, but also show cross-regulation. For example, signalling through the integrin pathway influences cadherin levels at the cell junctions. This study identified components of the EGFR pathway (discussed in section 6.3.7), Src family members (*Src42A, shark*) and a MEK kinase (*MEKK1*). Initiation of, exit from and correct execution of mitosis also depend upon the integration of signals from cell junction proteins (Pugacheva *et al.*, 2006). As discussed previously, altering the progression of the cell cycle would be predicted to have a significant effect on the resolution of chromosome segregation.

The cell adhesion molecules also have a structural role in mitosis. Cadherins and integrins have been demonstrated to be involved orienting in the mitotic spindle in mammalian epithelial cells (den Elzen *et al.,* 2009; Streuli, 2009; Toyoshima and Nishida, 2007). Cell junctions are also involved in orienting the cell division apparatus in *Drosophila* (Lecuit and Wieschaus, 2002). Cell contacts are reduced during mitosis, with cell attachment proteins being relocated and focal adhesions disrupted to allow reduction in attachment-associated signalling and movement of necessary proteins to the mitotic spindle. Later, integrin attachments are required for the abscission event in cytokinesis (Pugacheva *et al.*, 2006). As discussed

previously in section 6.3.4, correct orientation of the spindle and correct execution of cytokinesis is essential to maintain genomic stability.

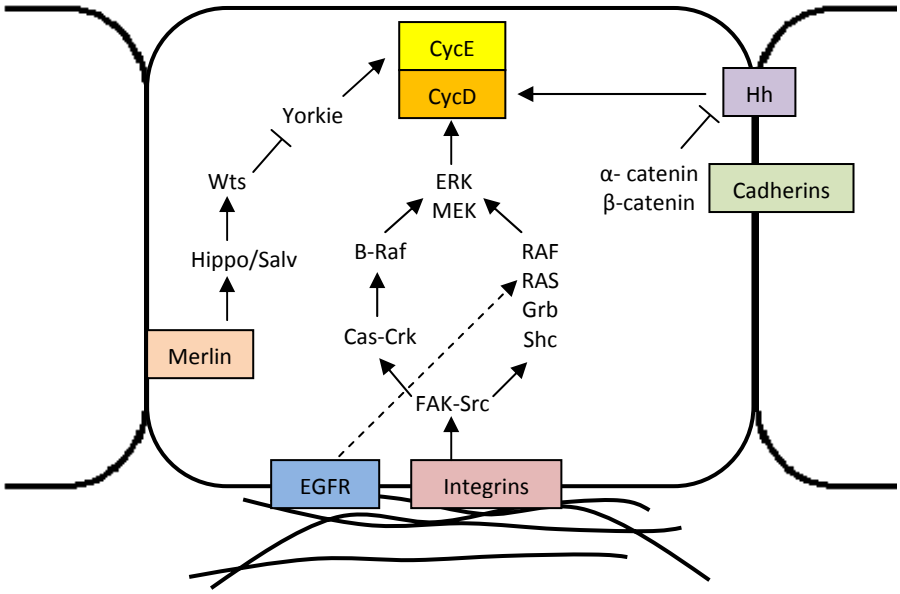

Figure 6.6: Cell adhesion regulation of the G1-S cell cycle transition. The signalling pathways initiated by integrins, cadherins and Merlin intersect to regulate the G1-S transition and cell proliferation rates.

6.3.6 DNA repair factors and centrosome duplication

DNA double-stranded break (DSB) repair factors have been linked to regulation of centrosome duplication. The centrosomes regulate spindle formation, with two centrosomes normally producing two spindle poles. An abnormal centrosome number has been linked to aneuploidy in tumourigenesis (Chng and Fonseca, 2009; Lingle *et al*., 2002; Nigg, 2006). The cohesin subunit SMC1 has an identified role in DNA damage repair and also localises to the centrosome (Shar *et al.*,. 2004; Kitagawa *et al.*, 2004; Shimada and Komatsu, 2009), providing another mechanism for SMC1 alleles to modify chromosome segregation. Another modifier locus identified in this study is *Parg*, the protein product of which antagonises the activities of PARP1 (Amé *et al.*, 2009) which localises with SMC1 at the centrosomes and is part of the DNA DSB repair pathway (Haince *et al.,* 2007; Tulin *et al*., 2006). In further of support of this as a mechanism of chromosome segregation modification, NBS1 is also central to DNA damage, localises at the centrosomes and modifies the GMR>*Rad21*^{NC} eye phenotype (Keall, unpublished). *Plk1* (*polo*) recruits γ-tubulin to the centrosome where it forms a part of the pericentriolar matrix and is the point of regulation targeted by the DSB repair factors (Haren *et al*., 2009). The proteins SMC1 and NBS1 are recruited to the centrosomes along with BRCA1, BRCA2, ATM, ATR and PARP1 (Shimada and Komatsu, 2009) and these proteins provide a link to the cell cycle and checkpoints to regulate the duplication of centrosomes, which occurs in preparation of cell division (Shimada *et al*., 2009; Parvin, 2009). This group of proteins also have a well established role in DNA DSB repair where they act in concert (Canman and Lim, 1998; Carney *et al*., 1998; Jackson 1996).

Two other genes, *asf1* and *haywire* (*hay*), with DNA repair functions were indentified in this study. *Asf1* forms part of the replication-coupled assembly factor (RCAF) complex, which assembles nucleosomes following DNA replication and repair of DNA DSBs (Tyler *et al*., 1999). Therefore *asf1* is closely linked to the DNA repair functions of SMC1, ATM and ATR, and may also have a role in centrosome regulation. The protein product of *hay* is involved in nucleotide excision repair and also acts as an RNApolII transcription factor and has been functionally associated with the tubulin molecules of the *Drosophila* meiotic spindle (Regan and

Fuller, 1990). It is most likely that modification of the GMR>*Rad21*^{NC} phenotype by hay was through the microtubules of the mitotic spindle.

6.3.7 Epidermal growth factor receptor (EGFR) pathway and Ras/MAPK signalling

A significant number of the genetic modifiers identified in the GMR>*Rad21*^{NC} screen are associated with the EGFR pathway (Figure 6.7, red squares). EGFR, a cell surface receptor, is activated by a variety of ligands and elicits a wide variety of cellular responses including cell proliferation, cell survival and cell differentiation (Jost *et al.*, 2000; Prigent and Lemoine, 1992). EGFR activation is recognised as the main trigger for cell differentiation during compound eye development (Freeman, 1998). However, the fate of cells is tempered through the interaction of the EGFR pathway with other signalling pathways such as Notch and Wingless, which are generally antagonistic to EGFR signals (Freeman, 1997). EGFR signalling is activated by the Spitz ligand and inhibited by the secreted protein, Argos (Figure 6.7), which forms a negative feedback loop. The downstream effectors of the EGFR (including *Jun, pnt* and *Yan*) are all targeted through the Ras/MEK/MAPK pathway. These effectors regulate expression of target genes that influence cell proliferation, survival (*hid*), growth and differentiation (*lilli*). Mutants of EGFR and Argos, the negative regulator of EGFR, both modify the GMR>*Rad21*^{NC} phenotype, confirming the link between the GMR>*Rad21*^{NC} phenotype and EGFR signalling cascade. Interaction with the EGFR pathway is another indication that cell differentiation and cell survival are underlying factors the can modify the GMR>*Rad21*^{NC} eye phenotype.

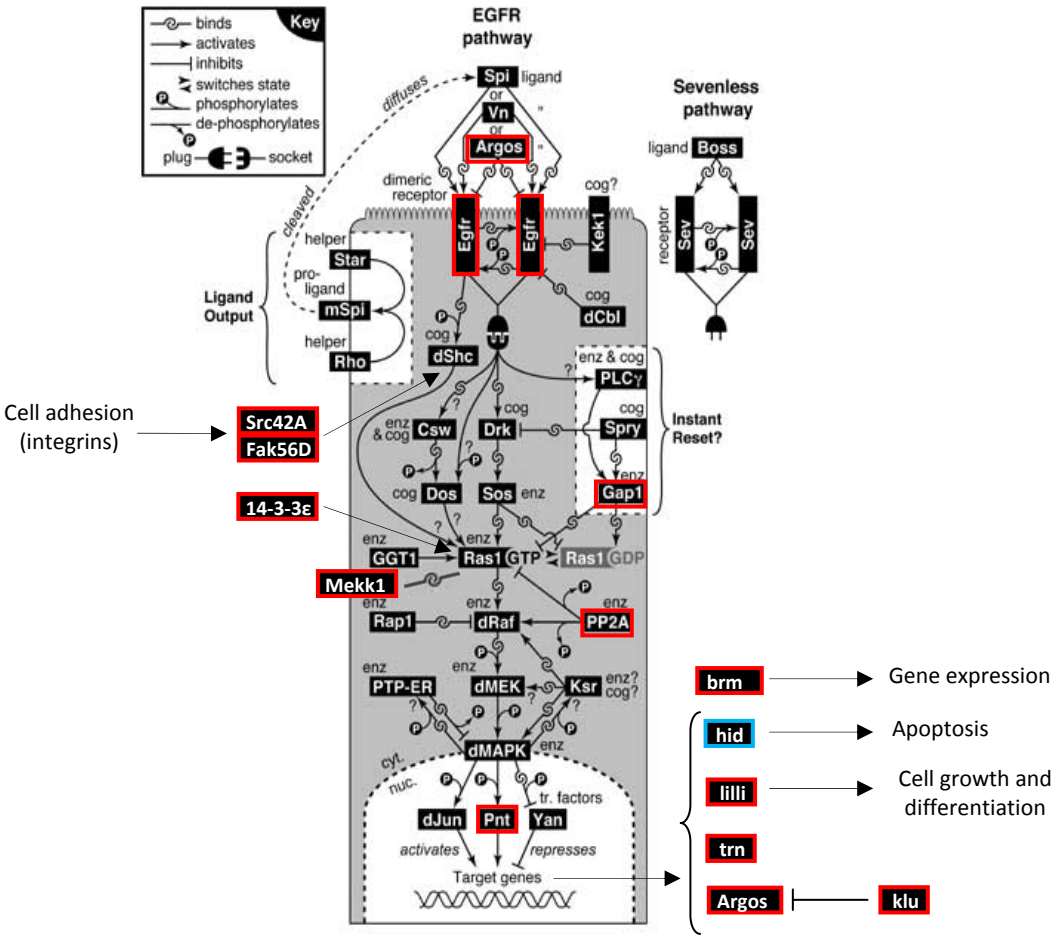

Figure 6.7: The EGFR signalling pathway. The activated EGFR primarily signals through the Ras/Raf/MAPK pathway to elicit a range of cellular responses through targeting of specific effector genes. Target genes include Argos, which downregulates EGFR in a negative feedback loop. Proteins boxed in red indicate identified modifiers of the GMR>RAD21^{NC} phenotype.

6.3.8 Gene product expression

The expression of genes is regulated at many different levels. This study identified a number of transcription factors (*CG6272, dl, dm, EcR, kni, Taf6*) and co-activators (*bon, brm, nej/CBP*), transcriptional repressors (*dl, kni*) and negative regulators (*lin-52*) of mRNA production. Modifiers identified in this study also included regulators of post-transcriptional events, including mRNA splicing (*CG3542, hay, Hrb27C, snf*) and mRNA degradation (*pcm*). Translation factors were also identified, such as translational repressors (*cup*), translation initiation factors (*eIF-4a, eIF-3p66, hay*)

and ribosome biogenesis factors. (*Mys45A)*. Almost all of these factors are not general regulators of gene expression, but instead are known to be specifically associated with the regulation of select genes within particular cellular processes. A number of the genes identified have known links to mitosis and cell-cycle regulation (*brm, cup, eIF-3p66, nej/CBP*) (Somma *et al*., 2009; Martinez *et al*., 2006; Bjorklund *et al.*, 2006; Okada *et al.*, 2002) and several have known links to the EGFR pathway (*brm, dm, EcR, kni*) (Terriente-Felix and de Celis, 2009; Orian *et al.*, 2007; Hackney *et al.*, 2007; Diaz-Benjumea and Garcia-Bellido, 1990). The fact that a significant number of these genes are linked to the cell cycle and cell proliferation suggests that these genes are more likely to be influencing cell cycle progression and potentially chromosome segregation, rather than simply affecting transgene expression levels.

6.3.9 Anaphase promoting complex/cyclosome (APC/C) and the proteasome

The proteasome is a very large protein complex that is responsible for the majority of homeostatic protein degradation in the cell. Proteins are directed for degradation through the addition of a poly-ubiquitin tag by ubiquitin ligases. This study identified subunits of the proteasome (*Tbp-1/proteasome 26S regulatory subunit 6A* and *Rpn9*), a ubiquitin conjugating enzymes (*vih*ar) and a ubiquitin-ubiquitin ligase (*CG11070*) and ubiquitin ligase regulators (*cortex*, the COP9 signalosome subunit *CSN3* and *Regulator of Cylin A 1*) as modifiers of the GMR>*Rad21*^{NC} phenotype. Mutations in these factors are predicted to alter the ubiquitination and degradation of key protein targets. The proteasome is made up of over 62 subunits, with Rpn subunits being the dominant factor in the regulatory particles or "lids" and the 20S core being made up a range of subunits that form a hollow barrel structure (Wollenberg and Swaffield, 2001). Degradation of essential proteins is a common way for the cell to limit a cellular process, for example, the APC/C ubiquitin ligase targets securin for degradation at the onset of anaphase and the ubiquitin conjugating enzyme vihar together with the APC/C targets Cyclin B for degradation to initiate exit from mitosis (Straight *et al.*, 2003; Peters, 2002; Yanagida, 2000). Cortex has previously been identified as a meiosis-specific regulator of APC/C activity (Pesin and Orr-Weaver, 2007), however, modification of the GMR>*Rad21*^{NC} phenotype would suggest that this function may be conserved in at least some somatic tissues or

at certain points in development. The COP9 signalosome complex regulates the APC/C and another ubiquitin ligase complex, Cullin (Kob *et al.*, 2009). Altering the activity of the APC/C is predicted to alter securin degradation thereby influencing Separase activity and the cleaving of the cohesin rings on the chromosomes. The APC/C also regulates the levels of the mitotic cyclins (Cyclins A and B) and Rca1 functions to specifically inhibit APC/C destruction of the mitotic cyclins in early mitosis (Zielke *et al,* 2006; Grosskortenhaus and Sprenger, 2002). It is therefore highly likely that mutations in APC/C and proteasome-related factors can also affect cell cycle progression (Wojcik and DeMartino, 2002). In further support of this, COP9 subunits (including CSN3) have been identified, in a *Drosophila* RNAi screen, regulators of cell size and cell cycle (Bjorklund *et al.,* 2009).

6.3.10 Circadian rhythm genes

The PP2A regulatory subunit *widerborst* (*wdb*), identified as a GMR>*Rad21*^{NC} modifier in this study, has been demonstrated to stabilise the circadian clock protein PERIOD (PER), which is a binding partner and regulator for TIMELESS (TIM) (Sathyanarayanan *et al.*, 2004; Landskron *et al.*, 2009). The *C. elegans* gene *tim-1*, a homologue of the *Drosophila* circadian rhythm regulators *timeless* (*tim*) and *timeout*, has been found to bind directly to the cohesin complex and is necessary for the loading of the RAD21 (Rec8) and SA subunits onto chromatin (Chan *et al*., 2003). Reduction of *tim-1* via RNAi mimics the cohesion defects observed when cohesin subunits are removed (Chan *et al.*, 2003). TIM-1 and TIMEOUT also share protein domains with SCC2 and PDS5, which have been identified in other species as essential for cohesin loading and establishment and maintenance of cohesion, respectively (Golden and Cohen-Fix, 2003).

The link between TIM-1 and cohesin has demonstrated a novel and unexpected function for circadian rhythm and related proteins in chromosome segregation. The GMR>*Rad21*^{NC} modifier loci *CG5618*, *CG9643*, *nej*, *Nep4*, and *Pdp1* all have been identified in circadian rhythm screens or linked with other components of the clock. PDP1 has been demonstrated as an integral component of the CLOCK/CYCLE feedback loop (Ueda *et al.*, 2002; Cyran *et al*., 2003; Allada, 2000), which regulates the *Drosophila* clock, while NEJ/CBP physically binds to CLOCK and co-activates

CLOCK/CYCLE regulated transcription (Hung *et al*., 2007). The expression levels of hundreds of *Drosophila* genes have been found to be regulated by the circadian rhythm (Ueda *et al*., 2002) and it may be that the circadian rhythm genes listed above are influencing gene expression in general rather than having a direct effect on chromosome segregation. Alternatively, these modifiers may be modifiers of the interphase role(s) of cohesin via CTCF and associated chromatin remodelling factors.

6.3.11 Immune and stress response genes

A number of immune and stress response genes were identified as modifiers of GMR>*Rad21*^{NC} phenotype: *Toll-9, Pli, smt3, nmo* and *dl* are involved in the Toll/NFkappaB (NFκB) pathway, *vir-1* and *r2d2* are the RNA interference (RNAi) response to viral infections and *Ect4* is poorly understood. It is not immediately obvious why immune system genes have been identified in this screen, however, other research groups have identified cellular immune response and surveillance genes and environmental stress response genes as being upregulated in aneuploid lymph node tumour cells (Grade *et al.*, 2007). Aneuploidy results in disruption of delicate gene dosage balances and it may be that these stress response genes are able to modulate the influences of these gene dosage imbalances. Altering the expression profile of these stress response genes may significantly alter the ability of a cell to survive aneuploidy and alteration of immune response gene expression may affect the ability of the immune system to detect and eliminate abnormal cells.

The majority of the loci identified in this study with an immune response role function in the Toll pathway, which classically responds to fungal pathogens and most Gram-positive bacteria (De Gregorio *et al.*, 2002; Tanji *et al*., 2007). Activated Toll receptors initiate the Toll signalling pathway, which leads to activation of the NFκB transcription factor, the *Drosophila* homologue of which is *dorsal* (*dl*). Dorsal activation results in the upregulation of a variety of antimicrobial peptides (Tanji *et al.,* 2007; De Gregorio *et al.*, 2002). Dorsal activity is inhibited by Cactus (IκBα homologue), which is degraded by activated the IκB Kinase (IKK) complex (activated by the NEMO subunit) (Prajapati and Gaynor, 2002), followed by Tube, Pelle and Pellino (Pli)-mediated (Grosshans *et al*., 1999) transportation of dl and Dif

(IKK2 homologue) into the nucleus (Silverman *et al.,* 2000). Dorsal activity is promoted by smt3 (ubiquitin-like protein) conjugation (Bhaskar *et al.*, 2002). In contrast to the Toll/NFκB genes identified, no members of the immune deficient (IMD) response pathway, which typically responds to infections by Gram-negative bacteria (Tanji *et al*., 2007; De Gregorio *et al.*, 2002), were identified. Dorsal function is not limited to the immune response and has been functionally linked to dorsoventral patterning in the *Drosophila* embryo (Biemar *et al.,* 2006; Letsou *et al.*, 1999).

The mouse NFκB inhibitor kinase IKK2 (homologue of *Drosophila* Dif) has been found to regulate the stability of the mitotic spindle. Reduced IKK2 deregulates Aurora A kinase resulting in misregulation of the kinesin-like motor protein KIF11 and destabilisation of the mitotic spindle (Irelan *et al.,* 2007). Although Dif was not tested in this study, this evidence provides a direct link between the factors of the NFκB pathway and the physical structure that segregates chromosomes during anaphase. An ubiquitin- and sumoylation-mediated DNA damage response provides an intriguing link between several modifier loci. DNA damage results in SUMO (smt3) modifying NEMO (nmo) via sumoylation, causing NEMO to be phosphorylated by ATM kinase followed by ubiquitination by unknown E3 ligases. This modified NEMO population then activates the IKK complex, which in turn promotes the degradation of IκB, resulting in the activation of NFκB (dl) (Huang *et al*., 2003; Sun and Chen, 2004). The presence of non-cleavable cohesin complexes on chromosomes in dividing cells is anticipated to produce DNA damage as a result of impeded separation of the chromatin mass. Therefore, modification of the GMR>*Rad21*^{NC} by *smt3, nmo* and *dl* may be a result of change in the cellular response to this DNA damage.

The loci *r2d2* and *vir-1* are involved in RNAi-mediated anti-viral response and both associate with Dicer-2 (Liu *et al.*, 2003; Galiana-Arnoux *et al.*, 2006). The role of the Dicer-2 complex is not limited to immune response; it has also been shown to regulate endogenous gene expression through microRNA (miRNA)-mediated silencing (Liu *et al.*, 2003) and to be involved in regulating the stability of heterochromatin (Peng and Karpen, 2009). Therefore, these RNAi factors may be influencing the GMR>*Rad21*^{NC} eye phenotype by modulating the expression of

essential genes or modifying the levels of heterochromatin and consequently the number of cohesin complexes loaded onto the chromosomes. No functional analyses have been carried out on *Ect4*, however, *in silico* analysis has linked this locus to the innate immune response (Flybase, 2009)

6.3.12 Compound eye development genes

Drosophila compound eye development is a tightly regulated process that results in the highly structured ommatidial array observed in the adult eye. The formation of this organ involves the integration of many different levels of structural development and organisation, including cell differentiation, recruitment of cells into ommatidia, selective cell proliferation and programmed cell death (*klu, ninaE*), and ommatidial rotation (*nmo*). This study identified a range of genes involved in eye development, some of which are recognised as eye-specific factors (*gl*), others that are involved in imaginal disc development generally (*in*), and others that have very specific roles in eye development but have unique functions in other tissues (*ninaE*, *Six4)*. These genes are considered unlikely candidates for chromosome cohesion regulation.

6.3.13 Neuronal genes

A number of the genes identified in this study are linked to human mental retardation syndromes, as the *Drosophila* homologues of the human disease genes (Table 6.1). This suggests these modifier loci are influencing the GMR>$Rad21^{NC}$ phenotype through a cohesin role other than chromosome segregation. Although expression of these genes is not restricted to the nervous system, the foremost disease manifestations associated with mutations in these genes are neuronal indicating the particular sensitivity of neurons and the nervous system.

A post-mitotic role for cohesin has been identified in neuronal cells, which are distinctly sensitive to cohesin removal from chromosomes after cells have finished dividing (Pauli *et al.*, 2008). This removal of cohesin was found to reduce the expression of the steroidal hormone receptor *EcR* and to lead to failure of axon pruning in mushroom body neurons (Pauli *et al.*, 2008; Schuldiner *et al.*, 2008). A growing body of evidence supports a role for cohesin in developing neurons, with

the cohesin loading factor Scc4 identified as a neuron migration factor in *C. elegans* (Seitan *et al.,* 2006; Takagi *et al.*, 1997), and the cohesin subunits SMC1 and SA/STAG1 have been implicated in axon pruning (Schuldiner *et al*., 2008).

Table 6.1: *Rad21*^{NC} modifier genes implicated in human mental retardation

***Drosophila* homologue**	**Gene function**	**Human disease gene**	**Associated syndrome**
wds (*will die slowly*, other)	DNA repair (transcription-coupled): CNS development/ function (myelin)	*CKN1* (*CSA*)	Cockayne syndrome type I
nej *(nejire*)	Transcription regulation: CNS development/function; chromosome structure	*CREBBP* (*CBP*) CREB-binding protein	Rubinstein-Taybi syndrome
hay *(haywire)*	Transcription/DNA repair: CNS development/ function	*ERCC3* (*XPB*) Xeroderma pigmentosum type B	XPB/Cockayne syndrome
lilli *(lilliputian)*	Transcription regulation: CNS development/ function (neuronal differentiation)	*FMR2* Fragile site mental retardation 2	X-linked nonspecific MR
nbs	DNA repair: CNS development/function	*NBS1*	Nijmegen breakage syndrome
CG4288, others	Lysosomal pathway (various): MR 2° local toxicity (neuron, glia)	*SLC17A5*	Infantile sialic acid storage disorder; Salla disease
CG3947	Metabolic (oxidation): CNS development/ function (neuron migration, glia)	*PEX16*	Zellweger syndrome

(Inlow and Restifo, 2004)

Neurons may be uniquely sensitive to changes in cohesin function, as evidenced by the mild variant of Cornelia de Lange syndrome (CDLS), which is associated with mutations in human SMC1α and SMC3 in that are hypothesised to modify the ability of cohesin to associate with chromatin (Revenkova *et al.*, 2008; Deardorff *et al*., 2007). Individuals with this milder variant of CDLS typically display mental retardation and very few of the physical development issues normally associated

with CDLS (Deardorff *et al*., 2007). The most likely explanation for the neuronal effects observed is that modulation of cohesin association with chromatin disturbs the expression profile of essential genes, as cohesin has been shown to influence the ability of insulators and long-range enhancers to regulate the expression of select genes in yeast and metazoans (Wendt *et al.*, 2008; Rollins *et al.*, 2004; Donze *et al.,* 1999).

In terms of the *Drosophila* GMR>*Rad21*^{NC} model, the neural origins of the photoreceptor cells is a reasonable explanation for the identification of neuronal genes in the GMR>*Rad21*^{NC} screen. Each individual ommatidium contains eight photoreceptor neurons, four cone cells and two primary pigment cells. There are nine additional cells, six secondary pigment cells and three tertiary pigment cells, shared between adjacent ommatidia (Figure 6.8). Five of the eight photoreceptor cells are present and recruited as the morphogenetic furrow progresses, forming a precluster of cells that form the basis of an ommatidium. Another three photoreceptor cells and the other ommatidial cells are recruited in the passing of the second mitotic wave (Figure 6.9) (Ready *et al.,* 1976) and therefore are likely to be directly affected by the ectopic expression of RAD21^{NC} under the control of the GMR driver.

On the basis that approximately 750 ommatidia make up the adult compound eye and that three photoreceptor cells are formed in the second mitotic wave (Ready *et al.,* 1976), it is predicted that around 2,250 cells destined to become photoreceptors will be expressing RAD21^{NC} and undergoing cell division in the developing eye. The effect of RAD21^{NC} on the developing eye is likely to sensitise the developing tissue to changes in expression levels of genes involved in neuron development and function, resulting in a change in the final eye phenotype. Several genes identified in this study have recognised roles in nervous system function, such as synaptic transmission (*CG5559, Hip14* and *Shal*), or have been linked to neurological development and neurodegeneration phenotypes (*CG31163, Gyc76C, hb, mam, mle, Nep4, oaf* and *Pka-C3*). Several of these genes have other well known functions that are not specific to the nervous system.

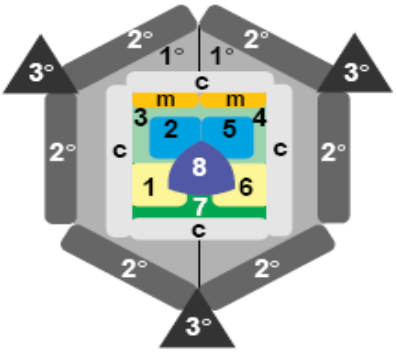

Figure 6.8: *Drosophila* ommatidial cell cluster in the developing eye imaginal disc. Cells 1-8 are the photoreceptor cells, surrounded by the four cone cells (c). Two primary (1˚) pigment cells are also part of the individual ommatidium, with six secondary (2˚) and three tertiary (3˚) pigment cells being shared between the ommatidia. The 'mystery cells' (m) are only present in the 3rd instar imaginal disc and later disappear. (Figure adapted from Freeman, 1997).

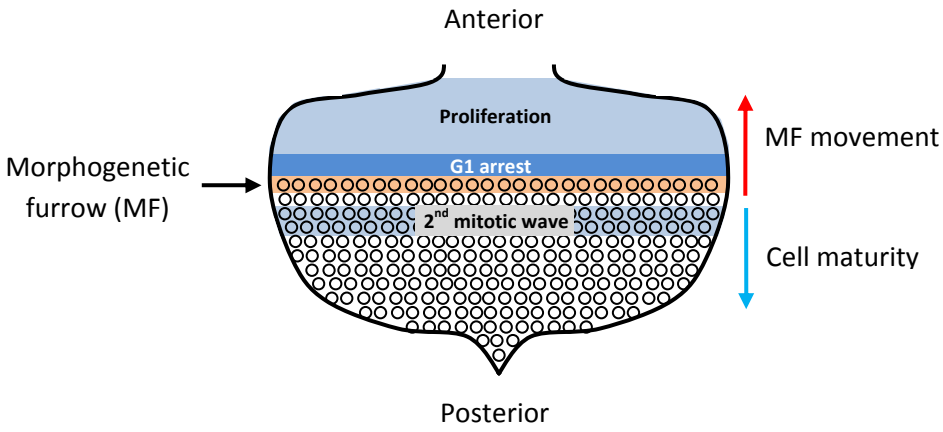

Figure 6.9: *Drosophila* eye development in the eye-imaginal disc. In the developing eye cells proliferate asynchronously until the morphogenetic furrow passes from the posterior to the anterior of the eye imaginal disc, inducing a G1 arrest ahead that synchronises the cells followed by a final round of division of a subset of cells termed the 2nd mitotic wave. Cells posterior to the MF undergo differentiation as they mature. (Adapted from Freeman, 1997).

6.3.14 Genes of unknown or miscellaneous function

A significant number of the GMR>*Rad21*^{NC} modifiers identified in this study have not been studied or studied in insufficient detail to identify their true molecular and cellular function. Approximately half of these genes from this group (in Table 4.48) have no predicted molecular or cellular functions (*CG9368, CG11523, CG12885, CG13255, CG30484, CG32432*) and therefore their potential as chromosome cohesion and segregation regulator cannot be speculated upon at this juncture. Other genes with predicted molecular activities such as protein binding (*CG2709, CG8786*), DNA binding (*sba*), ATPase activity and intracellular transport activity (*CG9330*) have little additional evidence linking these activities to other genes or cellular functions. The gene *six-banded* (*sba*), has undergone limited study but is known to be a DNA-binding protein that is expressed in a six-banded pattern in the developing embryo and is also expressed in the eye-imaginal disc (Zeidler and Mlodzik, 1997). This eye-specific expression is suggestive that *sba* is unlikely to be a general somatic regulator of cohesin and chromosome cohesion. The remaining genes have diverse functions that do not have any obvious link to chromosome function or regulation, including olfactory receptor (*Or85d*), alcohol metabolism (*Fdh*), and isoleucyl-tRNA aminoacylation (*Aats-ile*).

6.3.15 A consolidated chromosome cohesion regulator candidate list

The identified genetic modifiers of GMR>*Rad21*^{NC} are all potential regulators of chromosome cohesion and chromosome segregation. These modifiers can be classified as 'good' or 'poor' candidates for further investigation based on a variety of factors. As discussed above, the focus of this study is to identify regulators of chromosome cohesion and segregation; therefore, modifiers that may directly interact with the cohesin complex in other cellular roles, such as neuronal genes, are considered poor candidates for further study in regards to chromosome cohesion. 'Good' candidates have been selected based on function, identification in similar studies and the outcome of the secondary assays. It is unlikely that all of these genes are influencing chromosome segregation and further testing is required, as discussed below in section 6.4.3.

Table 6.2: Modifier alleles as candidates for chromosome cohesion regulation		
"Good" candidates for further study		**"Poor" candidates for further study**
SMC1	*CadN*	*CG2709*
SMC3	*CadN2*	*CG6272*
SA	*cora*	*CG8786*
san	*Src42A*	*CG9330*
polo	*Ten-m*	*CG30484*
PP2A-B'	*ha*	*sba*
gwl	*Parg*	*bowl*
cdc2	*CG5618*	*CG2264*
cdc2c	*CG9643*	*CG4288*
cort	*nej/CBP*	*CG4570*
CycA	*Nep4*	*Or85d*
Dp	*Pdp1*	*Vha100-2*
koko	*wdb*	*Aats-ile*
Myb	*ari-1*	*CG3947*
Nup98	*CG11070*	*CG7304*
oaf	*CSN3*	*Fdh*
Rca1	*Rpn9*	*CG5559*
Rpn9	*Tbp-1*	*CG31163*
Scim13	*bon*	*Gyc76C*
Scim32	*brm*	*hb*
vih	*esc*	*Hip14*
asf1	*fs(1)Ya*	*mam*
crm	*JIL-1*	*Nep4*
DNApolΔ	*prod*	*Pka-C3*
dup	*Su(var)2-10*	*Shal*
lat	*14-3-3ε*	*gl*
Mcm2	*Fak56D*	*in*
Mcm3	*klu*	*klu*
Arp66B	*lilli*	*nej/CBP*
cdc14	*Mekk1*	*ninaE*
eIF-1A	*Gap1*	*Six4*
γTub23C	*pnt*	*dm*
Klp3A	*trn*	*Hrb27C*
mars	*Taf6*	*kni*
mit(1)15	*eIF-3p66*	*Dhh1*
pbl	*th*	*mle*
RhoBTB	*lin-52*	*CG6272*
Sep2	*cup*	*eIF-4A*
smt3	*rd2d*	*Eig71Ei*
mrj	*vir-1*	*EcR*
dl	*Toll-9*	*snf*
Pli	*Egfr*	*CG3542*
pcm	*Ect4*	
Mys45A	*CG13255*	
CG9368	*CG12885*	
CG11523	*CG32432*	

6.4 IMPLICATIONS

6.4.1 Human aneuploidy syndromes

The study of human aneuploidy risk factors in humans is an extremely complex undertaking due to the incomplete understanding of the numerous aetiological factors that are known or suspected to contribute to meiotic aneuploidy. Currently there are no recognised genetic risk factors for the maternal age effect on human gametic aneuploidy. The studies demonstrating a maternal age-like effect in mice and flies with null mutations in SMC1β and SMC1 (Hodges *et al*., 2005; Subramanian and Bickel, 2008) clearly implicate the cohesin complex as a molecular suspect in the gametic aneuploidy. Therefore, genetic risk factors of chromosome cohesion and segregation identified in this and similar studies offer insight into the potential cellular mechanisms underlying the maternal age effect.

6.4.2 Aneuploidy and cancer

Aneuploidy was first linked to cancer cells over a century ago when asymmetric mitoses were observed on bipolar spindles by German pathologist David von Hansemann in 1890. Aneuploidy is now recognised as a very common occurrence in cancer cells, with most solid tumours (>90%) containing of aneuploid cells, frequently with structural abnormalities caused by inversions, deletions and duplications (Medema, 2008; Rajagopalan and Lengauer, 2004). A chicken-or-the-egg debate has reigned in cancer research as to whether aneuploidy is a cause of or an effect of cancer development, as chromosome missegregation can have both tumour-promoting and tumour-inhibiting effects (Weaver *et al*., 2007; Schmidt and Medema, 2006; Marx, 2002). The majority of evidence is now leaning towards aneuploidy being an event on the road to tumourigenesis, possibly as an artefact of decreased cellular fitness and less efficient metabolic processes, or a deliberate path taken by cells to further destabilise their genome to promote tumourigenesis (Marusyk and DeGregori, 2008). Although over a century of research has yielded a wealth of data concerning genes that could individually contribute to aneuploidy, it is still unclear when and in what context somatic chromosome missegregation occurs and the mechanisms that link aneuploidy to tumourigenesis (Chandhok and Pellman, 2009).

Current evidence indicates that there are a number of different mechanisms by which somatic aneuploidy can arise. Aneuploidy may arise in diploid cells through missegregation of individual chromosomes or alternatively, may arise through whole genome duplication (via a tetraploid intermediate) (King, 2008), with subsequent loss and/or gain of individual chromosomes. Individual chromosomes can be lost and gained during cell division due to merotelic attachments, defective chromosome cohesion, and mitotic spindle and SAC errors (Cimini, 2008; King, 2008; Salmon *et al*., 2005; Medema, 2008; Vader and Lens, 2008;Buffin *et al.*, 2005; Karess, 2005; Cimini *et al*., 2001). These mechanisms are believed to underlie chromosomal instability (CIN), an accelerated rate of chromosomal gain and loss that correlates with tumour progression and poor prognostic outcome.

6.4.2.1 Defective chromosome cohesion and cancer

Failure of chromosomes to remain "cohesed" until the onset of anaphase results in the cell being unable to control segregation of the chromatids. Many proteins are involved in not only establishing and maintaining chromatid cohesion, but tightly regulating cell cycle events so that cohesion is removed at exactly the right moment. A multitude of these genes, including *Separase, securin, Cyclin B, polo, SGO1, BRCA1, WAPL, APC,* and *Mcm2,* have been identified as misregulated in certain types of cancers (Meyer *et al.*, 2009; Liu *et al.,* 2003; Iwaizumi *et al.*, 2009; Skibbens, 2008; Oikawa *et al*., 2008; Ohbayashi *et al.*, 2007; Uhrhammer and Bignon, 2008; Kulkarni *et al*., 2007) and chromosome missegregation can be induced by mimicking these altered expression patterns in cultured cells (Zhang *et al*., 2008; Iwaizumi *et al.*, 2009; Ohbayashi *et al.*, 2007). These strong links between cohesin and cohesin regulators as risk factors for somatic aneuploidy and tumourigenesis highlight the relevance of the outcomes of this study in identifying novel genetic factors that could increase and individual's susceptibility to cancer.

6.4.3 **Drosophila *and GMR*>Rad21^{NC} *as models for human disease***

The major recognised risk factor for gametic aneuploidy remains maternal age, with no established molecular causes for the rapid rise in aneuploid conceptions observed after the age of 35 years. Equally, no molecular causes have been identified for people with a history of recurrent and heritable risk of aneuploid conceptions and

miscarriages. *Drosophila melanogaster* and other multicellular eukaryotes offer a means to furthering understanding of cellular functions and regulatory pathways, and also anticipating the relevance of specific genes in humans through comparative genomics. In 2000 the *Drosophila* euchromatic genome sequence was published, with the total gene number reaching approximately 13,600 (Adams *et al.*, 2000), with more recent annotations bring this number to 14,500 (Eilbeck *et al*., 2009). This is roughly 1/2 to 2/3 of the human gene number which is estimated at 20,000-25,000 genes. Of the approximately 300 currently recognised human disease-associated genes 62% have identifiable homologues in *Drosophila* (Fortini *et al.*, 2000).

6.4.3.1 Robustness of the genetic modifier list

This study has assembled a strong list of contenders for regulators of chromosome cohesion and segregation. The GMR>*Rad21*^{NC} model mirrored the results of the Separase deficiency kit screen performed by Heeger *et al.* (2005) and the phenotype was consistently and predictably modified in the heterozygous mutant backgrounds of known regulators of cohesin and chromosome cohesion (Keall, 2005). Of the genes identified in this study 40% have functions directly related to cohesin regulation or directly underpinning chromosome segregation, such as DNA replication, cell cycle progression regulation, cytokinesis and mitotic spindle regulation, chromosome structure and chromatin regulation. Another 35% of the modifier loci have identified roles in cellular pathways and functions that are closely linked to cell proliferation. Approximately 10% of the identified modifier loci function in the maintenance of circadian rhythm and neuronal development, which have been linked to cohesin, although most likely through roles independent of the chromosome cohesion function. Another 10% of modifier loci have unknown or extremely diverse functions, while only 5% of the modifier loci are believed to solely influence eye development. It is clear from the outcomes of this study that the GMR>*Rad21*^{NC} is a viable model for identify regulators of chromosome cohesion and segregation, although the true strength of the list of modifier loci identified will become apparent through testing with an independent aneuploidy assay.

Despite the numerous links to cohesin regulation, chromosome segregation and cell cycle regulation, it remains to be shown definitively that these genetic modifiers are

modifying chromosome segregation. The nature of the *Drosophila* eye, being highly organised and sensitive to small perturbations during development, which makes it a useful genetic screening tool, introduces the potential for identifying "false positives" during the screening process that are influencing only a facet of eye development and not the process of interest. Additionally, Rad21 and cohesin have functional roles separate to the integral role in chromosome cohesion. In metazoans, cohesin has identified roles in DNA damage repair (Severin *et al.*, 2001), apoptosis (Chen *et al.*, 2002; Pati *et al*., 2002), kinetochore function (Sonoda *et al*., 2001), mitotic spindle assembly (Gregson *et al.*, 2001) and regulation of transcription as a trithorax-group protein (Lara-Pezzi *et al.*, 2004; Rollins *et al.,* 2004; Horsfield *et al*., 2007; Hallson *et al.,* 2008). It is unlikely that any of these functions of Rad21 or cohesin is having a significant effect on the phenotype, because as demonstrated in Chapter 3 overexpression of three copies of wildtype *Rad21* has no influence on the eye phenotype and as demonstrated by Dr. S. Page only cells undergoing DNA replication and cell division in the present of $Rad21^{NC}$ are affected in any way. However, it is plausible that these other function of *Rad21* and cohesin could influence the modifiers that have been identified and this issue would also be addressed by a direct measure of the influence on chromosome missegregation caused by these mutant alleles.

6.4.3.2 Value of the genetic screen and secondary assays

Working with a complex biological system to identify genetic regulators of chromosome segregation has provided both meaningful results and confounding amounts of sometimes conflicting information. Many of the genetic modifiers identified in this study are known regulators of cell cycle and chromosome segregation. However, a significant number of these modifiers have never previously been associated with chromosome cohesion or the cohesin complex, which may be indicative of an excessively sensitive eye phenotype or may reflect the true extent of pathways that regulate genomic stability, which is the foundation of life.

The secondary assays, while providing insights into the nature of the interaction of individual alleles, were difficult to employ as a means of categorising modifiers. This is most likely due to the diverse functions of the genes identified and also the

multifunctional nature of proteins depending on the cellular context. The cohesin subunits and direct cohesin regulators had a strong and consistent set of characteristics, causing suppression of the wing phenotype, non-modification of the GMR*hid* phenotype, modification of the GMR>*Rad21*^{NC}*, p35* phenotype and variable modification of the GMR-Gal4 phenotype. However, the apparent lack of consistency produced by the other modifier loci in the secondary assays has proved less informative than hoped. Modification of the wing phenotype and the GMR>*Rad21*^{NC}*, p35* eye phenotype is most common amongst the strongest candidates based on known functions and therefore these assays would be most useful in future studies. The GMR*hid* phenotype may prove particularly useful in identifying regulators of MAPK function that are able to influence chromosome segregation through mis-regulation of the centrosomes. There was no apparent pattern to the ability of alleles to modify the GMR-Gal4 phenotype and no correlation between types of mutant alleles and modification of the GMR-Gal4 phenotype, therefore this phenotype is not recommended for further use without further characterisation. Some variability was observed in the modification of the primary GMR>*Rad21*^{NC} phenotype and the secondary assay phenotypes by different mutant alleles of the same gene, which may be indicative of secondary mutations that are able to influence these sensitive phenotypes. The variability observed between different mutant alleles in both the primary genetic screen and the secondary assays may be explained in part by the differential effects of increasing or decreasing gene expression in a complex regulatory system. Some of the observed variability may be reduced through "chromosome cleaning", crossing out all chromosomes except the one of interest and using the same balancer chromosomes for each cross. This variability made it difficult to draw strong conclusions from the combined assay results, and points to the necessity for a direct and objective assay to determine the influence of mutant alleles on chromosome segregation.

Further investigation into the putative regulators of chromosome segregation identified in this study is required, firstly to distinguish between those modifiers that act on chromosome segregation and those that are merely influencing the processes of eye development, and secondly to determine the exact nature of any modification of chromosome segregation. The establishment of a robust and informative meiotic aneuploidy assay that recapitulates the maternal age effect would be a priority in

further investigation of these potential regulators of chromosome cohesion and segregation. Such a meiotic model would be informative in the investigation of these candidate genes and their influence on meiotic missegregation. Further experiments to analyse the effects of individual mutant alleles on cohesin function could be performed using the *Rad21*-GFP transgenes, which allow visualisation of changes in cohesin loading levels and sites. Analyses carried out using the non-cleavable Rad21 transgene would be most informative if carried out in the eye as this is organ used for the majority of assays performed and as constitutive expression of this transgene in the neurons, most commonly used for visualising chromosome and their defects, is lethal. Other informative lines of investigation would be to determine particular defects in cell division, identification of cellular localisation of proteins of interest during cell division (e.g. spindles, chromosomes) and also to identify any changes in cohesin subunit expression levels.

6.6 FINAL COMMENTS

Fertility and wellbeing are of great interest and importance to the human race and therefore understanding the complex molecular and cellular events underlying infertility and cancer is essential. Many questions remain to be answered regarding the molecular aetiology of the maternal age effect and why certain people are at increased risk of aneuploid conceptions. Additionally, much remains to be understood about the mechanisms that lead to aneuploidy in tumour cells. Therefore the list of candidate genes generated from this and similar studies will provide a useful shortlist of genes capable of influencing chromosome segregation in a subtle way. Variations in these loci may increase or decrease an individual person's risk of producing gametes with abnormal chromosome numbers. Perhaps one day, similar to testing of hereditary risk factors for cancer, people will be able to undergo routine testing for increased risk of aneuploid conceptions that allows more informed reproductive planning.